IRE
Transactions
on ANTENNAS and PROPAGATION

Paul Weaver

VOLUME AP-3 NUMBER 2 APRIL 1955

Published Quarterly

PUBLISHED BY THE
Professional Group on Antennas and Propagation

IRE TRANSACTIONS PGAP IS A QUARTERLY PUBLICATION DEVOTED TO EXPERIMENTAL AND THEORETICAL PAPERS ON ANTENNAS AND WIRELESS PROPAGATION OF ELECTROMAGNETIC WAVES

MANUSCRIPTS should be submitted to John B. Smyth, Editor, U. S. Navy Electronics Laboratory, San Diego, California. Manuscripts should be original typewritten copy, double spaced, plus one carbon copy. References should appear as footnotes and include author's name, title, journal, volume, initial and final page numbers, and date. Each paper must have an abstract of not more than 200 words. News items concerning PGAP members and group activities should be sent to the News Editor, Mr. H. A. Finke, Polytechnic Research and Development Company, 55 Johnson Street, Brooklyn, New York.

ILLUSTRATIONS should be submitted as follows: All line drawings (graphs, charts, block diagrams, cutaways, etc.) should be inked uniformly and ready for reproduction. If commercially printed grids are used in graph drawings, author should be sure printer's ink is of a color that will reproduce. All half-tone illustrations (photographs, wash, airbrush, or pencil renderings, etc.) should be clean and ready to reproduce. Photographs should be glossy prints. Call-outs or labels should be marked on a registered tissue overlay, not on the illustration itself. No illustration should be larger than 8 x 10 inches.

Copies can be purchased from
THE INSTITUTE OF RADIO ENGINEERS
1 East 79 St., New York 21, N.Y.

PRICE PER COPY: members of the Professional Group on Antennas and Propagation, $1.60; members of the IRE, $2.40; nonmembers, $4.80.

ANNUAL SUBSCRIPTION PRICE: IRE members, $8.50; Colleges and public libraries, $12.75; nonmembers, $17.00.

Entered as second-class matter, at the post office at Menasha, Wisconsin, under the act of August 24, 1912. Acceptance for mailing at a special rate of postage is provided for in the act of February 28, 1925, embodied in Paragraph 4, Section 412, P. L. & R., authorized October 26, 1927.

news and views

PGAP

Membership—As of the beginning of this year, PGAP membership has grown to

Paid —	1,274
Unpaid —	40
Student —	62

Chapter Chairmen of the PGAP local chapters are: *Albuquerque-Los Alamos*—Frank J. Janza, Sandia Corp., Sandia Base, Albuquerque, N. M.; *Chicago*—Lawrence R. Krahe, Andrew Corp., 363 East 75th St., Chicago, Ill.; *Los Angeles*—Stanley M. Kerber, North American Aviation, 12214 Lakewood Boulevard, Downey, Calif.; *Orange Belt (Los Angeles Section)*—Andrew W. Walters, Antenna Group, Naval Ordnance Lab., Corona, Calif.; *Philadelphia*—Charles Polk, Moore School of Electrical Engineering, University of Pennsylvania, Philadelphia, Pa.; *Washington*—Dr. John I. Bohnert, U. S. Naval Research Lab., Washington, D. C.

Although Boston and New York represent areas fertile in antenna and propagation workers, neither have local chapters. This situation is, of course, deplorable. This apparent localized PGAP apathy may be rationalized by the fact that the IRE headquarters is located in New York and also because of the easy access of New York IRE people to the National Convention, while the Boston area is the scene of scientific colloquia several times each week. This problem could be met by a local PGAP chapter that jointly sponsors activities with organizations of compatible interests, thus producing a strengthened program. So, are there energetic spirits in the New York and Boston areas to get this organizing action started?

The Professional Groups are maintaining desks at the Waldorf Astoria and the Kingsbridge Armory during the IRE National Convention for the promotional work of our groups. This is a good opportunity to promote the formation of local group chapters and their membership.

Proceedings—Further progress has been made in establishing liaison with the PROCEEDINGS on papers procurement. Copies of papers submitted to the PROCEEDINGS will also be transmitted by E. K. Gannett to Roy Spencer. Roy will get a special reviewer to examine them as to whether they are more suitable for publication in the TRANSACTIONS or in the PROCEEDINGS. Also, Vic Rumsey and A. W. Straiton are moving into high gear in the matter of paper procurement. Henry Booker and A. H. Waynick are going after foreign authors. Abstracts of all papers presented at the four sessions (out of a total of fifty-five) of the IRE National convention sponsored by the PGAP are being forwarded to George Sinclair. These will be screened for potentially good papers. There is no legal restriction on publication of a paper in both the TRANSACTIONS and the PROCEEDINGS, although it would undoubtedly be limited to exceptional cases. Some authors have been reluctant to publish in the Professional Group Transactions. Some of this feeling may stem from the supposed restricted audience and the consequent lack of recognition. It must be pointed out that the circulation of the Transactions of all the progressional groups exceeds that of the PROCEEDINGS. We are inaugurating soon the policy of printing photos and biographical sketches of authors of the PGAP TRANSACTIONS.

There are still a few copies of all back issues of the PGAP TRANSACTIONS. Anyone wishing to buy any to fill out his library and insure a complete set, may purchase them from the Technical Secretary, IRE Headquarters, 1 East 79th Street, New York 21, N. Y.

Meetings—A Convention Record of the IRE National Convention will again be published this year. W. C. Jakes has represented the PGAP on the Convention Record Committee. This year we are fortunate in having Part I of the Convention Record, and this section will deal exclusively with antennas and propagation. We will not have to divide our section with other sponsoring

groups, and consequently the price will be low enough to encourage wider distribution.

As you know, we are sponsoring four technical sessions again this year. One of the sessions will be a panel discussion dealing with extended range propagation. The subject has caused considerable popular interest over the last several months and should make an interesting session. The Chairman is J. B. Wiesner of Lincoln Laboratories.

The International Symposium on Electromagnetic Theory is being held at the University of Michigan from June 20 to 25. This symposium is sponsored by URSI. We are not serving as co-sponsors. However, we have offered our assistance in helping them make this meeting a success. The session speakers are all invited, and they represent a rather imposing array of scientists of international fame. We have been approached about the question of publication of these papers. They could be handled either as a regular part of our TRANSACTIONS, or as a supplement to them. In view of the nature of the symposium, this does not necessarily represent a departure from our policy of publishing only qualified and thoroughly edited papers. To have these papers all published in a single issue of some publication with a reasonably good circulation, would be valuable and a service to our profession. It would be a single edition considerably larger than our normal publication. It may be possible to take care of the financial questions by distributing copies at a stipulated price to registrants of the symposium. In order to handle this successfully, it would be almost necessary for the registrants to pay for them in advance of the printing, in a manner similar to that handled by other conferences, such as the National Electronic Conference. The Administrative Committee of the PGAP is interested in suggestions on how this matter should be handled.

Awards—It is again time to consider the question of awards and incentives for worthy individuals, particularly in our Professional Group. Harry Wells is responsible for the nomination of appropriate individuals, and requests that all recommendations and suggestions be forwarded to him. The IRE editor's award has been discontinued. Some Professional Groups are establishing their own award system and members of their groups are eligible as recipients. Should we consider establishing a PGAP award? Let us hear from you.

GROUP CHAPTERS AND CHAPTER NEWS

Los Angeles—A talk on "Some Microwave Antenna Problems" by Samuel Silver of the University of California highlighted the most recent meeting on January 25th of the Los Angeles Chapter of the PGAP. Dr. Silver discussed some of the areas of the microwave antenna field which seem to offer the most challenging problems, and stimulated a lively discussion afterwards The Chapter has been enjoying a series of excellent meetings under the Chairmanship of S. M. Kerber, with an average attendance of fifty to sixty people at the bimonthly meetings.

The Los Angeles section also sponsored the February meeting of the Los Angeles Section of the IRE. Two outstanding papers were presented on the program. R. S. Elliott of the Hughes Aircraft Company spoke on "Surface Wave Antennas," and D. A. Watkins of Stanford University discussed the status of traveling-wave tubes and backward-wave oscillators.

At the regularly scheduled meeting in March, a paper entitled "Recent Research on Tropheric Propagation at the National Bureau of Standards" will be presented by Robert S. Kirby of the Central Radio Propagation Laboratory at Boulder, Colorado. As is customary, there will be a pre-meeting social get-together for dinner at the Encore Restaurant. A program of additional interest to Los Angeles PGAP members was presented by the UCLA Department of Engineering during the first week of March. Eric Hallen of the Royal Institute of Technology, Stockholm, Sweden, presented a series of three lectures on "Antenna Integral Equations," "Methods of Solution of Antenna Problems," and "Antenna Response to an Incoming Field."

Nominations for new officers will be made at the March meeting, and elections will be held in May.

Washington, D. C.—The Washington, D. C. Chapter of the PGAP held its first meeting on January 31, 1955. A paper entitled, "Some Recent Progress in Radio Astronomy," was presented by Frederic T. Haddock of the Naval Research Laboratory. The following Chapter officers were elected: *Chairman*—John Y. Bohnert; *Vice-Chairman*—Coleman Goatley; *Secretary*—Clarence H. Stewart, II.

The group plans to hold its next meeting on March 28, 1955.

ANTENNAS AND PROPAGATION PEOPLE

Harold A. Thomas has been appointed chief of the Radio Standards Division of the National Bureau of Standards Boulder Laboratories in Colorado. Dr. Thomas will head the continuing NBS program for the establishment, maintenance, and improvement of basic standards of measurement in the radio frequency range.

A. W. Straiton of the Electrical Engineering Research Laboratory of the University of Texas has been appointed Chairman of the Institute of Radio Engineers advisory committee to the NBS Central Radio Propagation Laboratory in Boulder, Colorado. This committee is one of 12 technical area advisory committees established to provide a direct, continuing link between the National Bureau of Standards and the organized science and technology of the nation.

Oswald J. Villard, Jr., Associate Professor with the Radio Propagation Laboratory at Stanford University, was named the "Outstanding Young Bay Area Engineer of 1955" for his contributions to radio engineering, particularly in the field of isonospheric propagation.

Meetings

URSI—The Spring Meeting will be held May 3–5 at the National Bureau of Standards, Washington, D. C. Symposia have been tentatively planned on the following subjects: The forward scattering of radio waves; The theoretical aspects of ferrites at microwaves; The mechanisms and limitations of microwave noise sources; and Multi-mode microwave transmission systems.

International Council of Scientific Unions Mixed Commission on the Ionosphere—A Symposium under the general title "Solar Eclipses and the Ionosphere" will be held in the rooms of the Royal Society, Burlington House, London, August 22–24, 1955. Topics to be discussed include: Ionospheric and other geophysical eclipse phenomena; Recent ionospheric eclipse results; Ionospheric processes—ion production and recombination; Sources of ionizing radiation; Radio astronomical eclipse observations. Contributors include S. Chapman, H. S. W. Massey, J. A. Ratcliffe, M. Nicolet, J. Bartels, L. V. Berkner, D. R. Bates, J. Sayers, R. P. Lejay, K. Weekes, C. W. Allen, W. R. Piggott, and C. M. Minnis. The Proceedings of the Symposium will be published as a Special Report by the International Union of Scientific Radio (URSI). Those wishing to attend the Symposium or to submit written contributions are invited to communicate with Dr. W. J. G. Beynon, Secretary, Mixed Commission on the Ionosphere, Department of Physics, University College, Swansea, U. K.

Correspondence

Ted Hunter, editor of the *IRE Student Quarterly*, wishes to call attention to the prominence that publication is giving to Professional Group activities. We heartily agree that an important way of building the strength of the Professional Groups is through encouraging student interest and activity. Mr. Hunter writes,

"As editor of this magazine I am sure that one of the things which will bring success to this publication will be that of keeping it youthful by bringing to the student at least one article in each issue dealing with current engineering accomplishments which the student can understand. This means that the Professional Groups should supply me with articles in a quantity greater than is needed to allow the Committee on the *Student Quarterly* to choose material for this publication. It is my earnest hope that you will accept this challenge. Some papers may not be published at all, others will be placed in the backlog to serve as material for future issues in order to give "balance" to the issues printed. The point is that I hope you will provide these papers and be willing to take the chance of not having them published and still be happy about it."

Work of the CCIR (International Radio Consulting Committee)

A service this section of the Transactions aims to provide for our Professional Group is that of keeping the membership advised of activities and affairs pertinent to our field of interest. Considerable work is being done under the CCIR dealing directly and indirectly with antennas and propagation at all frequencies, but with emphasis on those frequencies below the UHF range. The work is conducted largely by individuals or study groups. The activities in progress are various and many. The complete list is too long to be published here, but some of the groups in the U.S. and chairmen in charge are listed below. Copies of reports are available for inspection at IRE Headquarters. They may also be obtained by a request to the chairman of any one of the study groups.

Study Group	Title	U.S. Chairman
1	Transmitters	Mr. John B. Coleman Asst. Director of Engineering, RCA Victor Division, Camden, N. J.
2	Receivers	Mr. J. H. Gough Bureau of Ships, Room 1, No. 8 Navy Dept., Washington 25, D. C.
3	(Complete radio systems employed by different services)	Mr. Wayne Mason RCA Frequency Bureau, 60 Broad Street, New York 4, N. Y.
4	Ground Wave Propagation	Mr. Jack Herbstreit Boulder Labs., National Bureau of Standards, Boulder, Colo.
5	Tropospheric Propagation	Mr. E. Q. Allen, Jr. Chief Engineer, Federal Communications Commission, Washington 25, D. C.
6	Ionospheric propagation	Dr. J. H. Dellinger RCA Frequency Bureau, 1625 K Street, N.W., Washington 5, D. C.
7	Radio time Signals and Standard Frequencies	Mr. William D. George, Chief CRPL—Boulder Labs., Nat'l Bureau of Standards, Boulder, Colo.
8	International Monitoring	Mr. George Tuner, Chief Field Engineer & Monitoring Division, Federal Communications Commission, Washington 25, D. C.
9	General technical questions	Mr. E. W. Bemis American Tel. & Tel Co., 195 Broadway, New York 7, N. Y.
10	Broadcasting including questions relating to single sideband	Mr. A. Prose Walker, Dir. Eng., NARTB, 1171 N. Street, N.W., Washington 6, D. C.
11	Television including related to single sideband	Mr. Donald G. Fink Dir. of Res., R, T & A, Philco Corporation, C & Tioga Sts., Philadelphia 34, Pa.
12	Tropical broadcasting	Mr. Prose Walker Dir. Eng., NARTB, 1771 N Street, N. W., Washington 6, D. C.
13	Operation questions depending principally on technical considerations	Mr. Nathaniel White O. C. Sig. O., Dept., of the Army, Pentagon Building, Washington 25, D. C.
14	Vocabulary	Mr. A. G. Jensen Bell Telephone Lab. Murray Hill, N. J.

contributions

Synthesis of Radio Signals on Overwater Paths*

A. H. LaGRONE† A. W. STRAITON†, AND H. W. SMITH†

Summary—**The fluctuations of radio signals at microwave frequencies on overwater paths are explained on the basis of a periodic rise and fall of the water level. From this study, it is seen that the variations in the radio signal strength will contain the frequency of the water-level cycles and also the second and third harmonics of the water-level cycles.**

This same model predicts that the cross-correlation function of the fluctuations of the radio signal at two vertically-spaced antennas will drop from unity to zero as the separation distance is changed from zero to one-half of a lobe width of a height-gain interference pattern.

Although the model assumes reflection from a plane surface, the results of the study successfully explain most of the features of the observed fluctuations of the radio signals on two overwater paths.

Introduction

A STUDY OF the propagation of microwave radio signals on overwater paths is confused by the absence of a suitable model of the rough-water surfaces. Reflection from hemisphere, semi-cylinder and broken mirror-type surfaces have been considered, but the results obtained are very unwieldy and the appropriateness of the models for actual sea surfaces is questionable.

Many of the characteristics of the overwater radio signal fluctuations can be explained in terms of a plane reflecting surface which rises and falls periodically. This report investigates some of the effects of this simplified model and compares the results with measured overwater propagation data. The comparison indicates that at small grazing angles the simplified model is adequate to explain a number of measured characteristics.

It is not implied that the plane surface model gives a complete explanation of the radio signal fluctuations. It is felt that the plane surface model does give a very good solution where a large coherent reflected component is present. It is felt, further, that a clear understanding of the plane surface case will be of value in approaching the problem of reflections from rough surfaces.

* Original manuscript received by the PGAP, May 21, 1954; revised manuscript received, November 24, 1954. This work was sponsored under the Office of Naval Research Contract NOnr 375(01) NR 071 031.

† The University of Texas, Austin, Texas.

The Radio Signal on an Overwater Path

It is assumed that the path length is short enough so that straight line propagation may be used and that the effect of the earth's curvature may be neglected. With these assumptions, the phase difference, θ, between the direct and the reflected waves at the receiver can be expressed as accurately as needed by the following equation:

$$\theta = \frac{4\pi h_1 h_2}{\lambda D} - \pi, \tag{1}$$

where

h_1 = transmitter height in feet
h_2 = receiver height in feet
D = path length in feet
λ = wavelength in feet.

The reflecting surface is assumed to rise and fall sinusoidally with time and the deviation of the reflecting plane from its average value is given by

$$\Delta h = b \sin(\omega t), \tag{2}$$

where b is the maximum displacement of the reflecting plane from its average value, measured in feet.

The height of the receiver and of the transmitter are given by

$$h_1 = h_{1_0} + \Delta h \quad \text{and}$$
$$h_2 = h_{2_0} + \Delta h,$$

respectively.

The equation for θ can now be written to show the changes in h_1 and h_2 which result from the reflecting-

surface height variations. The equation for θ is

$$\theta = \frac{4\pi}{\lambda D}(h_{1_0} + \Delta h)(h_{2_0} + \Delta h) - \pi \tag{3}$$

$$= \frac{4\pi}{\lambda D}[h_{1_0}h_{2_0} + (h_{1_0} + h_{2_0})\Delta h + (\Delta h)^2] - \pi. \tag{4}$$

If we assume that Δh is small compared to $(h_{1_0}+h_{2_0})$, we can rewrite (4) as follows:

$$\theta = \left[\frac{4\pi}{\lambda D}(h_{1_0}h_{2_0}) - \pi\right] + \left[\frac{4\pi}{\lambda D}(h_{1_0} + h_{2_0})\right]\Delta h \tag{4}$$

$$= \left[\frac{4\pi}{\lambda D}(h_{1_0}h_{2_0}) - \pi\right] + \left[\frac{4\pi}{\lambda D}(h_{1_0} + h_{2_0})b\right]\sin \omega t \tag{5}$$

$$= \theta_0 + \phi \sin \omega t. \tag{6}$$

The equation for the resultant received signal, E, is

$$E = E_0(1 + Ke^{i\theta}), \tag{7}$$

where

E_0 = electric field strength of the direct ray or free-space signal at the receiver.

K = reflection coefficient.

The ratio R of the resultant signal to the direct or free-space signal is given by

$$R = (E/E_0) = 1 + Ke^{i\theta} \tag{8}$$

$$= [1 + K^2 + 2K\cos\theta]^{1/2} < \delta \tag{9}$$

where

$$\delta = \arctan\left[\frac{K\sin\theta}{1 + K\cos\theta}\right]. \tag{10}$$

Since our primary interest is in the time fluctuations in the total signal amplitude, we will consider only the scalar magnitude of R in (9), which is

$$|R| = +[(1 + K^2) + 2K\cos\theta]^{1/2}. \tag{11}$$

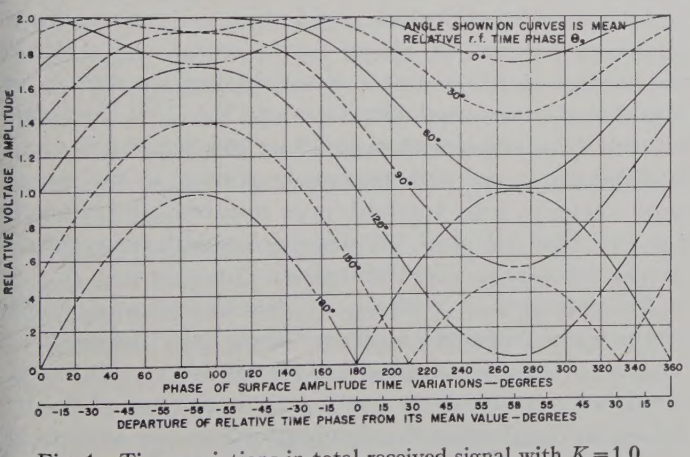

Fig. 1—Time variations in total received signal with $K = 1.0$.

Fig. 1 shows a plot of $|R|$ for $K = 1.0$ and $\phi = 1.012$ radians (58 degrees). The time fluctuations in $|R|$ are readily apparent in this set of curves. The nature of the time fluctuations can be obtained by expanding $|R|$ in a binominal series and then expanding Cos θ in terms of $(\theta_0+\phi \sin \omega t)$. Such an expansion shows that the time fluctuations in $|R|$ are functions of the ocean surface amplitude fundamental (ωt) and its harmonics $(n\omega t)$, $n = 1, 2, 3$, etc., as follows:

$$|R| = B_0 + B_1 \sin \omega t + B_2 \cos 2\omega t + B_3 \sin 3\omega t + B_4 \cos 4\omega t + \cdots \tag{12}$$

where B_n is a function of the path geometry [1], the reflection coefficient K, and the surface amplitude coefficient b.

An expression similar to (12) can be obtained for the total relative power received if $|R|^2$ is expanded through cos θ in terms of the ocean-surface amplitude fundamental (ωt).

$$|R|^2 = (1 + K^2) + 2K\cos\theta \tag{13}$$

$$|R|^2 = C_0 + C_1 \sin \omega t + C_2 \cos 2\omega t + C_3 \sin 3\omega t + C_4 \cos 4\omega t + \cdots, \tag{14}$$

where C_n is a function of the path geometry [1], the reflection coefficient K and the surface amplitude coefficient b.

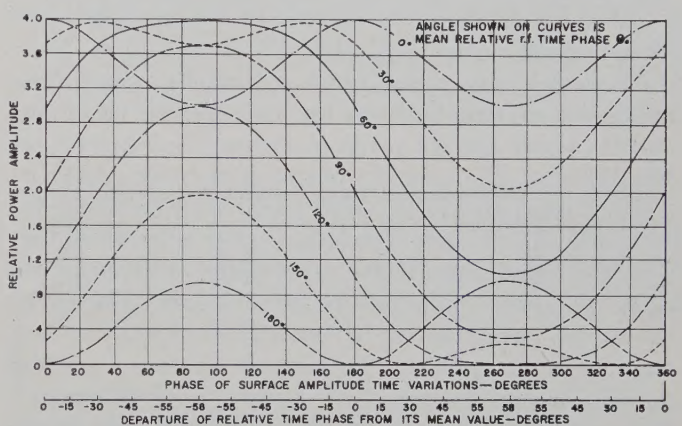

Fig. 2—Time variations in relative power received with $K = 1.0$.

Fig. 2 is a plot of $|R|^2$ for $K = 1.0$ and $\phi = 1.012$ radians (58 degrees). Fig. 3 (next page) is a plot of the three primary frequency components in $|R|^2$. Note that only the even harmonics are present at $\theta_0 = 0$ degrees, or 180 degrees. This would correspond to having the signal fluctuate about a signal maximum or a signal minimum, respectively, in a height-gain curve.

Correlation Characteristics of Radio Signal with Water-Surface Variations

The normalized cross-correlation [2] coefficient $\rho_{12}(\tau)$ is computed at $\tau = 0$ between the water-surface variation and the fluctuations in the total received radio signal. The mathematical expression for $\rho_{12}(\tau)$ is

$$\rho_{12}(\tau) = \frac{1}{y_1(t)\ y_2(t)}\int_{-\pi}^{\pi} y_1(t)\, y_2(t + \tau)\, dt, \tag{15}$$

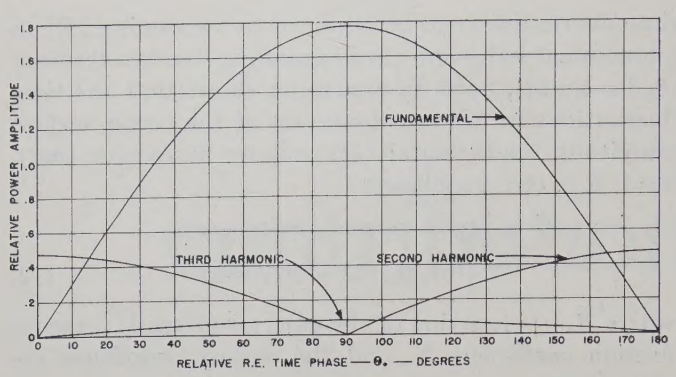

Fig. 3—Power distribution of the frequency components in the time fluctuations of the radio signal for $K=1.0$.

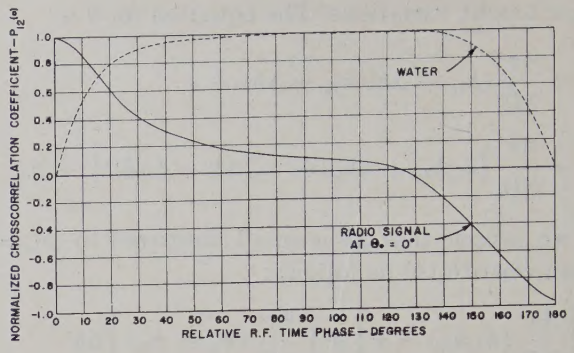

Fig. 4—Cross correlation of water data and ac component of total radio signal at $\Theta_0=0°$ with ac component of total radio signal at other values of Θ_0, for $K=1.0$.

where

$y_1(t)=1.0 \sin \omega t$ (assumed water surface amplitude variation)

$y_2(t)=$ fluctuating part of R (ac component of curves in Fig. 1)

$\overline{y_1(t)}=$ effective value of $y_1(t)$

$\overline{y_2(t)}=$ effective value of $y_2(t)$.

A plot of the water cross-correlation coefficient for $\tau=0$ is shown in Fig. 4 as a function of θ_0 for $K=1.0$. Curves for $K=0.8$ and 0.6 were also computed but are not shown as there was no significant difference between them and the curve for $K=1.0$.

The water cross-correlation curve shows a correlation coefficient of zero between the radio-signal variations and the water-surface variations when $\theta_0=0$ degrees, or 180 degrees; or in terms of height-gain curves, when at a signal maximum or at a signal minimum respectively.

A radio-signal cross-correlation curve is shown in Fig. 4 for the fluctuations in the raido signal at other values of θ_0. This was computed for $K=1.0$ only. The curve shows the correlation to be expected between the fluctuations in the signal at a height-gain maximum and the fluctuations in the signal at nearby receiver heights. This curve, of course, is directly applicable only to the numerical example in this paper.

Analysis of Field-Measured Radio Signals on Overwater Path

Signal-strength measurements were made on an overwater path, 16,200 feet long, across the Golden Gate Inlet, San Francisco, Calif. The transmitter was 87 feet above mean sea level and the receiver approximately 50 feet above mean sea level. The water-level data [3] were obtained at a point about 200 yards offshore at the receiver end. A nominal value for the swell amplitudes as measured was two feet, peak to trough.

Spectral density studies [4] were made of the variations with time of the water level and also of the radio signal. Sample curves are shown in Figs. 5 and 6.

Fig. 5 shows a water-level spectral-density curve that is typical of all the water data samples taken. The frequency at which the peak occurred varied slightly from day to day but, otherwise, the curve remained essentially the same. The spectral-density curve of the fluctuations in the associated radio signal is also shown. The radio spectral-density curve was not always a single peak curve as Fig. 5 might indicate, however. It was more often a variation of the two or three peak-type curves as shown in Fig. 6. There were no cases in which a definite fourth peak was found.

The very good agreement between the central frequency at which the peak occurs in the water level spectral-density curve and the central frequency of the first peak in the associated radio spectral-density curve, Fig. 5, suggests very strongly that one results from the other. Also the second and third peaks in the radio data are so near the second and third harmonic frequencies of the first peak central frequency, Fig. 6, that it must be assumed that they are the harmonics of the first peak central frequency.

The power distribution curves in Fig. 3 show how a proper choice of θ_0 would yield, by theoretical analysis, curves of $|R|$ having the same fluctuation characteristics as found in the measured data. In Fig. 3, for example, a constant amplitude reflected wave with a mean relative time phase of 80 or 100 degrees, and a relative time-phase variation of 58 degrees sin ωt would have produced in the total received signal a time-varying component having a strong fundamental and a small second and third harmonic of the driving frequency, as found in the measured data shown in Fig. 5. If the mean relative time phase had been 15 or 165 degrees, a spectral-density curve with two peaks similar to the measured curve in Fig. 6 would have resulted, and a mean relative time phase of 130 degrees would have resulted in the three-peak spectral-density curve in Fig. 6.

The theoretical analysis, of course, is for a single water-wave frequency and thus gives only line spectra, whereas the field-measured curves are for conditions of continuous water-wave spectra. It is not too difficult, however, to visualize the driving force in the numerical example as a band of frequencies, in which case the spectra would be a band spectra similar to the field-measured case. Thus, we see that the patterns in Figs. 5 and 6, plus many others, could be obtained from a single specularly-reflected wave of constant amplitude.

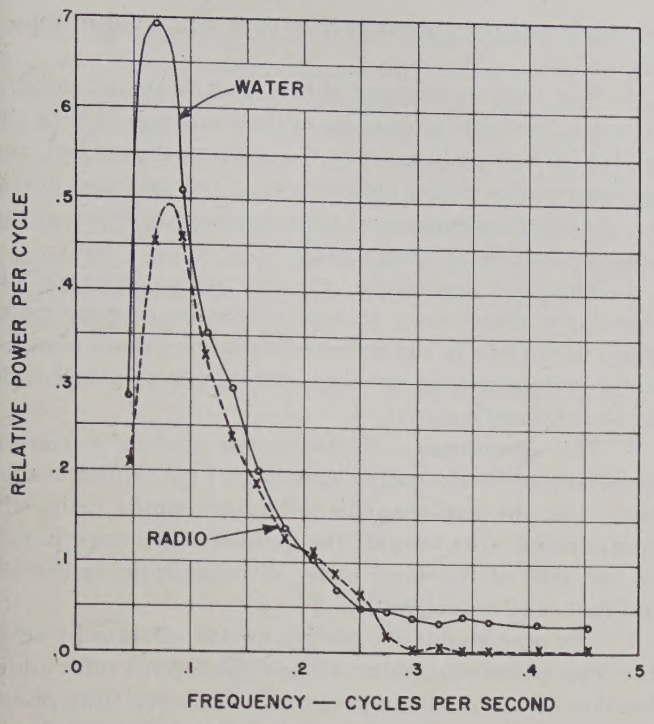

Fig. 5—Frequency spectrum of water-surface variations and of associated radio signal.

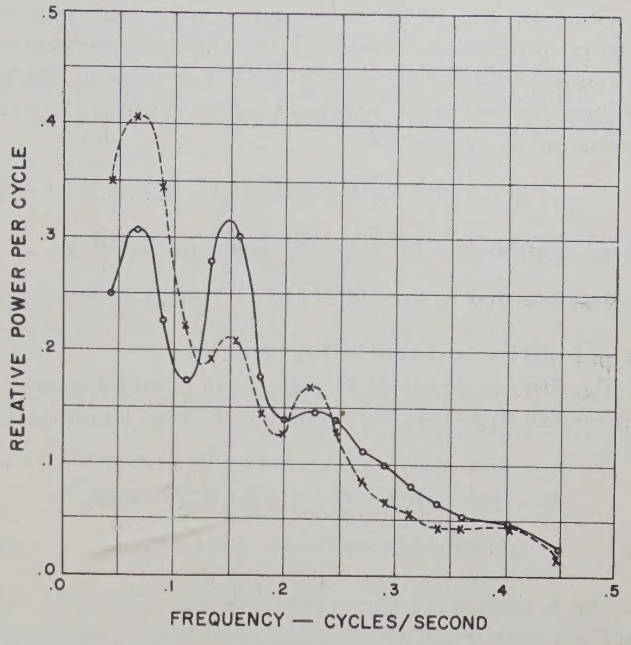

Fig. 6—Frequency spectrum of ac components of total radio signal showing prominent harmonics.

The mean relative phase θ_0 in the field-measured data was essentially constant over short periods of time; however, changes in water level due to the tide did change θ_0 considerably over longer periods of time. Tides varied from four to six feet during the period of measurement and thus changed the effective terminal heights h_1 and h_2 such that θ_0 varied during the day as much as 232 or 348 degrees, depending on the tide that day. This range of variation was sufficient to cover almost all of the possible combinations of components shown in Fig. 3.

Synthesis of Radio Signals on an Overwater Path

The ocean model assumed in the first section is used to explain the time variation observed in a field-measured height-gain run, Fig. 7(a), made on a second overwater path. The path is 2,780 feet long and is across Baratraia Pass near Grand Isle, La. The transmitter is at 61.7 feet mean sea level, and the swell amplitude two inches, peak-to-trough. The wavelength of the radio signal is $\lambda = 0.105$ foot.

The hypothetical height-gain runs, Fig. 7(b), (c) and (d), are obtained by using (8). The time variations in the height of the reflecting surface are arbitrarily related to the time factor in the height-gain run in such a way that 7.12 cycles of the surface variations are completed in one cycle of the height-gain variation. If we neglect π in the θ_0 component of (5) and assume an initial phase angle for the reflecting surface variations, the equation for θ is

$$\theta = 2.656h_2 - \left(\frac{61.7 + h_2}{278.8}\right) = \sin\,(18.9\,h_2 - 3.037). \quad (16)$$

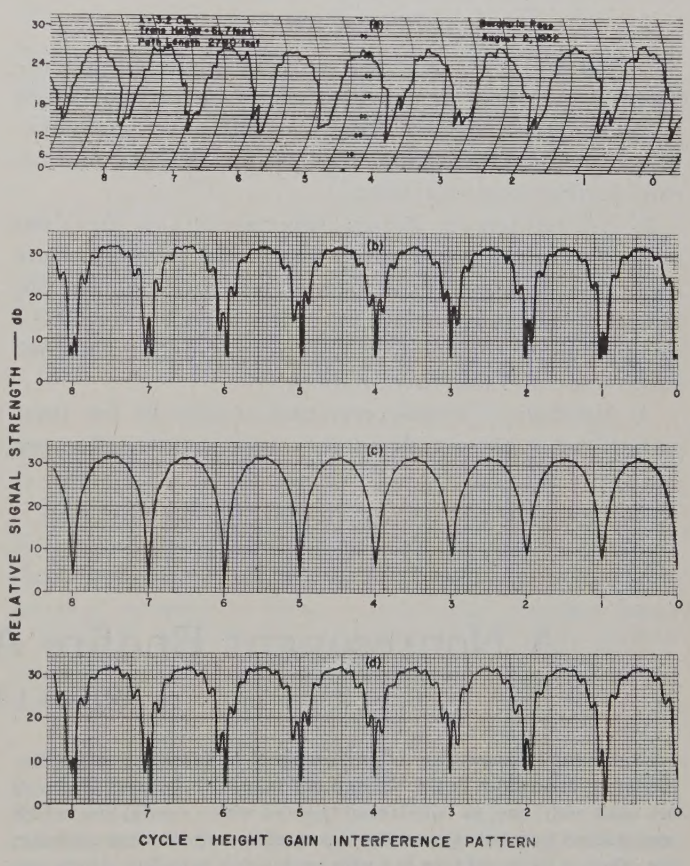

Fig. 7—Field measured and theoretical height-gain curves.

A value of 0.9 is assumed [5] for K, so that the equation for R is

$$R = 1 + 0.9e^{j[2.656h_2 - (61.7+h_2)/278.8 \sin\,(18.9h_2 - 3.037)]}. \quad (17)$$

Eq. (17) is shown plotted in Fig. 7(b).

The synthesis of the radio signal is carried one step further in order to investigate the effect on the pattern of the height-gain curve of a small variation in the reflection coefficient. Accordingly, K is assumed to vary in the following manner.

$$K = 0.9 - 0.05 \sin (18.9h_2 - 3.037). \quad (18)$$

If we assume ϕ to be zero, the equation for R is

$$R = 1 + [0.9 - 0.05 \sin (18.9h_2 - 3.037)]e^{i2.656h_2}. \quad (19)$$

A plot of (19) is shown in Fig. 7(c).

Fig. 7(d) is a plot of R with both K and θ having a sinusoidal time-varying component. The equation for R is

$$R = 1 + \{[0.9 - 0.05 \sin (18.9h_2 - 3.037)] \cdot e^{i[2.65h_2 - (61.7+h_2)/278.8 \sin (18.9h_2 - 3.037)]}\}. \quad (20)$$

The agreement of the synthesized signals in Fig. 7(b) and (d) with Fig. 7(a) is very good and indicates the extreme importance of the relative phase of the reflected wave in the total signal.

Conclusions

1. Variations in the relative time phase of the reflected wave generates, in the combination of the direct wave and the reflected wave in the receiver, a fundamental and higher harmonics of the driving motion causing the phase variations.

2. Normalized cross-correlation studies of the time variations in the amplitude of a radio signal taken on an overwater path and the associated time variations in the height of the ocean surface may vary from zero to unity, depending on the relative time phase of the reflected radio wave and the direct radio wave.

3. Normalized cross-correlation studies of the time variations in the amplitude of radio signals taken on vertically-spaced antennas may vary from plus or minus one to zero.

4. The good agreement of the spectral-density distribution of the time variations in the radio signal with the predicted spectral-density distribution based on the assumed ocean model indicates that the assumed model is a good approximation of the true ocean existing at the time the field data were taken.

5. The good agreement referred to in paragraph (4) above also shows very strongly that the relative time-phase variations in the reflected radio signal are a major factor in determining the time stability of the amplitude of the total radio signal.

6. The prominence of the ocean surface variation fundamental in the radio signals in Figs. 5 and 6 suggests that the surface-reflected wave comes primarily from a small area around the geometrical image point, i.e., an area of the same order of magnitude as the individual swell wavelength.

7. The reproducibility of field measured data by relative time-phase variations in the reflected ray offer additional evidence of the importance of relative time-phase variations in time stability of the total radio signal.

Bibliography

1. LaGrone, A. H., Straiton, A. W., and Smith, H. W., "Synthesis of Radio Signals on Overwater Paths," Rep. No. 71, Elec. Eng. Res. Lab., The Univ. of Texas, Austin, Texas, April, 1954.
2. James, H. M., *Theory of Servomechanism*. New York, McGraw-Hill Book Co., Inc., 1947.
3. Jehn, K. H., Gerhardt, J. R., Metcalf, D. F., and Prosser, S. J., "Some Meteorological and Oceanographic Characteristics of the Golden Gate California Area," Rep. No. 3–13, CM-760, Elec. Engrg. Res. Lab., The Univ. of Texas, Austin, Texas, February, 1954.
4. Brooks, F. E., Smith, H. W., and DuBose, G. P., "Power Spectra and Statistical Studies of Overwater Signal Strengths for the Golden Gate California Radio Path," Rep. No. 3–16, CM-813, Elec. Engrg. Res. Lab., The Univ. of Texas, Austin, Texas, July, 1954.
5. LaGrone, A. H. and C. W. Tolbert, "Reflection Studies of Millimeter and Centimeter Radio Waves for Gulf of Mexico Paths," Rep. No. 64, Elec. Engrg. Res. Lab., The Univ. of Texas, Austin, Texas, October, 1952.

A Nonresonant Endfire Array for VHF and UHF*

W. A. CUMMING†

***Summary*—A new type of endfire array is described which has moderate bandwidth in the vhf and uhf ranges. Two types of arrays are dealt with; one, an unbalanced type fed with a coaxial line, which was studied primarily to test the theory of operation of the antenna; the other, a balanced type fed with unshielded twin-line, which was developed as a receiving antenna for vhf television. This latter antenna has a gain varying from 6 db to 10 db above a dipole over a 50 per cent frequency range, and produces a voltage standing wave ratio of not greater than 2.5 to 1 on 300-ohm twin lead.**

* Original manuscript received by the PGAP, July 9, 1954; revised manuscript received, December 3, 1954.

† Radio and Electrical Engineering Division, National Research Council, Ottawa, Canada.

Introduction

THE DEVELOPMENT of this antenna grew out of a study of the well-known helical antenna.[1] A helix operating in the axial mode has been shown to perform as a circularly polarized endfire array with increased directivity over approximately a 2:1 frequency range. For many applications, however, circular polarization is not required and may even be undesirable. It was felt, therefore, that the need existed for an

[1] J. D. Kraus, "The helical antenna," Proc. I.R.E., vol. 37, p. 263–272; March, 1949.

antenna having the broadband characteristics of the helix, but having linear rather than circular polarization. Linear polarization can be achieved by suitably combining two helixes of opposite sense, but such an arrangement is cumbersome and attended by additional drawbacks with respect to side lobes and bandwidth, depending on the method chosen to combine the two antennas. It was decided, therefore, to attempt to design an antenna of linear current elements to obtain the required linear polarization.

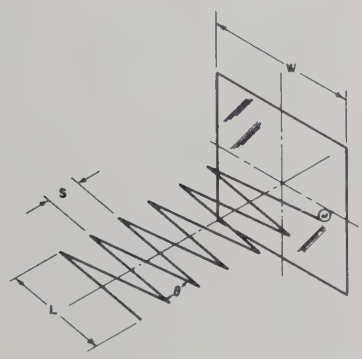

Fig. 1—Configuration of 6-element array.

The Experimental Antenna

The initial study was made on an antenna having the configuration shown in Fig. 1. To determine the most suitable geometry for this antenna, certain simplifying assumptions were made, the plan being to test an antenna designed in accordance with the principles of a simplified theory of operation, and then to amend this theory to fit the measured results.

Neglecting for the moment the effect of the ground screen backing the antenna, it was postulated that the conductor would carry a single traveling wave, and that reflections from the corners and the unterminated end of the wire would merely alter sidelobe levels and fill in the nulls. With this simplifying assumption the structure then becomes an array of V-shaped elements, as shown in Fig. 2.

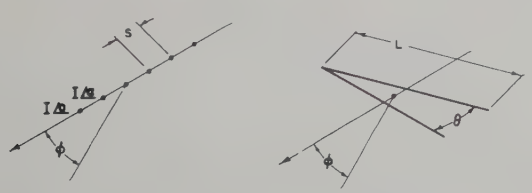

Fig. 2—(a) Equivalent array of isotropic point sources. (b) Basic element of equivalent array.

Looking first at a single V it is seen that if the geometry is chosen correctly, the unit becomes an endfire couplet formed by two wires, each carrying a traveling wave. If the velocity of propagation on the wire is v, then for the geometry of Fig. 2 the pattern of one wire in the plane of the wire is given by[2]

$$F_1(\phi) = \frac{K \cdot \sin \frac{\pi L}{\lambda_a}\left(\frac{c}{v} + \sin\left(\phi - \frac{\theta}{2}\right)\right)}{\frac{c}{v} + \sin\left(\phi - \frac{\theta}{2}\right)} \cdot \cos\left(\phi - \frac{\theta}{2}\right), \tag{1}$$

and the pattern of the other wire by

$$F_2(\phi) = \frac{K \cdot \sin \frac{\pi L}{\lambda_a}\left(\frac{c}{v} - \sin\left(\phi - \frac{\theta}{2}\right)\right)}{\frac{c}{v} - \sin\left(\phi + \frac{\theta}{2}\right)} \cdot \cos\left(\phi + \frac{\theta}{2}\right). \tag{2}$$

It will be noted that these equations have implied that the two wires carry currents equal both in amplitude and time phase. However, by taking the centers of the two wires as reference points, it is seen that the phase angle of the current in one wire with respect to that in the other is given by

$$\alpha = \frac{2\pi L}{\lambda_a} \cdot \frac{c}{v} - \pi,$$

where the phase delay of π is due to the phase reversal in space. In the plane of the wires, then, the phase angle of the radiation from one wire relative to that from the other is

$$\psi = \frac{2\pi L c}{\lambda_a v} - \pi - \frac{\pi S}{\lambda_a} \cos\phi, \tag{3}$$

where the wire remote from the generator is taken to be the reference.

An examination of the pattern functions for each wire and of the phase function for one wire with respect to the other shows that ideally two conditions should be satisfied in order to obtain a satisfactory pattern from a single V. In order that the V operates as an endfire couplet, L and S should be so related that when $\phi = 0$, $\psi = 0$; i.e.,

$$\left(\frac{c}{v}\right)L - \frac{S}{2} = \frac{\lambda_a}{2}. \tag{4}$$

The second condition is that the major radiation lobes from the two wires should be coincident along the axis of the endfire couplet. An examination of (1) and (2) shows that if the individual wire patterns are to have their maxima in the direction $\phi = 0$ degrees, then, provided the tilt of the individual beam is not too great, θ must be chosen so that

[2] J. A. Stratton, "Electromagnetic Theory," McGraw-Hill Book Co., Inc., New York, ch. VIII, sec. 8.8, p. 445; 1941.

$$\sin \theta/2 = c/v - \lambda_a/2L.$$

From the geometry it is seen that $\sin \theta/2 = S/2\ L$, and thus the condition for alignment becomes

$$\frac{S}{2} = L\left(\frac{c}{v}\right) - \frac{\lambda_a}{2},$$

which is also recognized as the condition for endfire operation. In the first experimental array a value of $c/v = 1$ was assumed and the values chosen for L and S were $0.6\ \lambda_a$ and $0.2\lambda_a$, respectively, making θ approximately 20 degrees.

Referring now to an endfire array of n such V-shaped elements, it is seen that the phase of equivalent current in one V relative to that in an adjacent V is given by

$$\alpha = \frac{4\pi L}{\lambda_a} \cdot \frac{c}{v} - 2\pi, \tag{5}$$

where again the phase delay of 2π is due to the double reversal in space. With the V-elements spaced a distance S apart, the array factor then becomes[3]

$$A(\phi) = \frac{\sin\left(\frac{n\psi}{2}\right)}{n \sin\left(\frac{\psi}{2}\right)}, \tag{6}$$

where

$$\psi = \frac{4\pi L}{\lambda_a} \cdot \frac{c}{v} - 2\pi - \frac{2\pi S}{\lambda_a} \cos \phi. \tag{7}$$

Having assumed $c/v = 1$, and having chosen L and S to give endfire operation of the individual V-elements, (7) becomes

$$\psi = \frac{2\pi S}{\lambda_a}(1 - \cos \phi). \tag{8}$$

Thus on the axis of the array the contributions from the individual V-elements add in phase and the array is an ordinary endfire type.

An experimental 6-element array, backed by a one-wavelength-square ground plane, was constructed on the basis of the foregoing analysis. A design frequency of 1,400 megacycles/second was chosen for convenience in pattern taking, and measured E- and H-plane patterns are shown in Figs. 3 and 4, opposite. Comparison of the measured E-plane pattern with the calculated E-plane pattern of Fig. 5 shows the measured beamwidth to be considerably smaller than that calculated. The measured pattern is in fact quite similar to that obtained from an endfire array with increased directivity. It has been shown by Hansen and Woodyard[4] that an endfire array of n elements, spaced a distance S apart, has a considerably higher gain if the phase of one element relative to the next is made greater than the value of $2\pi S/\lambda_a$ required to give in-phase radiation on the array axis.

Again writing the array factor

$$F(\phi) = \frac{\sin\left(\frac{n\psi}{2}\right)}{n \sin\left(\frac{\psi}{2}\right)},$$

where now

$$\psi = \frac{2\pi S}{\lambda_a}(1 - \cos \phi) + \delta, \tag{9}$$

Hansen and Woodyard show that if δ is made approximately π/n rather than zero, as is the case for the ordinary endfire array, the gain is considerably increased.

Returning now to this particular array, we had

$$\psi = \frac{4\pi L}{\lambda_a} \cdot \frac{c}{v} - 2\pi - \frac{2\pi S}{\lambda_a} \cos \phi,$$

which can be written

$$\psi = \frac{2\pi S}{\lambda_a}(1 - \cos \phi) + \delta,$$

where

$$\delta = \frac{4\pi L}{\lambda_a} - \frac{c}{v} - 2\pi - \frac{2\pi S}{\lambda_a}. \tag{10}$$

Recalling that

$$L - \frac{S}{2} = \frac{\lambda_a}{2},$$

this becomes

$$\delta = \frac{4\pi L}{\lambda_a}\left(\frac{c}{v} - 1\right). \tag{11}$$

Thus it is seen that if the velocity of propagation on the wire is less than in free space, the array could be expected to operate with increased directivity.

A number of values were chosen for the velocity ratio $\rho = v/c$, and the corresponding unit patterns, array factors, and hence complete patterns were calculated for the E-plane. It was found that a ratio of 91 per cent gave the best fit with the measured pattern. The pattern calculated under these new assumed conditions is shown in Fig. 6. It will be noted that insofar as the main beam is concerned, the agreement is excellent. The wide-lobe detail, however, is different in the two cases, which is not too surprising considering the assumptions made in calculating the pattern, and also considering the effects of the ground plane. It would appear then that the array, to a first approximation, operates as a nonresonant antenna, and that the velocity of propagation on the wire is reduced, due to the geometry of the structure.

[3] J. D. Kraus, "Antennas," McGraw-Hill Book Co., Inc., New York, ch. 4, sec. 4.6, p. 78; 1950.

[4] W. W. Hansen and J. R. Woodyard, "A new principle in directional antenna design," Proc. I.R.E., vol. 26, pp. 333–345; March, 1938.

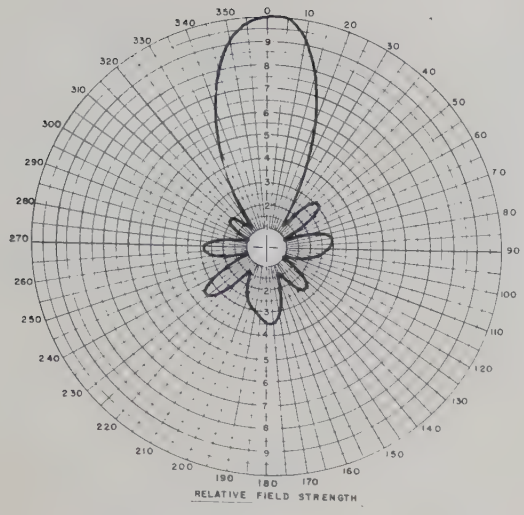

Fig. 3—Measured *E*-plane pattern of 6-element array.

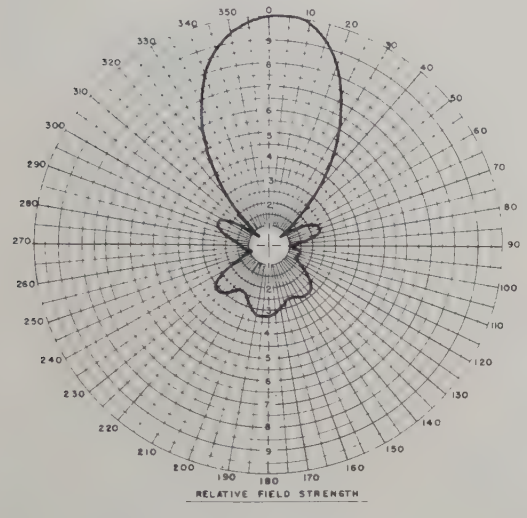

Fig. 4—Measured *H*-plane pattern of 6-element array.

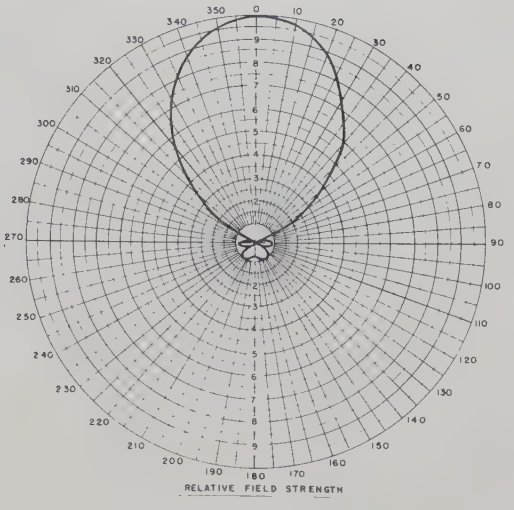

Fig. 5—Calculated *E*-plane pattern of 6-element array with $v/c=1$.

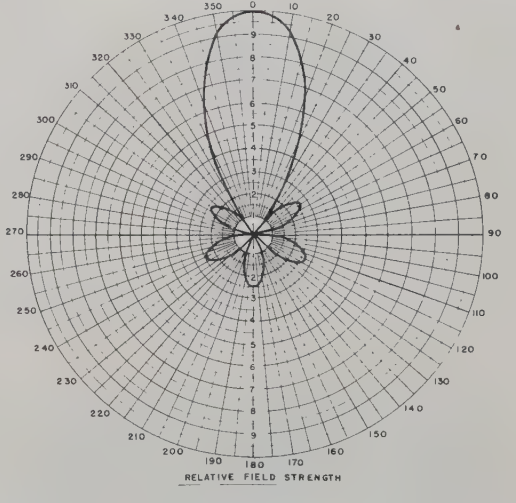

Fig. 6—Calculated *E*-plane pattern of 6-element array with $v/c=0.91$.

A series of patterns were measured on this same antenna to determine its operating bandwidth. It was found that in this case satisfactory operation was obtained from 1,250 to 1,450 mc—a bandwidth of some 15 per cent. The patterns at 1,250 mc were considerably broader than those at 1,400 mc and had lower sidelobes; while those at 1,450 mc had a narrower beam and slightly higher sidelobes. In order to explain this performance it was assumed that v/c remained 91 per cent over the frequency range 1,250–1,450 mc, and δ was calculated for the frequency limits. It was found that under these conditions δ varied from 0 degrees at 1,250 mc to 55 degrees at 1,450 mc. With $\delta=0$ degrees the conditions are satisfied for operation as an ordinary endfire array, while with $\delta=55$ degrees, the array is again operating with increased directivity. Patterns were calculated for these new values of δ, and reasonable agreement was once more obtained. It is thus evident that the assumption of a constant velocity of propagation is valid. This fact of course limits the bandwidth of the antenna to a smaller value than that obtainable with the helical antenna in which the velocity of propagation varies with frequency in such a way as to hold δ constant. If δ is permitted to vary with frequency from 0 degrees to a specified maximum value, then it is readily seen that the bandwidth of this antenna varies inversely as the number of elements in the array. It is, however, difficult to assign a maximum value for δ in the case of short arrays. For the 6-element antenna, which has been described, satisfactory patterns were obtained with a maximum of 55 degrees, considerably greater than the value of π/n derived by Hansen and Woodyard. However, this is not too surprising when it is remembered that their analysis assumed long arrays, and did not take into account the directivity of the array elements.

Since the array which has been described was built primarily to check the validity of the assumed current distribution, the impedance characteristics have not

been studied carefully. The input impedance is, of course, influenced by the size of the ground plane backing the array, and it can be said only that for this particular unbalanced antenna the input resistance varied from 100 to 150 ohms.

While further fundamental studies remain to be carried out on this antenna, with a view to further broadbanding, one practical application has already been investigated, and is described in the following section.

A Balanced Antenna for *VHF*

The nonresonant properties of the antenna which has been described suggest an application for the relatively broad bands required for VHF television reception. As was pointed out previously, the bandwidth of this antenna varies inversely with the number of elements, and it was felt that a shorter array could be designed which would cover the 50 per cent band occupied by Channels 2 to 6, while providing moderate gain.

For this application a balanced antenna which can be connected directly to 300-ohm twin-lead is most desirable. Such a balanced antenna could easily be devised by placing two of the units already described side-by-side. It is readily seen that this arrangement consists really of a number of small rhombic antennas, connected in series. However, when it is remembered that Channel 2 extends down to 54 mc, it is seen that such an antenna would be too large to be practical. It was therefore decided to sacrifice gain for convenient physical size, and to mount one unit above the other, as shown in Fig. 7.

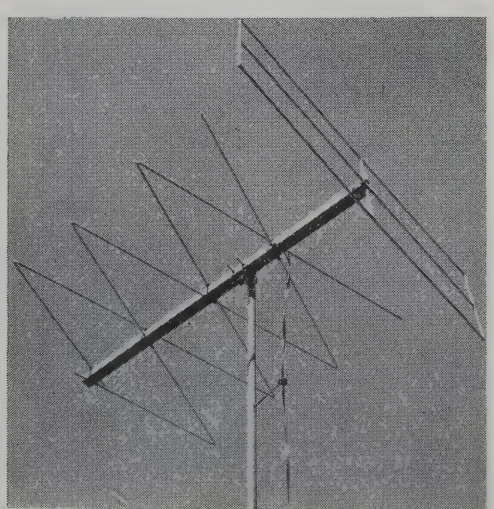

Fig. 7—Photograph of array for VHF TV (Channels 7 to 13).

Referring to Fig. 8, it is seen that while the basic configuration of the antenna is similar to that of the experimental antenna, it differs in detail. In order to obtain slightly better alignment of the radiation lobes from the individual wires, the included angle of the *V* was increased to 30 degrees. The dimensions of the antenna for the general case are shown in the table of Fig. 8, where λ is the free-space center-frequency wavelength.

The first prototype-balanced antenna was constructed by supporting the radiating members on stand-off insulators mounted in a metal pipe. Pattern tests on this arrangement showed that the shunt capacity introduced by the pipe reduced the velocity of propagation of the antenna still further, thus permitting a slightly smaller structure. However, this same capacity reduced the input impedance to an unworkable level, and it was concluded that for satisfactory operation the antenna elements would have to be mounted on a dielectric support.

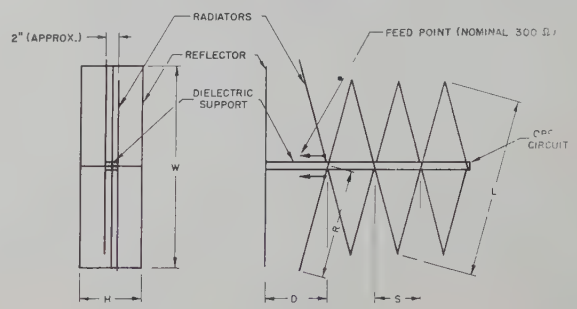

	LOW BAND (CHANNELS 2-6)	HIGH BAND (CHANNELS 7-13)	GENERAL CASE
S	30·5"	12·25"	·18λ
L	115"	46"	·69λ
D	39"	15·5"	·23λ
W	130"	52"	·78λ
H	40·5"	16"	·24λ
R	70"	28"	·42λ

Fig. 8—General configuration of series-rhombic antenna.

The agreement between theory and measurement was not nearly so good on such a short antenna, with the result that final adjustments were made by trial and error. For example, it was found that the termination on the antenna had only a small effect on patterns, so it was left open-circuited. Likewise, it was found by experiment that the front-to-back ratio could be improved considerably by placing a small grid-type reflector behind the antenna.

Referring again to Fig. 8, it is seen that the input elements extend back towards the reflector a distance *R*. It was observed that the length of these members provided an excellent control over input impedance without affecting the patterns to any great extent, and so their length was chosen to provide the best match on 300-ohm line.

For the sake of convenience in pattern-taking, an antenna based on this design was constructed to operate in the frequency range 135–220 mc, a band of some 50 per cent. The measured *E*-plane and *H*-plane patterns of this antenna are shown in Fig. 9 and Fig. 10. It will be seen that as in the case of the unbalanced antenna, the broad patterns of the ordinary endfire array are obtained at the low end of the band, while a much more directional pattern is produced at the high end. For convenience in comparing patterns on the lower TV channels, the frequencies at which the measurements were made have been scaled down to the band 54–88 mc; i.e., Channels 2 to 6.

Fig. 11, next page, shows a gain comparison between this and a standard commercial 5-element Yagi antenna. In both cases gain figures were obtained from patterns,

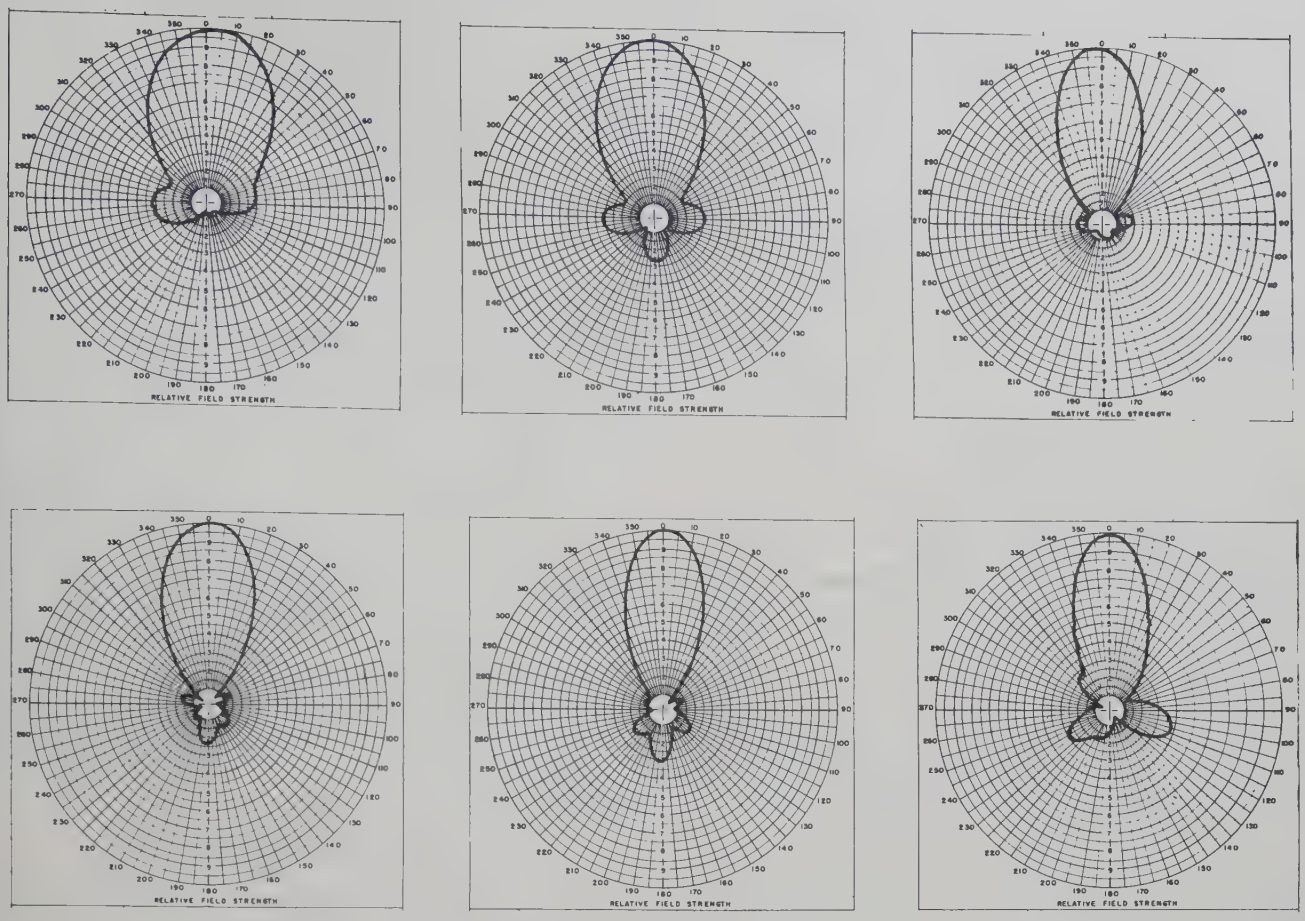

Fig. 9—*E*-plane patterns of series-rhombic antenna.

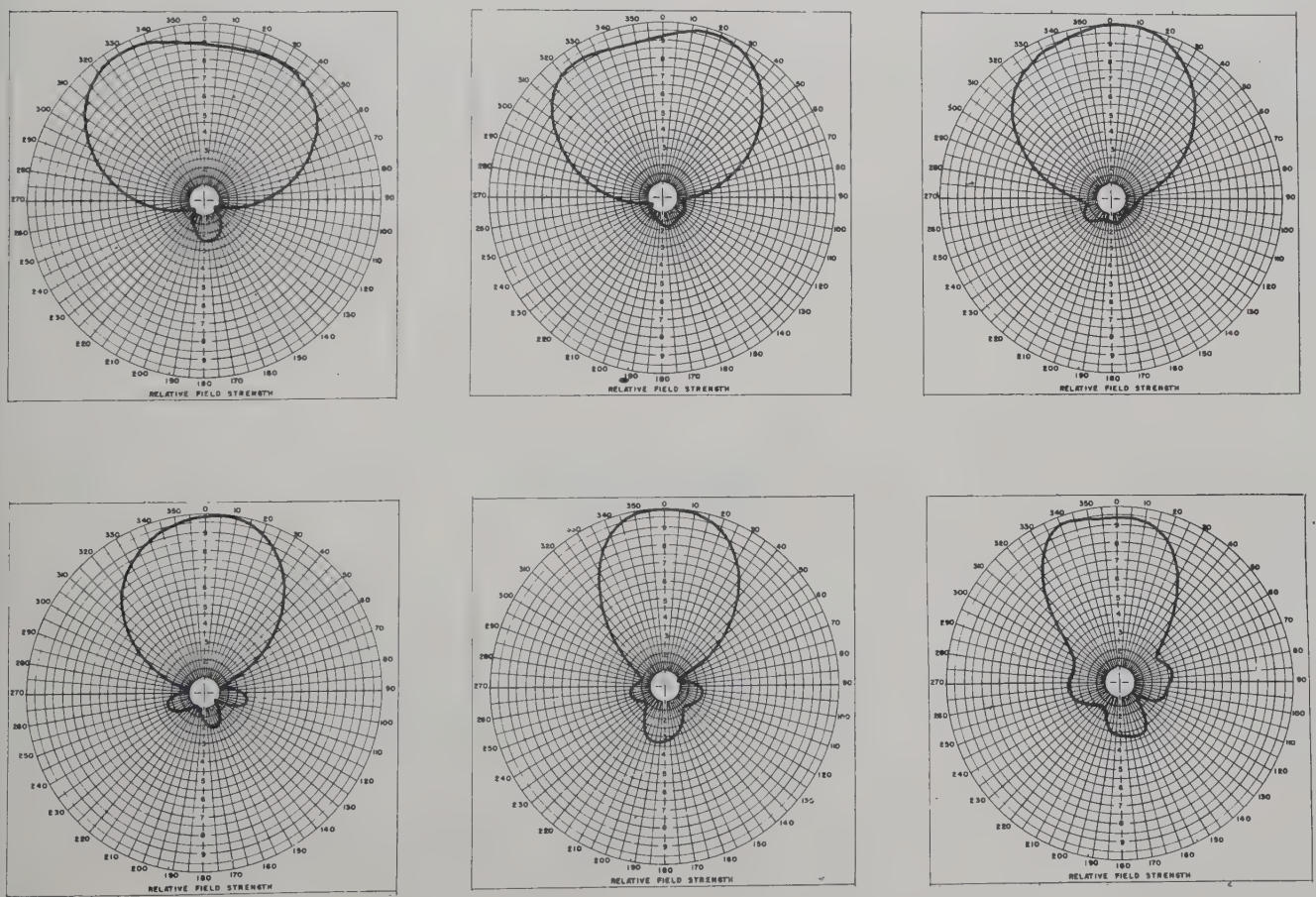

Fig. 10—*H*-plane patterns of series-rhombic antenna.

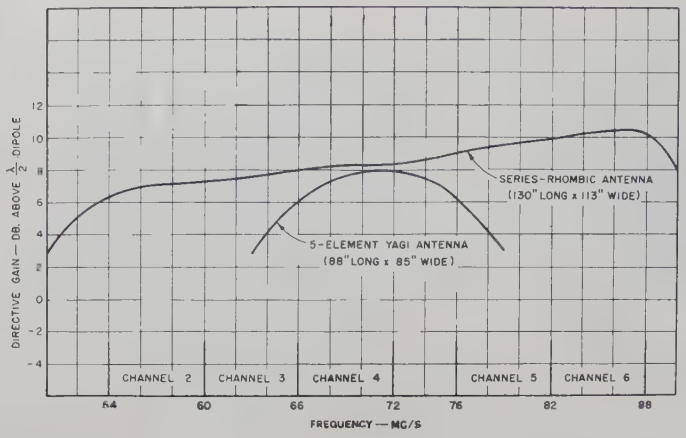

Fig. 11—Gain curve of series-rhombic antenna.

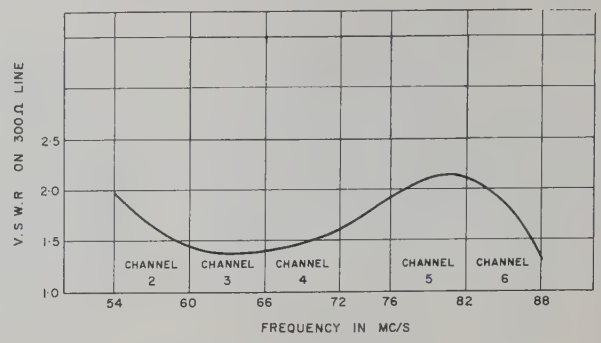

Fig. 12—Match curve of series-rhombic antenna (referred to 300-ohm line).

so that while the absolute gain figures are subject to error, the relative figures are quite reliable. It is seen that this antenna has considerably greater bandwidth than the Yagi, with approximately the same center-frequency gain. This is obtained, however, at the expense of greater physical size.

A measured voltage standing wave ratio curve for the antenna on 300-ohm line is shown in Fig. 12. This curve was obtained by measuring the antenna impedance on a standard slotted line, and computing the voltage standing-wave ratio that this load would produce on twin-lead. The resulting curve is considered to be quite satisfactory for a receiving antenna operating in this frequency range.

Conclusion

While the detailed behavior of this antenna is not yet fully understood, it has been shown that its operation can be partially explained in terms of simple array theory. When the mechanism of propagation along the radiator is more thoroughly understood, it may be possible to load the structure in such a way as to produce a variable velocity of propagation, which in turn would yield a greater bandwidth. In the meantime it has been shown that where gains of from 6 to 10 db are required, a bandwidth of 50 per cent can be readily obtained, and while the prototype antenna has been designed for television applications, it may have other uses in the VHF and UHF bands.

Acknowledgment

This investigation was carried out at the laboratories of the Radio and Electrical Engineering Division, National Research Council of Canada. The author is indebted to Dr. G. A. Miller for his suggestions and guidance concerning this project, and to Mr. J. R. Dawson and Mr. E. P. Deloli for their assistance with pattern and impedance measurements.

Radio Transmission Loss vs Distance and Antenna Height at 100 Mc*

P. L. RICE† AND F. T. DANIEL†

Summary—**This report describes curves of transmission loss vs distance and antenna height derived from an analysis of approximately 159,000 hourly median field-strength observations between 90 and 110 mc. These observations extend over a period of several years and are distributed geographically over the whole United States. The curves contained in this report are believed to be more precise for engineering use than the FCC Ad Hoc Committee curves published in 1949.**

Introduction

THIS REPORT depends upon long-term records of radio transmission loss observed beyond radio line of sight over 44 overland propagation paths. The paths are listed in Appendix I. Prediction curves are derived to represent what might have been obtained if data had been available from each station monitored for twenty-four hours of every day in an average year.

Hourly medians were recorded either as field strengths or in terms of transmission loss, defined as the ratio of total radiated power to the resulting signal power available from a loss-free receiving antenna.[1] Transmission loss is an easily measured, dimensionless quantity which lumps together the gains and losses arising from the characteristics of the transmitting and receiving antennas and the transmission medium.

The effective gains of transmitting and receiving antennas are not always separable into their respective free-space gains G_t and G_r, but sometimes depend upon each other and upon the transmission medium in a very complicated manner.[2] The Booker-Gordon tropospheric radio scattering theory[3,4] was used to derive a "combined effective gain," G_p,[5] of transmitting and receiving antennas. Crude preliminary estimates of the effective loss of antenna gain, $(G_t+G_r-G_p)$, will be found in Fig. 1.

Data and curves in this report are presented in terms of the transmission loss expected between isotropic antennas, called the "basic" transmission loss. Expressing the transmission loss L and the basic transmission loss L_b in decibels, and G_t, G_r, and G_p in decibels relative to an isotropic antenna:

$$G_p \leqq G_t + G_r, \tag{1}$$

and

$$L_b = L + G_p. \tag{2}$$

If it is assumed that the transmitting antenna realizes its free-space gain G_t, then a simple relationship exists between L_b and the field strength E expressed in decibels above one microvolt per meter for one kilowatt of effective radiated power:

$$E = 139.37 + 20 \log_{10} f_{mc} - L_b, \tag{3}$$

where f_{mc} is the frequency in megacycles. When G_t and G_r are not separable, the concepts of field strength and effective radiated power are misleading, since only the ratio of two such quantities can then be determined; neither quantity could be separately determined.

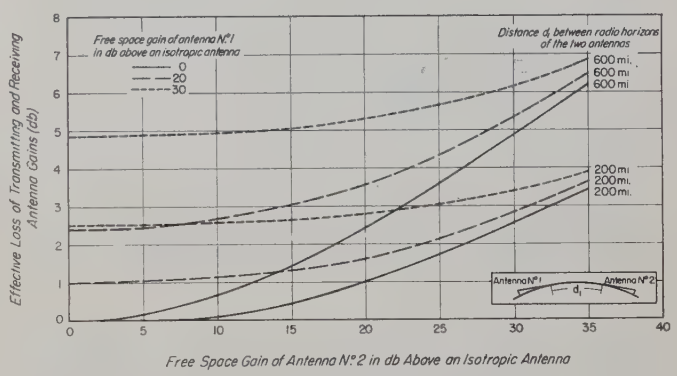

Fig. 1—Tentative estimate of loss of antenna gain relative to the free-space gain.

Description of Data

Transmission loss at certain times is consistently greater than at other times. In order to allow to some extent for such systematic effects, the year was divided into two parts and the day into four parts, making eight "Time Blocks." These are defined in a table in Fig. 3. The hours of the day were divided in the fashion shown mainly because the low point of the diurnal cycle in this type of data usually occurs between 1 P.M. and 6 P.M. The year was divided in half to distinguish between high summer field strengths and low winter fields.

The prediction curves are valid only for a receiving antenna height of 30 feet, but extrapolation to transmitting antenna heights beyond the range of the data was believed to be worthwhile. Where complete terrain profiles were not available, transmitting antenna height was defined as the FCC Ad Hoc Committee defined it:

* Original manuscript received by the PGAP, July 12, 1954; revised manuscript received, December 17, 1954.

† National Bureau of Standards, Boulder, Colo.

[1] K. A. Norton, "Transmission loss in radio propagation," PROC. I.R.E., vol. 41, pp. 146–152; January, 1953.

[2] F. W. Schott, "On the response of a directive antenna to incoherent radiation," PROC. I.R.E., vol. 39, pp. 677–680; June, 1951.

[3] H. G. Booker and W. E. Gordon, "A theory of radio scattering in the troposphere," PROC. I.R.E., vol. 38, pp. 401–412; April, 1950.

[4] H. Staras, "Scattering of electromagnetic energy in a randomly inhomogeneous atmosphere," *Jour. Appl. Phys.*, vol. 23, pp. 1152–1156; October, 1952.

[5] J. W. Herbstreit, K. A. Norton, P. L. Rice, and G. E. Schafer, "Radio Wave Scattering in Tropospheric Propagation," 1953 IRE Convention Record, Part 2, "Antennas and Communications," pp. 85–93.

the average height above terrain two to ten miles from the transmitter in the direction of the receiver. For the lower (receiving) antennas, structural height was chosen to define their effective heights; all but four of these receiving antenna heights were between 20 and 60 feet above ground. All but seven of the transmitting antenna effective heights were between 200 and 700 feet, and these seven ranged from 1,000 to 8,000 feet above a smooth curve fitted to the terrain extending from the antenna to its radio horizon.[6]

Steps in the Analysis

Field strengths exceeded 1, 10, 20, 50, 80, 90, and 99 per cent of the time for each path and time block were determined. Each of these percentage fields was then plotted vs the distance between the four-thirds earth radio horizons of the transmitting and receiving antennas. Fig. 2 is an example of such a graph. There were 56 of these graphs, one for each of the 7 percentage fields in each of the 8 time blocks.

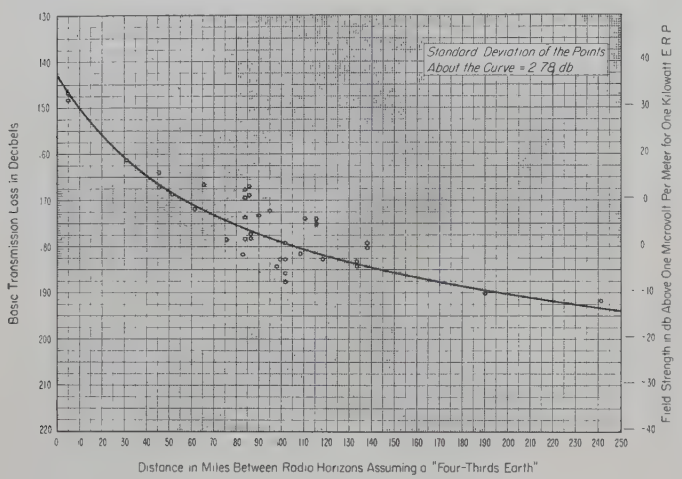

Fig. 2—Transmission loss as a function of distance between the radio horizons of two antennas. Points correspond to the median of all hourly medians recorded between 6 P.M. and Midnight, May through October of a single year.

Next, cumulative distributions were obtained for each of a number of distances and for each time block. A set of cumulative distributions for each of the 8 time blocks and for a distance of 100 miles is shown in Fig. 3. From the 8 cumulative distributions corresponding to each distance, a combined distribution was derived which is believed to be representative of what would have been obtained if data had been available all day and all year from every propagation path. The combined distribution was obtained by averaging the 8 percentages at several convenient levels of transmission loss.

Having thus obtained an estimate of the attenuation to be expected between the radio horizons of any two antennas, without regard to their height or the distance between them, this estimate was then combined with various theories in order to produce tentative semi-empirical height-gain curves by means of which the data could be reduced to standard antenna heights before evaluating their dependence on distance.

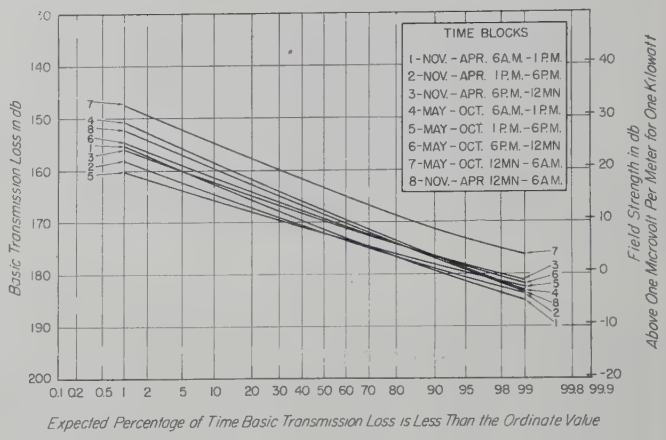

Fig. 3—Expected basic transmission loss at 100 miles and 100 mc. Transmitting antenna height—500 feet; Receiving antenna height—30 feet.

It was tentatively assumed that the attenuation from transmitter to receiver may be considered as the sum of two independent quantities, (a) the attenuation between the radio horizons of the antennas, and (b) the attenuation from the transmitter to its radio horizon plus the atttenuation from the radio horizon of the receiving antenna to the receiver. The estimation of (a) has been described. The quantity (b) was assumed to be the same for antennas which are not within line-of-sight of each other as for antennas which are just barely within line-of-sight of each other, and calculations for this latter situation were made using standard four-thirds earth diffraction theory. In the construction of preliminary height-gain curves for the region beyond line-of-sight, the curves were made to correspond to the quantity (a) plus (b). Within line-of-sight, the curves were made to correspond to the free-space field at a substantial elevation above the radio horizon of one antenna with the other antenna height fixed at 30 feet.

When the distance between the radio horizons of two antennas becomes large, the above tentative assumption is invalid; consequently the Booker-Gordon scattering theory was used for construction of the portions of the preliminary height-gain curves which correspond to points well beyond the horizon of the transmitter.

For each propagation path, the average deviation Δ of data from estimates of L_b obtained from the curves fit through the data in each of the time blocks indicated how much better or poorer than average the path was. An estimate of basic transmission loss for all-day, all-year conditions for each path was obtained by subtracting Δ from the estimate of basic transmission loss

[6] A. P. Barsis, J. W. Herbstreit, and K. O. Hornberg, "Cheyenne Mountain Tropospheric Propagation Experiments," NBS Circular No. 554; January, 1955.

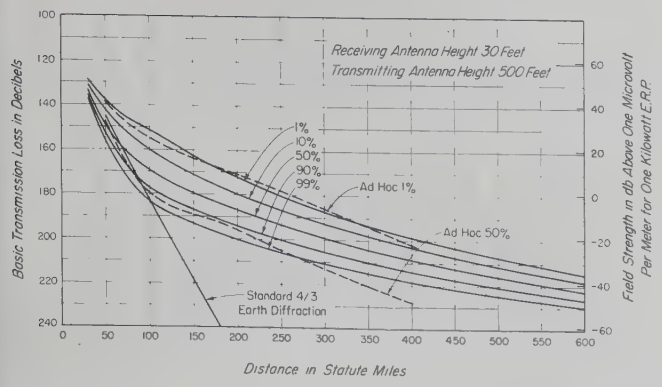

Fig. 4—Expected transmission loss for propagation at 100 mc over land in the United States.

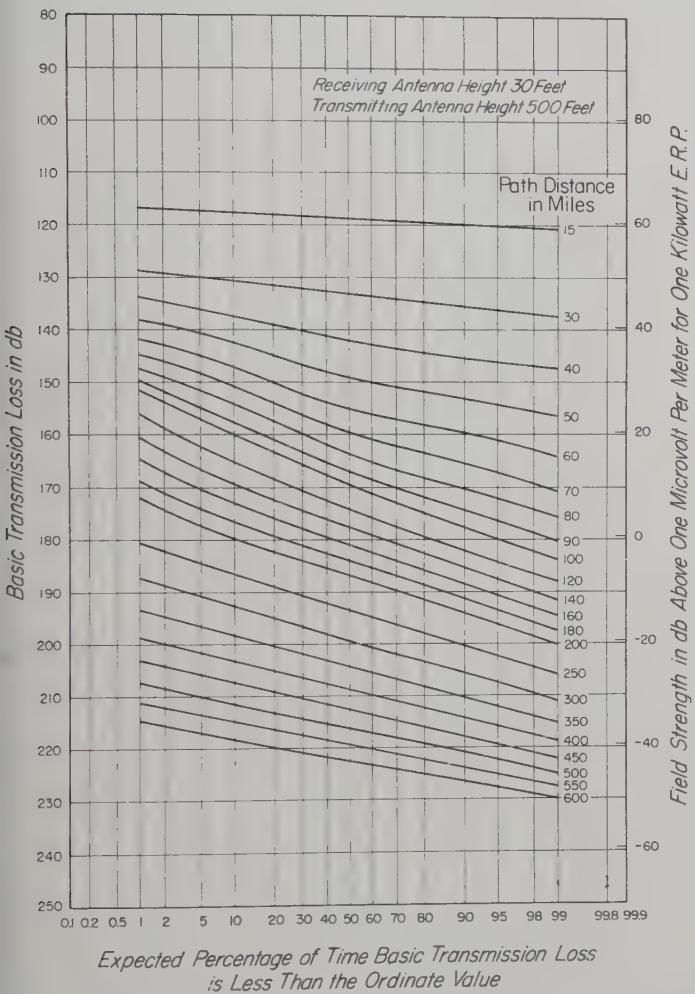

Fig. 5—Expected transmission loss for propagation at 100 mc over land in the United States.

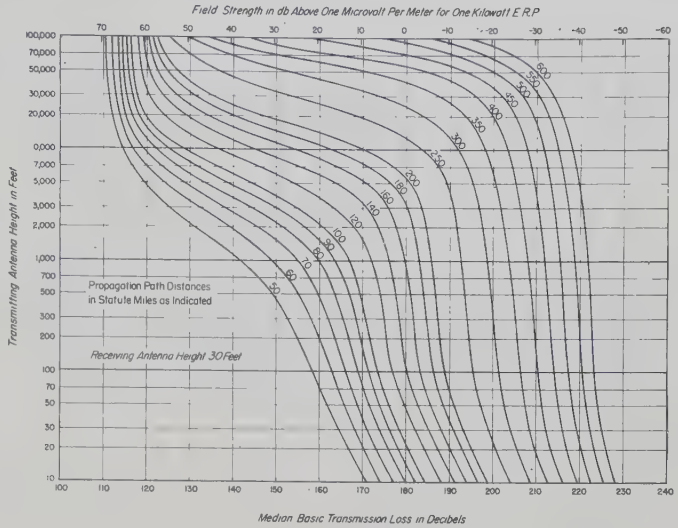

Fig. 6—Median basic transmission loss vs transmitting antenna height and distance at 100 mc.

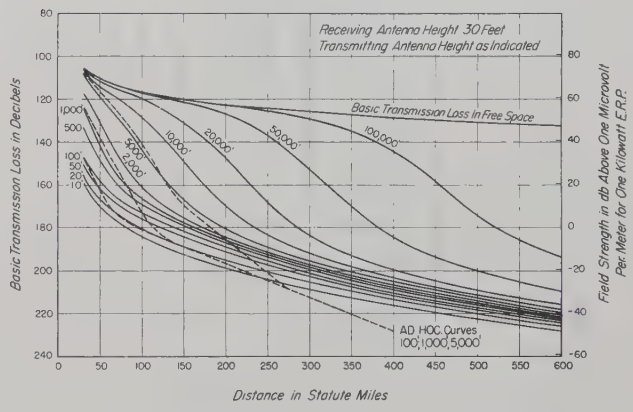

Fig. 7—Expected median transmission loss for propagation at 100 mc over land in the United States.

obtained from the preliminary set of height-gain curves. These data were then plotted vs total path distance after being corrected to standard antenna heights of 500 feet and 30 feet. Curves were drawn for each of the percentage fields (see Fig. 4), and cumulative distributions for each of a number of distances were obtained from these curves. These are shown in Fig. 5.

Considerable additional work was done in order to insure a certain amount of self-consistency to the curves and also to insure that slightly different methods of analysis (such as correcting to some other antenna-height combination) gave substantially the same results. Tentative estimates of height-gain were adjusted (Fig. 6) to agree with final estimates of distance attenuation for various antenna height combinations. These are shown in Fig. 7.

Figs. 4 and 5 show the long-term or "all-day, all-year" variance of hourly medians corresponding to propagation between a 500-foot and a 30-foot antenna. This variance, however, is expected to be essentially a function of the distance d_s between the radio horizons of two antennas:

$$d_s = d - \sqrt{2h_t} - \sqrt{2h} \qquad (4)$$

where d is the total path distance in miles, h_t and h_r are the antenna heights in feet, and d_s is in miles. In order to estimate the variance for a total path distance d and antenna heights h_t and h_r, Fig. 4 or Fig. 5 should be read at a distance equal to $(d_s+39.4)$ miles.

Conclusion

It is believed that Figs. 4 through 7 represent the best available estimates of average distance attenuation and height gain at 100 mc for the United States. They show much less distance attenuation than that calculated using standard smooth-earth diffraction theory, and except for one per cent fields, they show less distance attenuation than the FCC Ad Hoc Committee curves.[7] At distances less than radio line-of-sight, the curves were made to agree with the FCC curves.

Additional detailed information about the data and analysis in this report is available at the National Bureau of Standards and may be obtained by writing the authors.

[7] Report of the Ad Hoc Committee for the "Evaluation of the Radio Propagation Factors Concerning the Television and Frequency Modulation Broadcasting Services in the Frequency Range between 50 and 250 Mc; FCC Mimeos Nos. 36728, May 26, 1949; 36830, May 31, 1949, and 54382, July 7, 1950.

Appendix 1

TABLE I

Path. No.	Transmitter	Receiver
1	KARM, Fresno, Calif.	FCC, Livermore, Calif.
2	KFOR, Lincoln, Neb.	FCC, Grand Island, Neb.
3	KING, Seattle, Wash.	FCC, Portland, Oregon
4	KVCI, Chico, Calif.	FCC, Livermore, Calif.
5	WCAC, Anderson, S. C.	FCC, Powder Springs, Ga.
6	WEEU, Reading, Pa.	FCC, Laurel, Md.
7	WFRO, Fremont, Ohio	FCC, Allegan, Mich.
8	WIP, Philadelphia, Pa.	FCC, Laurel, Md.
9	WMRC, Greenville, S. C.	FCC, Powder Springs, Ga.
10	WTIC, Hartford, Conn.	FCC, Millis, Mass.
11	WEST, Easton, Pa.	Pa. State College, State College, Pa.
12	WJAS, Pittsburgh, Pa.	Pa. State College, State College, Pa.
13	WTOP, Washington, D. C.	Pa. State College, State College, Pa.
14	KXOK, St. Louis, Mo.	Univ. of Ill., Urbana, Ill.
15	WCSI, Columbus, Ind.	Univ. of Ill., Urbana, Ill.
16	WMBI, Chicago, Ill.	Univ. of Ill., Urbana, Ill.
17	WCOL, Columbus, Ohio	United Broadcasting Co., Hudson, Ohio
18	WCOL, Columbus, Ohio	United Broadcasting Co., 20 sites near Hudson, Ohio
19	WHKC, Columbus, Ohio	United Broadcasting Co., Hudson, Ohio
20, 21, 22	WHKC, Columbus, Ohio	United Broadcasting Co., Hudson, Ohio
23	WHKC, Columbus, Ohio	United Broadcasting Co., 20 sites near Hudson, Ohio
24	WKBN, Youngstown, Ohio	United Broadcasting Co., Hudson, Ohio
25	WVKO, Columbus, Ohio	United Broadcasting Co., Hudson, Ohio
26	KDKA, Pittsburgh, Pa.	United Broadcasting Co., Hudson, Ohio
27	KIXL, Dallas, Texas	Univ. of Texas, Austin, Texas
28	KLTI, Longview, Texas	Univ. of Texas, Austin, Texas
29	KPRC, Houston, Texas	Univ. of Texas, Austin, Texas
30	KRBC, Abilene, Texas	Univ. of Texas, Austin, Texas
31	KTSA, San Antonio, Texas	Univ. of Texas, Austin, Texas
32	KWKH, Shreveport, La.	Univ. of Texas, Austin, Texas
33	KXYZ, Houston, Texas	Univ. of Texas, Austin, Texas
34	KYFM/KTSA, San Antonio, Tex.	Univ. of Texas, Austin, Texas
35	WFAA, Dallas, Texas	Univ. of Texas, Austin, Texas
36	CRPL, Cheyenne Mt., Colorado Springs, Colo.	CRPL, Garden City, Kansas
37	CRPL, Cheyenne Mt., Colorado Springs, Colo.	CRPL, Anthony, Kansas
38	CRPL, Cheyenne Mt., Colorado Springs, Colo.	CRPL, Fayetteville, Arkansas
39	CRPL, Camp Carson, Colo.	CRPL, Garden City, Kansas
40	CRPL, Camp Carson, Colo.	CRPL, Anthony, Kansas
41	CRPL, Camp Carson, Colo.	CRPL, Fayetteville, Arkansas
42	CRPL, Pikes Peak, Colo.	CRPL, Garden City, Kansas
43	CRPL, Pikes Peak, Colo.	CRPL, Anthony, Kansas
44	CRPL, Pikes Peak, Colo.	CRPL, Fayetteville, Arkansas

Spacing-Error Analysis of the Eight-Element Two-Phase Adcock Direction Finder*

D. N. TRAVERS†

Summary—**In the design of a modern high-frequency radio direction finder utilizing the Adcock principle, the sensitivity and spacing error limitations of the conventional four-element array requires the use of several arrays in order to cover a large portion of the frequency spectrum. An eight-element array is described which has an operating frequency range considerably greater than that of the familiar Adcock, while still maintaining the simplicity of two-phase goniometer azimuth scanning. Spacing error curves are plotted and an optimum design is selected. It is shown that element spacing values greater than one wavelength are possible, and that frequency coverage is sufficiently great to render considerations other than spacing error the limiting factors.**

List of Symbols

θ = azimuth of signal arrival.
s = diagonal spacing of elements.
$\phi = 2\pi s/\lambda$.
2ρ = angular separation of paired elements.
γ = phase of the emf induced in antenna A.
α = phase of the emf induced in antenna B.
δ = phase of the emf induced in antenna C.
ζ = phase of the emf induced in antenna D.
E_k = emf induced in kth antenna.
E_{NS} = emf output of the north-south quartet.
E_{EW} = emf output of the east-west quartet.
E_0 = amplitude of emf induced in any antenna.
ϵ = observed bearing.
λ = wavelength
Δ = error in observed bearing.

Introduction

ADCOCK antenna arrays have been very successfully used in modern direction finder systems for several decades. Many modifications have been introduced during recent years to improve accuracy, but until very recently little attention has been directed toward extending the frequency range of the array.

It is a well established fact that the familiar four-element Adcock array is limited in frequency coverage by decreasing sensitivity at the lowest operating frequency and octantal spacing error at the highest frequency.[1–3] Within these limits reliable frequency coverage in excess of a six-to-one frequency range is almost impossible without poor performance. This condition is particularly restricting since it necessitates employing a multiplicity of widely displaced direction-finding arrays to cover a representative portion of the spectrum.

In recent years a number of suitable designs have been investigated which appreciably reduce the spacing error and thereby increase the possible operating bandwidth. These designs have in each case accomplished the error reduction by the addition of extra antennas in arrangements which modify the normal geometry of the array. A general treatment of the entire subject of multi-element Adcock arrays was given by Redgment, Struszynski and Phillips in 1947.[1] It is the purpose of this paper to call attention to a particular design of this type which incorporates eight antennas unequally spaced on a circle, and connected for conventional two phase goniometer azimuth scanning.

The Spacing Error Equation

The array configuration is shown in Fig. 1. The eight antennas are disposed on a circle and fed by transmission lines which are shown by double lines. T-connectors are employed at the four indicated junction points to provide parallel connection of the two paired antennas. In this manner only four transmission lines are required to feed the array allowing the use of a conventional two-phase goniometer.

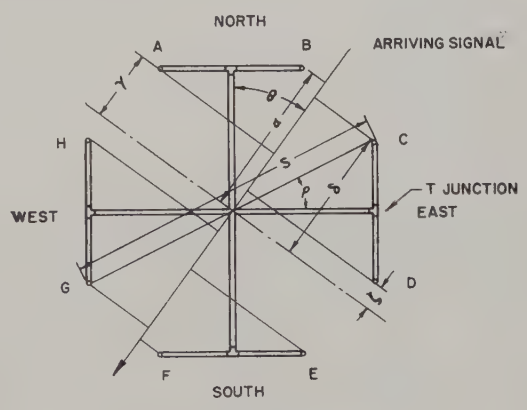

Fig. 1

Choosing the center of the array to be the point of zero phase, and noting that the differential connection is used, the output voltage of the north-south quartet will be

$$E_{NS} = E_A + E_B - (E_E + E_F). \quad (1)$$

* Original manuscript received by the PGAP, June 2, 1954; revised manuscript received, November 8, 1954.
† Southwest Research Institute, San Antonio, Texas.
[1] P. G. Redgment, W. Struszynski, and G. J. Phillips, "An analysis of the performance of multi-aerial Adcock direction-finding systems," *Jour. IEE*, vol. 94, Part IIIA, pp. 751–761; 1947.
[2] James G. Holbrook, "An analysis of errors in long range radio direction-finding systems," Proc. I.R.E., vol. 41, pp. 1747–1749; December, 1953.
[3] R. Keen, "Wireless Direction Finding," Iliffe and Sons, Ltd., London, England; 1947.

The phase relations between these voltages are evident from the array geometry, and are

$$\gamma = \frac{\phi}{2}\cos(\rho+\theta) \tag{2}$$

$$\alpha = \frac{\phi}{2}\cos(\rho-\theta). \tag{3}$$

Hence it follows that

$$E_{NS} = E_0\left[e^{j\phi/2\cos(\rho+\theta)} + e^{j\phi/2\cos(\rho-\theta)} - e^{-j\phi/2\cos(\rho+\theta)} - e^{-j\phi/2\cos(\rho-\theta)}\right]; \tag{4}$$

or

$$\frac{E_{NS}}{2jE_0} = \sin\left(\frac{\phi}{2}\cos(\rho+\theta)\right) + \sin\left(\frac{\phi}{2}\cos(\rho-\theta)\right). \tag{5}$$

By trigonometric substitution this becomes

$$\frac{E_{NS}}{2jE_0} = 2\sin\left(\frac{\phi}{2}\cos\rho\cos\theta\right)\cos\left(\frac{\phi}{2}\sin\rho\sin\theta\right). \tag{6}$$

Similarly, by noting the phase relationships of the east-west antennas the output voltage of this quartet becomes

$$\frac{E_{EW}}{2jE_0} = 2\sin\left(\frac{\phi}{2}\cos\rho\sin\theta\right)\cos\left(\frac{\phi}{2}\sin\rho\cos\theta\right). \tag{7}$$

When these voltages are combined in the goniometer the observed bearing is ϵ, where

$$\operatorname{Tan}\epsilon = \frac{E_{EW}}{E_{NS}} = \frac{\sin\left(\frac{\phi}{2}\cos\rho\sin\theta\right)\cos\left(\frac{\phi}{2}\sin\rho\cos\theta\right)}{\sin\left(\frac{\phi}{2}\cos\rho\cos\theta\right)\cos\left(\frac{\phi}{2}\sin\rho\sin\theta\right)}. \tag{8}$$

The error is then

$$\Delta = \epsilon - \theta \tag{9}$$

There are two special cases of interest in (8).

1. When $\rho = 0$ degrees the configuration reduces to that of a conventional four element Adcock, or,

$$\tan\epsilon = \frac{\sin\left(\frac{\phi}{2}\sin\theta\right)}{\sin\left(\frac{\phi}{2}\cos\theta\right)}. \tag{10}$$

This is the well known octantal error formula for the four element Adcock.[2-3]

2. When the spacing between elements becomes small, or $s \ll \lambda$, both (8) and (10) reduce to

$$\tan\epsilon \approx \tan\theta, \tag{11}$$

in which case the error will be negligible. In the following section it is shown that in the eight element arrangement there is a particular value for ρ which will allow s to reach a value in excess of λ and still maintain the condition of (11) for all azimuths.

Spacing Error Curves

It is evident that (9) will reduce to zero when θ equals any multiple of $\pi/4$. In general the curve will be octantal and will reach maximum values of positive and negative error between zero and $\pi/4$. Fig. 2 has been plotted to determine the behavior of the error curve with respect to azimuth. For these curves the frequency was chosen so that $\phi = 6.8$ or $s = 1.08\lambda$, values which are considerably beyond the range of a four-element array. It can be seen that for values of ρ near 27 degrees an additional point of zero error is introduced in the vicinity of $\theta = 20$ degrees. The value of 27 degrees 15 minutes indicates that less than two degrees of error can be realized.

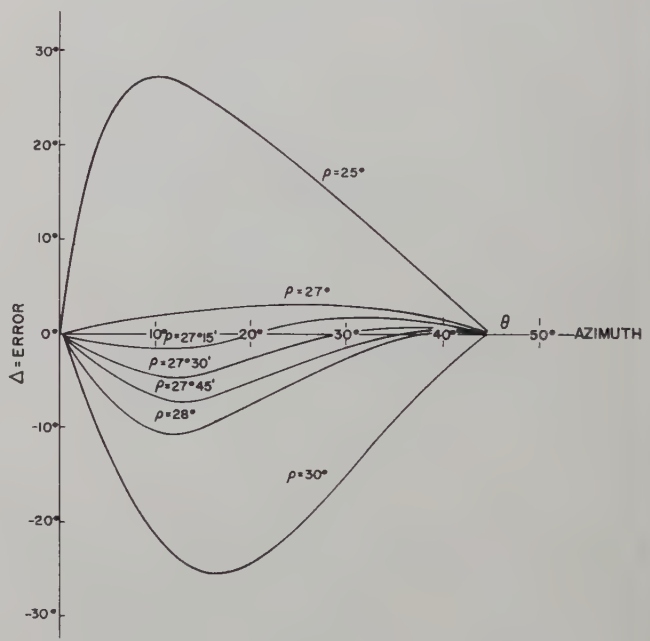

Fig. 2

In Fig. 3 the error has been plotted vs the spacing expressed in terms of s/λ units at the azimuth of $\theta = 20$ degrees. It can be seen that as the frequency is increased the spacing error slowly increases, reaches a maximum and suddenly drops off with a rapid increase in error. The optimum selection of ρ will then be a compromise between the maximum error which can be tolerated and the desired high-frequency limit. A value of ρ between 27 degrees and 27 degrees 15 minutes appears to be a good compromise and will permit operation up to a spacing of $s = 1.1\lambda$ without encountering serious error.

Similar curves can be plotted at the other azimuths of interest but unless the maximum possible bandwidth is

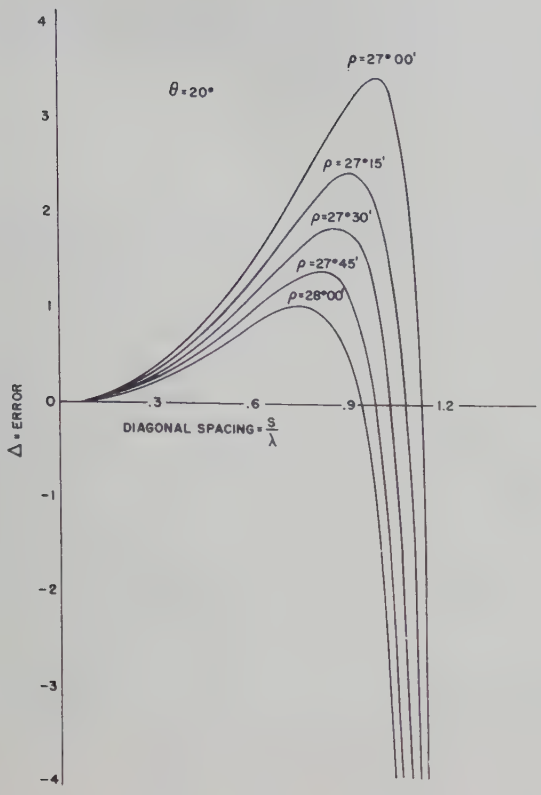

Fig. 3

desired it will not generally be profitable to produce the curves. For spacings below $s=\lambda$ the curves are low-valued and are not sensitive to either frequency or azimuth with proper selection of ρ. It has been established that the ultimate spacing obtainable in any multi-element Adcock is $s=1.22\lambda$,[1] which indicates that no more than a marginal improvement beyond the suggested values can be obtained by a more detailed analysis of (9).

Conclusions

The conventional four-element Adcock array is restricted in frequency range by the reduced accuracy caused by octantal spacing error at the high end of the band. This error is a function of the array geometry and by proper modification through the use of extra elements it can be considerably reduced.

A particular design which accomplishes this uses eight antennas distributed on a circle with alternate angular separations of 54 degrees and 36 degrees. With this configuration octantal error is kept to a very low value for all spacings up to approximately 1.1λ. The corresponding value for the four element array is about one-third wavelength.

The resulting increase in bandwidth permits operation over a twenty-to-one frequency range without undue loss of sensitivity or high octantal error. This is so wide, in fact, that other considerations such as antenna impedance or vertical pattern may limit the bandwidth.

Acknowledgment

The two-phase eight-element Adcock direction finder was first suggested by Mr. A. F. L. Rocke and is mentioned in Reference 1.

The End Correction for a Coaxial Line When Driving an Antenna over a Ground Screen*

RONOLD KING†

Summary—**Theoretical and experimental results obtained by Hartig[1] for the end correction for a coaxial line when driving an antenna over a ground screen are corrected. Improved theoretical and experimental curves of the quantity $-C_T/bc_0$ are obtained, where $-C_T$ is the lumped negative capacitance required as end correction, c_0 is the capacitance per unit length of the coaxial line, and b is the inner radius of the outer conductor of the line.**

CONSIDER a cylindrical antenna of length h that is the extension of the inner conductor of a coaxial line through a hole in a ground screen that is highly conducting and of great extent. As shown in Fig. 1, the radius a of the antenna is also the radius of the inner conductor of the line; the radius b of the hole in

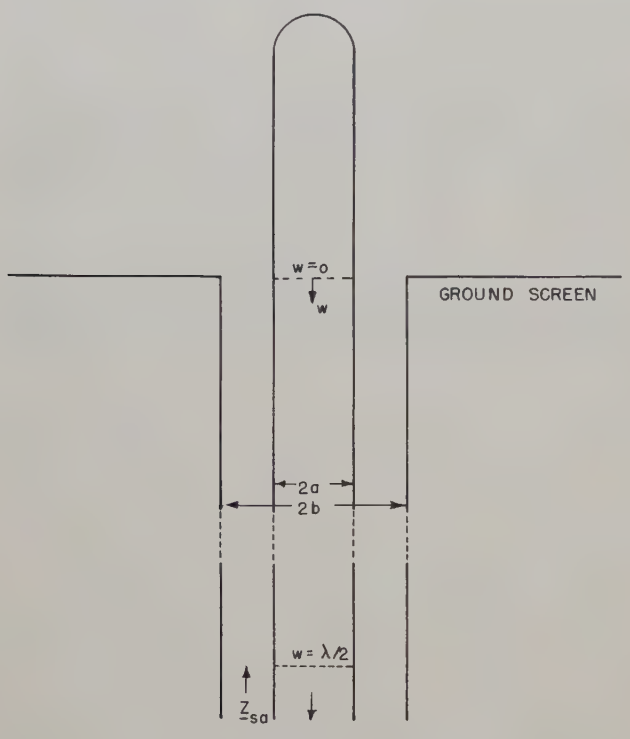

Fig. 1—Antenna driven from coaxial line.

the ground screen is also the inner radius of the coaxial sheath. The admittance apparently loading the line at its end $z=s$ or $w=s-z=0$ is Y_{sa}; with perfect conductors it is the admittance looking toward the load at $w=\lambda_0/2$.

Conventional transmission-line formulas are based on the assumptions that the charges per unit length $q(w)$ on the two conductors of the line at a given cross section w are equal and opposite; that the capacitance per unit length, defined as $c(w)=V(w)/q(w)$, is equal to the constant capacitance per unit length, c_0, characteristic of an infinitely long line for all values of w. These are good approximations at distances d (from the junctions of antenna and line at $w=0$) that are large compared with $b-a$. Near $w=0$, on the other hand, $q(w)$ is not exactly equal and opposite on the two conductors, and $c(w)$ is not constant. Note that since interest is in the current and charge on the antenna and inner conductor, $c(w)$ must be defined in terms of the charge per unit length on the inner conductor. Changes in $q(w)$ near $w=0$ and variations in $c(w)$ from c_0 are consequences of transmission-line end-effect and of essentially capacitive coupling between the line on the one hand and the antenna and ground screen on the other.

The ideal admittance $Y_0=1/Z_0$ of the antenna as calculated theoretically according to the King-Middleton method assumes the antenna to be driven by a discontinuity in scalar potential at $w=0$. The so-called "gap problem" associated with the cylindrical antenna is discussed in the literature[2-4]. The relation between Y_0 and Y_{sa} may be expressed approximately as follows:

$$Y_{sa} \to Y_0 \quad \text{as} \quad b/a \to 1 \tag{1}$$

$$Y_{sa} \doteq Y_0 + j\omega C_T; \quad b/a > 1, \tag{2}$$

where

$$C_T \doteq \int_0^d [c(w) - c_0]dw. \tag{3}$$

and $d \approx 10b$ includes the principal range over which $c(w) - c_0$ is significant.

Evidently, if use is to be made of the theoretical admittance Y_0 in conjunction with the measurable admittance Y_{sa}, knowledge of C_T is necessary. C_T may be determined experimentally or theoretically.

The experimental determination of C_T may be carried out by measuring the apparent susceptance B_{sa} as a function of the length h of the antenna over a range near antiresonance defined by $B_{sa}=0$. By repeating these measurements for a number of values of the ratio b/a and plotting B_{sa} as a function of $\beta_0 h=2\pi h/\lambda_0$ with b/a

* Original manuscript received by the PGAP, February 5, 1954; revised manuscript received November 8, 1954. The research reported in this document was made possible through support extended Cruft Laboratory, Harvard University, jointly by the Navy Department (Office of Naval Research); the Signal Corps of the U. S. Army; and the U. S. Air Force, under ONR Contract N5ori-76, T.O. 1.

† Cruft Laboratory, Harvard University, Cambridge, Massachusetts.

[1] E. O. Hartig, "Circular Apertures and Their Effects on Half-Dipole Impedances," Cruft Lab. Tech. Rep. No. 107; June, 1950.

[2] R. King, "The Gap Problem in Antenna Theory," Cruft Lab. Tech. Rep. No. 194; December 21, 1953. To be published in the *Jour. Appl. Phys.*

[3] P. A. Kennedy and R. King, "Experimental and Theoretical Impedances and Admittances of Center-Driven Antennas," Cruft Lab. Tech. Rep. No. 155; April 1, 1953.

[4] R. W. P. King, "Theory of Linear Radiators," Harvard University Press, Cambridge, Mass; in press.

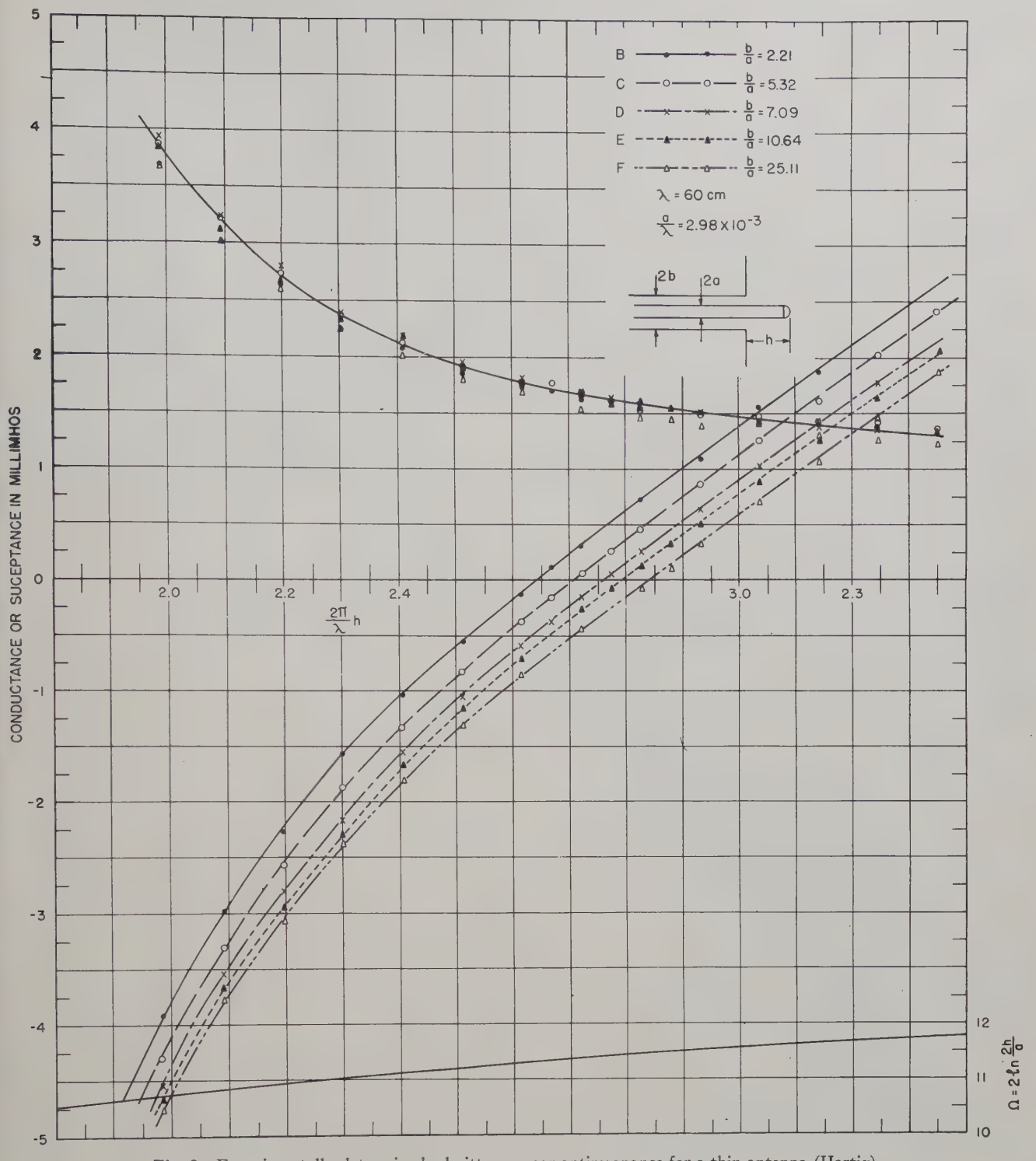

Fig. 2—Experimentally determined admittance near antiresonance for a thin antenna (Hartig). Upper curve G, lower curves B in $Y=G+jB$.

as a parameter, a family of nearly straight lines is obtained. Curves of this sort are reported by Hartig and are shown in Figs. 2 and 3, above and on page 24. The value of $\beta_0 h$ for antiresonance (defined by $B_{sa}=0$) may be taken from each curve and plotted as a function of b/a. The curve defined by these points may then be extrapolated to $b/a=1$ in order to locate $\beta_0 h$ (antiresonant) for B_0. Curves of this sort for four values of a/λ_0 are in Fig. 4 (page 69). With B_0 determined as a function of $\beta_0 h$ at antiresonance, it is possible to construct a curve of B_0 (as a function of $\beta_0 h$), near antiresonance, by drawing the curve parallel to the members of the family of experimental curves for

$$B_{sa}\left(\frac{b}{a}>1\right).$$

With the point $B_0=0$ determined as a function of $\beta_0 h$, the value of ωC_T for each value of b/a for which B_{sa} is available, is obtained at once from the relation

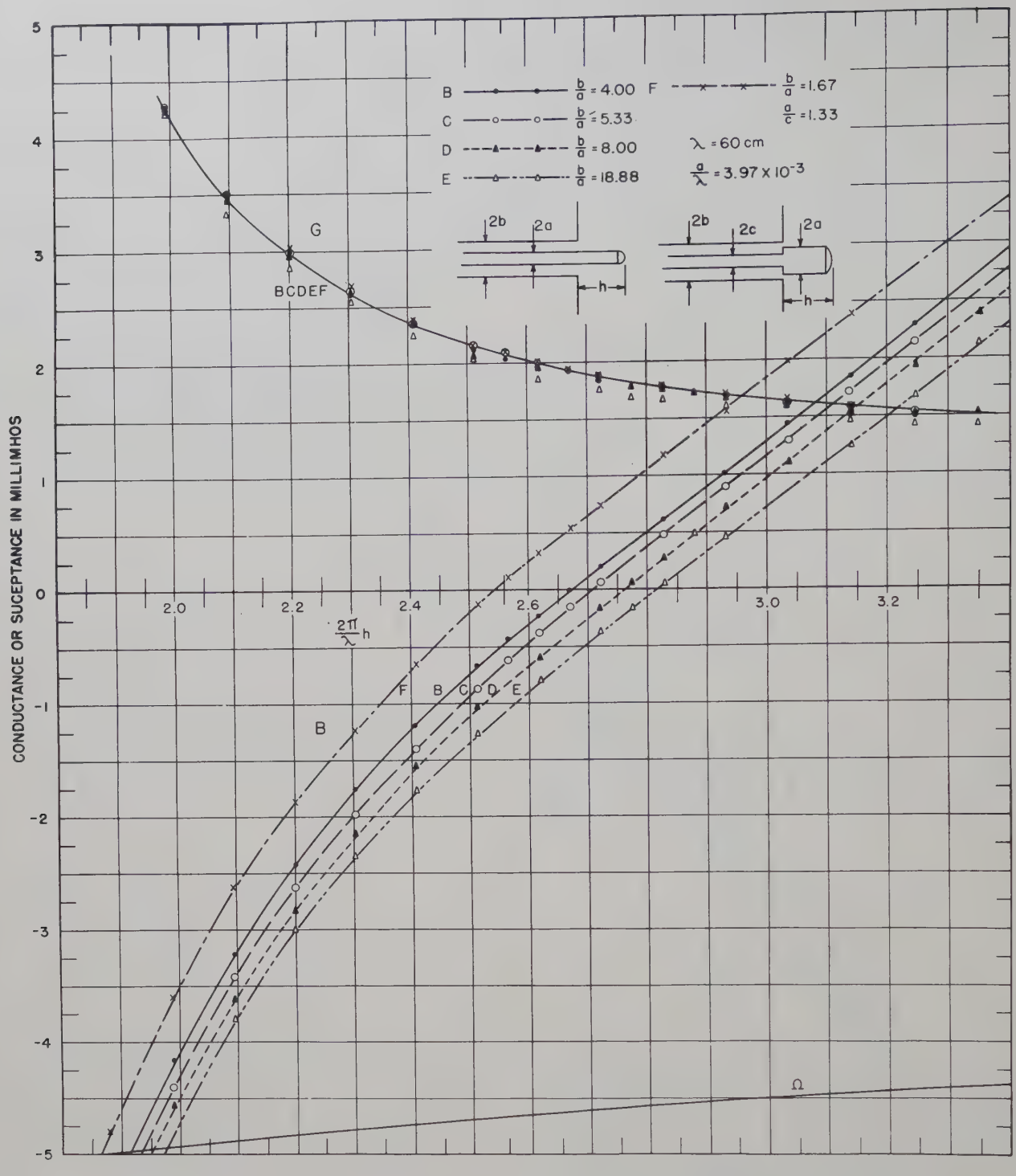

Fig. 3—Experimentally determined admittance near antiresonance for a moderately thin antenna (Hartig).

$$\omega C_T = B_{sa} \text{ (at } \beta_0 h \text{ for } B_0 = 0). \quad (4)$$

Values of C_T obtained in this manner *entirely from measurements* are in Table I for two values of a/λ_0. These values differ somewhat from those obtained by Hartig since they have been determined using the antiresonant value of $\beta_0 h$ obtained by extrapolating measured values of B_{sa} instead of the theoretical value of $\beta_0 h$ (antiresonant). For thin and moderately thin antennas the difference between these values is not great (as seen in Fig. 4), but still sufficient to show the experimentally determined values of C_T to be more self-consistent than was apparent in Hartig's report. Fig. 5 (page 70) gives experimentally determined values of $-C_T$.

TABLE I
MEASURED AND THEORETICAL TERMINAL-NETWORK CAPACITANCES

$a = 1.79 \times 10^{-3}$ m			$a = 2.38 \times 10^{-3}$ m		
b/a	C_T(theor.)	C_T(meas.)	b/a	C_T(theor.)	C_T(meas.)
2.21	−0.048 μμf	−0.048 μμf			
5.32	−0.111	−0.118	4.0	−0.127 μμf	−0.159 μμf
7.09	−0.123	−0.184	5.33	−0.147	−0.223
10.64	−0.139	−0.223	8.00	−0.186	−0.270
25.11	−0.193	−0.264	18.88	−0.226	−0.366

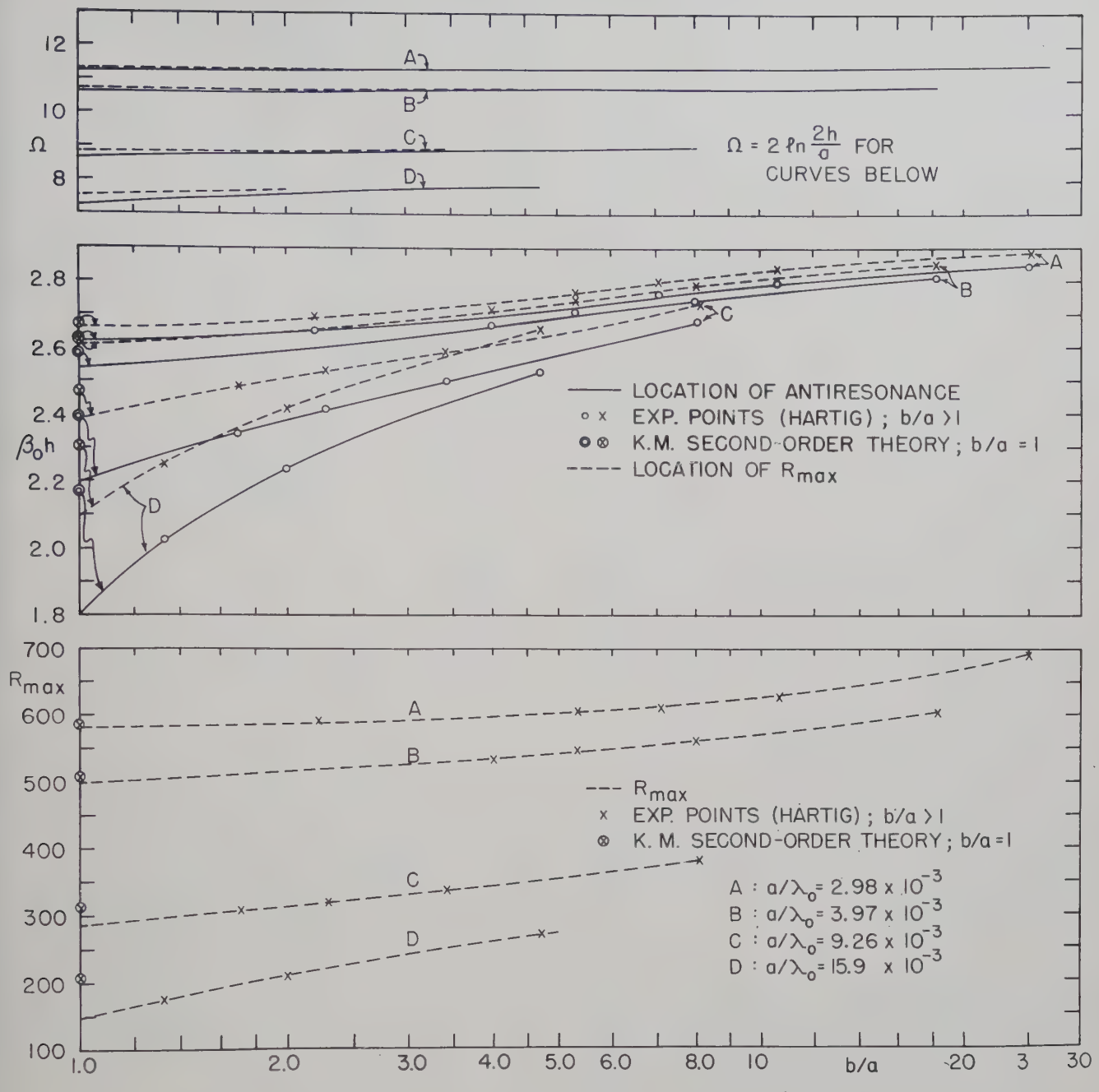

Fig. 4—Summary of critical values of antenna impedance near antiresonance.

A rigorous theoretical analysis to determine the admittance Y_{sa} does not involve Y_0 or C_T. However, since such an analysis is unavailable, the approximate evaluation of Y_{sa} using Y_0 and C_T is convenient. C_T may be calculated from (3) if $c(w)$ can be determined. This can be accomplished approximately by calculating the scalar potential difference V at a distance w from the end of the line (Fig. 1) with assumed zeroth-order distributions of charge on the line, the antenna, and the ground screen. Hartig carried out such an evaluation[1] by using the integral

$$\phi(z) = \frac{1}{4\pi\epsilon_0} \int q(z') \frac{e^{-j\beta_0 R}}{R} dz' \qquad (5)$$

for the scalar potential on the surface of the antenna. In (4), $R = \sqrt{(z-z')^2+a^2}$ is the distance from a point *on the axis* of the conductor at z' to the point of calculation at z on its surface. Similar integrals are used to obtain the contributions from charge distributions on the outer conductor and the ground screen. Actually, (5) is a good approximation of $\phi(z)$ *only* if the integration is extended over distances that are at least $5a$ in both directions from the point w.[4,5] Since the difference $c(w)-c_0$ is actually significant only over a range of w from zero to very small integral multiples of $b-a$, it is clear that in order to have $b-a$ greater than $5a$, b/a must be at least as great as 7. This fact was ignored by Hartig. Theoretical curves of $-C_T$ as evaluated using the approximate

[5] O. Zinke, "Grundlagen der Strom- und Spannungsverteilung auf Antennen," *Arch. für Elecktrotech.*, vol. 35, no. 2 p. 67; 1941.

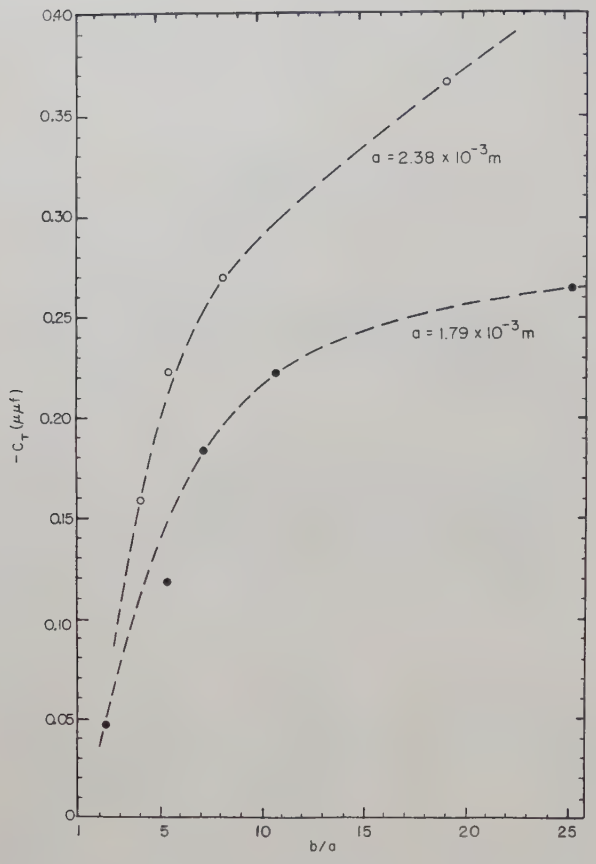

Fig. 5—Experimental end correction for coaxial-line driving an antenna.

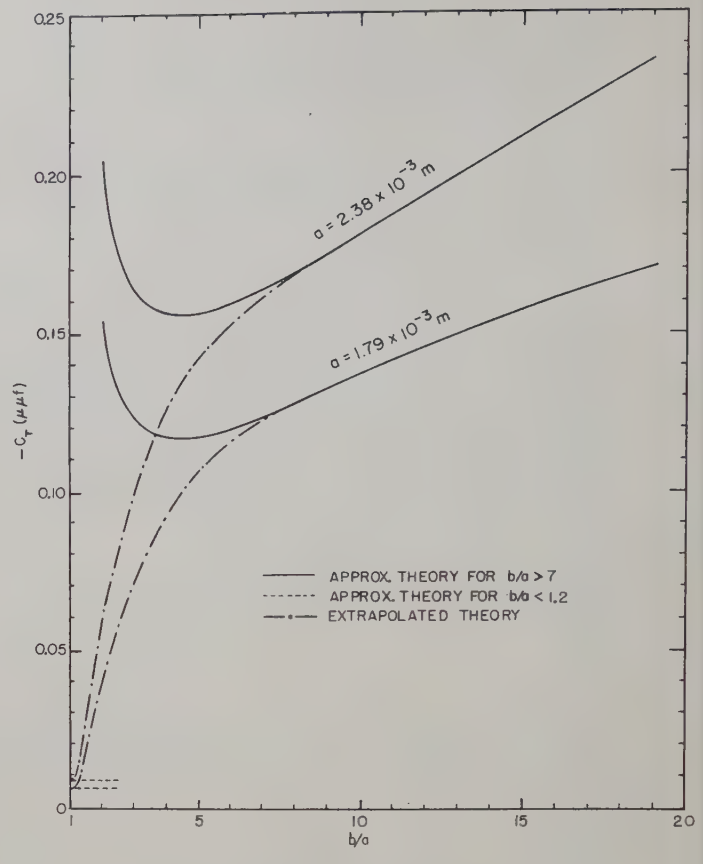

Fig. 6—Theoretical end correction for coaxial-line driving an antenna.

integral given by Hartig (Reference 1, (5.28) with (5.31)) are in Fig. 6 in solid line. They are shown over a range of values of b/a from 2 to 20, but it is to be expected that they become poorer approximations rapidly as b/a is reduced below about 7.

In order to obtain an expression for $-C_T$ for values of b/a quite near one, it is well to note that when $b-a$ is small compared with a and b, the potential at any point in the coaxial line is determined principally by the charges on the adjacent parallel surfaces so that they may be represented approximately by *parallel planes*, i.e., cylinders of infinite radius instead of sections of circular cylinders. Moreover, since $(b-a)/\lambda/_0$ is necessarily very small compared with unity, the distribution of charge near $w=0$ must correspond essentially to an electrostatic one. This suggests determining C_T for a coaxial line with $b-a$ very small by representing the coaxial line by a parallel-plate region extending from $w=0$ to $w=\infty$ and with plates separated a distance $b-a$. One of the plates extends over the range from $-\infty \leqq w \leqq \infty$; the other makes a right-angle bend at $w=0$ and then continues to $x=\infty$, (Fig. 7).

The distribution of surface charge η on both the straight and the bent plates may be determined by conformal transformations using the Schwarz-Chistoffel mapping. The solution of interest in the problem at hand is the distribution of charge on the straight plate in the range from $w=0$ to $w=\infty$ where it is parallel to the second plate. It is this range which corresponds to the inner conductor of the coaxial line when this has an infinite radius. The static distribution of charge may be obtained by applying a potential difference V across the two plates. The transformations involved in the solution for the charge η are described in the literature.[6-8] The pertinent result is the ratio of charge density $\eta(w)$ on the straight plate (at a distance w from the plane $w=0$ where the second plate is bent) to the charge density $\eta(\infty)$ sufficiently far into the parallel-plate region so that a constant value is reached. This ratio is

$$\frac{\eta(w)}{\eta(\infty)} = \frac{1}{\sqrt{1-t}}, \tag{6a}$$

where the relation

$$\frac{w}{b-a} = \frac{1}{\pi}\left[2\sqrt{1-t} - \ln\left(\sqrt{1-t}+1\right) + \ln\left(\sqrt{1-t}-1\right)\right]; \quad t \leqq 0 \tag{6b}$$

obtains. A plot of $\eta(w)/\eta(\infty)$ as a function of $w/(b-a)$ is in Fig. 7 for the part of the straight plate that forms half of the parallel-plate region near $w=0$. Note that the

[6] J. J. Thomson, "Recent Researches in Electricity and Magnetism," Oxford, Clarendon Press, Eng., pp. 225 ff.; 1893.
[7] E. Weber, "Electromagnetic Field," vol. 1, John Wiley and Sons, Inc., New York, p. 344; 1950.
[8] L. V. Bewley, "Two-dimensional Fields in Electrical Engineering," The Macmillan Co., New York, pp. 13 ff.; 1948.

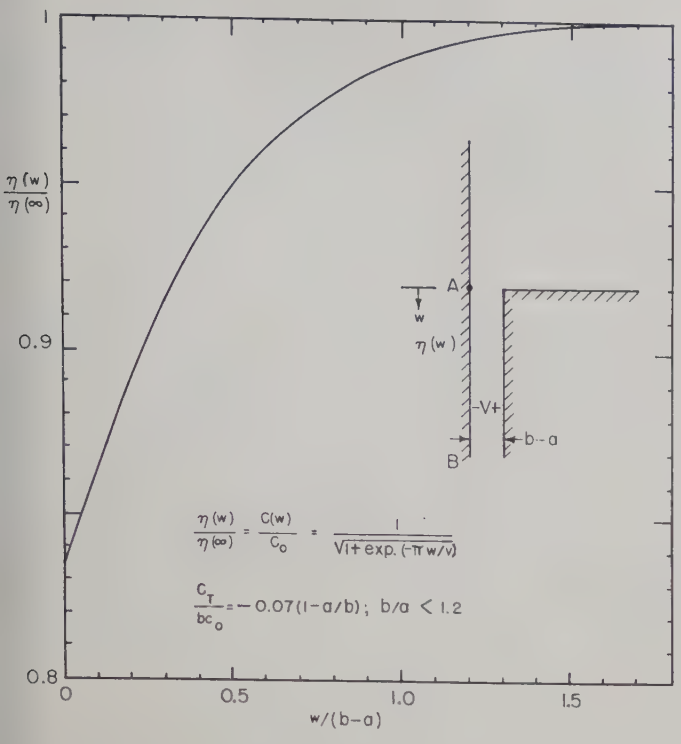

Fig. 7—Charge density distribution on plane AB

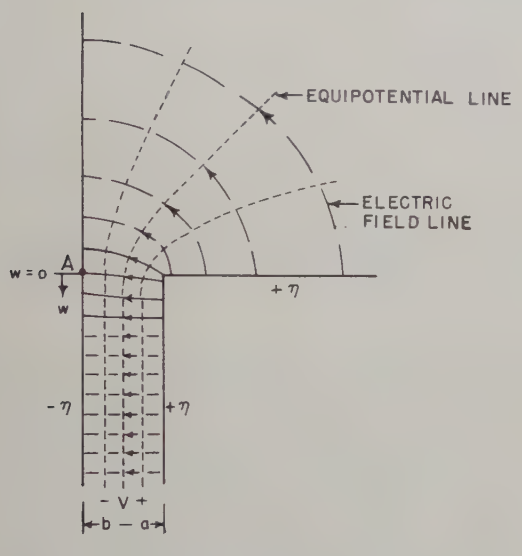

Fig. 8—Equipotential lines and lines of electric field.

charge density on this plate *decreases* as w approaches zero, whereas on the corresponding part of the bent plate, it is readily shown that the density of charge increases as $w=0$ is approached from within the parallel-plate region. A representation of the electric field lines and the equipotentials is in Fig. 8. It is significant to note that the electric lines are curved near $w=0$ so that the electric line which ends at A (Fig. 8) on the straight plate, originated at a point within the parallel-plate region that is not at $w=0$.

Since V is the *constant* potential difference, it follows that

$$\frac{\eta(w)}{\eta(\infty)} = \frac{c(w)}{c_0}, \tag{7}$$

where c_0 is the capacitance per unit length of an infinitely long line. Hence Fig. 7 is also a measure of change in capacitance per unit length as w approaches zero from ∞.

In order to determine the lumped capacitance C_T required to compensate for the error made in using c_0 instead of $c(w)$ even near $w=0$, it is necessary to form (3) and to choose d sufficiently great so that $c(d)=c_0$. The graphical evaluation of C_T from Fig. 7 gives

$$C_T \doteq -0.0683(2\pi a\epsilon_0) = -3.8a\ \mu\mu f. \tag{8}$$

For the two values of a involved in Fig. 6, $C_T=-0.0068$ $\mu\mu f$ for $a=1.79\times10^{-3}m$ and $C_T=-0.0090$ $\mu\mu f$ for $a=2.38\times10^{-3}m$. These are the limiting constant values which are good approximations for $b/a<1.2$. They are shown in Fig. 6.

With approximate theoretical values available for $b/a>7$ and for $b/a<1.2$, it is possible to construct smooth, continuous curves for the range of b/a between 1.2 and 7. Such curves are in Fig. 6. A comparison of the theoretical curves of Fig. 6 with the experimental ones in Fig. 5 shows a good agreement in shape and relative position. However, the theoretically determined values of $-C_T$ are somewhat smaller. This is also clear from Table I.

A good intercomparison of theoretical and experimental curves is obtained if the quantity $-C_T/bc_0$ is plotted against the logarithm of b/a or against b/a on a logarithmic scale. This ratio yields a single curve for all values of a/λ_0. For the range $b/a<1.2$ the formula is $C_T/bc_0=-0.0068\ (1-a/b)$. The two ranges of the theoretical curve and the extrapolated curve joining them are in Fig. 9 together with the experimental values (corrected) obtained by Hartig. Note that both of the extrapolated theoretical curves in Fig. 6 yield a single curve in Fig. 9. This is a check on the shape of the curves in Fig. 6.

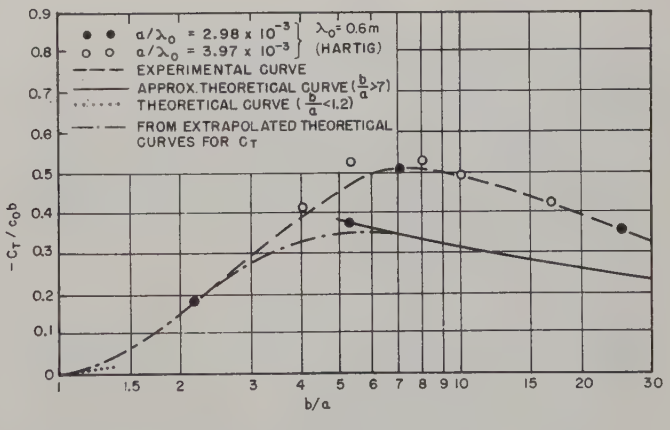

Fig. 9—Capacitive end effect correction for antenna driven from coaxial line.

It is clear from Fig. 9 that the result of the *approximate* theoretical analysis is a reasonable representation

of the capacitive end-effect of a coaxial line when this is used to drive an antenna as in Fig. 1. Since the experimental determination of the very small capacitance C_T involves several possible sources of error, it may not be concluded that the entire difference between theoretical and experimental results is necessarily a consequence of the approximate nature of the theory. Experimental errors may be as great as the theoretical ones. In view of the fact that the difference between experiment and theory corresponds to a difference in length along the coaxial line of only $0.001\lambda_0$ to $0.002\lambda_0$, it is clear that for most practical applications it is adequate to use either the theoretical or the experimental curves in Fig. 9.

The practical importance of an understanding of the end-correction described in this paper is well illustrated by a recent experimental study of the input impedance of thick cylindrical antennas.[9] In that study an attempt was made paralleling that of Hartig[1] to obtain a complete set of curves of the experimentally determined impedance of a cylindrical antenna over a wide range of thicknesses and lengths, the impedances to be so defined as to be independent of end effects. Instead of accomplishing this by extrapolating the measured impedances for different values of b and a to the ideal limiting value at $(b/a)=1$ (as was done by Hartig[1] and by Kennedy and King,[3]) Ehrenspeck[9] assumed that the end-effect is the same when the coaxial line has an open end as when its inner conductor is extended to form an antenna. Since C_T for the open end is *positive* its effect could be cancelled by a shunt inductance across the open end. This compensating inductance was then left in place as compensation for the end effect with an antenna as load. Unfortunately, as the theoretical and experimental results in Fig. 9 show, C_T for the line with the antenna as load is *negative*. It would have to be compensated by a positive shunt capacitance, not by an inductance. It follows that "compensated" impedance measurements of Ehrenspeak have little meaning. Also, since apparent terminal impedance Z_{sa} depends on b/λ_0 as well as b/a, the uncompensated impedances are correct only for the particular values of b and b/a for which they were made. Since Ehrenspeck does not give the value of b, his results cannot be compared with Hartig's.

[9] H. W. Ehrenspeck, "Der Eingangswiderstand dicker zylindrischer Strahler, *Fernmeldetech. Z.*, p. 497; November, 1952.

Acknowledgment

Dr. J. E. Storer pointed out the incorrect behavior of the theoretical curve in Fig. 49 of reference 3. Miss Phyllis Kennedy assisted with the computations and the graphical representations.

The Shielding of Radio Waves by Conductive Coatings*

E. L. HILL†

***Summary*—A theory is given of the shielding of radio waves by the conducting coatings which are placed over the cockpit dome and windows of an airplane. At low and medium frequencies the shielding arises primarily from the quasi-electrostatic charges which are induced on the surface, the effects of which increase strongly with decreasing frequency. At higher frequencies the shielding from this source diminishes in importance while that from the induced eddy currents increases in effectiveness.**

Introduction

AIRCRAFT in flight accumulate electrical charges on external plastic sections either directly from charged atmospheric particles or through frictional contact with uncharged particles. The accumulated charge on the highly insulated surfaces of common aircraft canopy materials is dissipated after sufficiently high concentrations are reached by streamering across the surfaces. The deleterious effects of such static charge streamering in inducing radio interference on nearby antennas can be minimized by covering the affected areas with slightly conducting coatings. This procedure makes it of importance to determine the magnitude of the attenuation to be expected for radio waves which must penetrate these openings in order to affect an internal antenna. This paper presents a theory of the shielding and such experimental data as are available to the writer.

Theory

The shielding effect of a conducting surface against an electromagnetic field has its origin in the charge and current distributions which are induced on the surface under the action of the field. These in turn give rise to secondary fields which interfere with the incident wave to produce the resultant field. The contributions to the secondary field from the charges and currents on the surface are not independent but, since they vary differently with the frequency of the incident field, it is profitable to consider them separately. At low frequen-

* Original manuscript received June 24, 1954; revised manuscript received December 13, 1954.

† Dept. of Physics, Univ. of Minnesota, Minneapolis, Minn. Consultant to Lightning and Transients Res. Lab., Foshay Tower, Minneapolis, Minn.

cies the charge distribution behaves almost electrostatically and is the primary cause of the shielding. With increasing frequency the shielding from the charges diminishes in effectiveness while that from the induced eddy currents grows in importance until it becomes the dominant effect. The usual theories of surface shielding are concerned with the effects from the eddy currents.

This paper is restricted to the case in which the wavelength of the incident radiation is large compared with the linear dimensions of the openings in the aircraft skin. In the opposite extreme, in which the wavelength is small compared with the size of the openings, the penetrability of the surface can be estimated from known formulas for eddy-current shielding, provided the radiation actually incident on the opening is known. The intermediate case of wavelengths which are comparable with the size of the openings is much more difficult than either of the extreme cases, and no general theory has been devised for it.

A method of solution of the field equations by successive approximations has been established by Rayleigh[1] for the case in which the wavelength is large compared with the linear dimensions of the conducting body on which it is incident. This theory has been extended recently by Stevenson[2]. The principle used is that of expanding the field variables as power series in the parameter d/λ, where d is the maximum linear dimension of the conductor and λ is the wavelength of the radiation, the expansion being convergent for $d/\lambda \ll 1$. This theory can be used to show that the field around a perfectly conducting body of any shape can be resolved into partial fields of electric and magnetic types, similar to the known electric and magnetic modes of a sphere, which reduce respectively to electrostatic and magnetostatic fields as $d/\lambda \to 0$. In principle one can employ the corresponding static solutions of the field equations as a starting point for the computation of the higher terms in the series expansions.

The application of the Rayleigh method becomes very difficult for shapes as irregular as those of aircraft, and in order to obtain significant results that can be compared with experimental data, one is obliged to introduce severe idealizations which cannot be justified strictly on theoretical grounds alone. This has been the case in the present calculation. As a consequence we do not strive for high accuracy in the result, but seek to estimate the numerical magnitude of the shielding and its dependence on the frequency of the radiation in an approximation which is useful for engineering applications, and which may also be of assistance in the development of more detailed theories of the shielding.

The metallic surface of an airplane can be considered to have infinite electrical conductivity at the frequencies of interest here. On such a conductor the resultant electrical field must be everywhere perpendicular to the surface. In the immediate neighborhood of a window or cockpit there will be fringing of the field with penetration into the interior of the plane. The problem is to estimate the change which is produced in the interior field by the placing of a poorly conducting coating over the window or cockpit dome. The calculation starts from the consideration which is inherent in Rayleigh's theory that for wavelengths which are long compared with the linear dimensions of the opening the electric field around the latter at any instant will be nearly that corresponding to the induced static charge distribution in a constant external field. A knowledge of the solution of the electrostatic problem permits an evaluation of the charges and currents which flow over the conducting coating on the opening, and from this the secondary shielding field can be estimated. Since the exact solution even of the electrostatic problem is unmanageable for an actual airplane shape, we shall neglect the curvature of the body of the aircraft and idealize its surface as an infinite conducting plane. The calculations will be carried out for some special shapes of the opening which approximate actual experimental conditions.

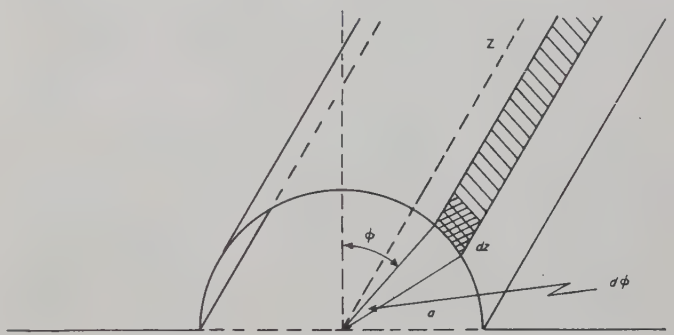

Fig. 1—Geometrical co-ordinates for the semicylindrical dome.

The Semicylindrical Dome

A long cockpit dome can be approximated as a semicylinder resting on a slit in an infinite conducting plane. The geometrical relations are shown in Fig. 1, the radius of the dome being a, with positions on the dome specified by two co-ordinates (ϕ, z). The symmetry of the problem allows us to neglect currents flowing along the length of the dome, the surface charge and current densities being functions of the angle ϕ and the time t only.

When the dome is nonconducting the basic electrostatic problem is that of a slit in an infinite conducting plane placed in an electrical field which is uniform and normal to the plane at large distances from the slit. The solution of this problem is known and from it the field at points on the dome can be evaluated.[3] However, in this idealized case one finds an infinite field and an in-

[1] Lord Rayleigh, *Phil. Mag.*, vol. 44, p. 28; 1897.
[2] A. F. Stevenson, *Jour. Appl. Phys.*, vol. 24, p. 1134; 1953.
[3] W. R. Smythe, "Static and Dynamic Electricity," McGraw-Hill Book Co., Inc., New York, N. Y., 2nd ed., sec. 4.23; 1950.

finite charge density at the edge of the slit. With a dome made of dielectric material, even though it is nonconducting in a practical sense, this strong local field will be smoothed out and the major part of the current flow over the dome will be produced by the field at some distance from the slit edge. Over the greater part of the surface of the dome the field is approximately uniform and normal to the plane.

As the dome is made slightly conducting charge will flow over it to make the resultant field approach that of a conducting plane with a semicylindrical conducting boss on it. If the external field is of very low frequency the latter case is achieved completely, the induced surface charge on the dome and plane being just sufficient at each instant to cancel the incident field in the interior of the dome.

Let $E_0(t)$ be the electric field when the dome is nonconducting, which we label as the incident field, while $E_s(t)$ is the secondary field which is produced by the additional charge and current distributions which are induced on the plane and the dome when the latter is made conducting. Following the qualitative arguments just given we make the approximation that, even when the external field varies at a moderate frequency, the *form* of the charge distribution which is induced when the dome is made conducting is that given by the electrostatic problem, although the rate of flow of charge over the surface and its phase relation to the external field will depend on the frequency. In this approximation both the incident and secondary fields are treated as uniform over the surface of the dome and the calculated shielding will not take into account local diffraction effects within the dome. When the experimental measurements are made sufficiently accurate to test these local field variations within the dome, the present theory will have to be improved.

The connection between the surface charge on the dome and the secondary electric field under these assumptions is that given by the electrostatic problem of a plane having a semicylindrical boss, and as a result takes the form

$$\sigma = 2\epsilon_v E_s \cos \phi. \tag{1}$$

Surface-current density on the dome is determined by the tangential component of the total field, which is continuous across the surface. Ohm's law gives the relation

$$k = \frac{E_0 + E_s}{R} \sin \phi, \tag{2}$$

where R is the surface resistivity in ohms per square. Finally, the relation between the surface charge and current densities given by the equation of conservation of charge is

$$\frac{\partial \sigma}{\partial t} + \frac{1}{a} \frac{\partial k}{\partial \phi} = 0. \tag{3}$$

The convention has been used that the fields are taken to be positive when they are directed towards the plane.

Substitution of relations (1) and (2) into (3) yields the differential equation

$$\frac{dE_s}{dt} + \frac{E_0 + E_s}{\epsilon_v R d} = 0, \tag{4}$$

in which $d = 2a$ is the diameter of the dome. Assuming a sinusoidal time variation with frequency f,

$$E_0(t) = e_0 e^{j2\pi f t}, \quad E_s(t) = e_s e^{j2\pi f t}, \tag{5}$$

one finds from (4) that

$$e_s = -e_0/[1 + j2\pi\epsilon_v f R d]. \tag{6}$$

The resultant field acting on an antenna inside the dome will depend on its position. In the absence of more detailed information we take as a measure of the mean resultant field inside the dome the quantity

$$E(t) = E_0(t) + E_s(t) = \frac{j2\pi\epsilon_v f R d}{1 + j2\pi\epsilon_v f R d} E_0(t), \tag{7}$$

from which one finds that

$$|E/E_0| = x/(1 + x^2)^{1/2}, \tag{8}$$

with

$$x = 2\pi\epsilon_v f R d. \tag{9}$$

The attenuation of the field inside the cockpit dome, in *db*, is defined to be

$$\begin{aligned} A &= -20[\log_{10} |E/E_0|] \\ &= -20\left[\log_{10} x - \frac{1}{2}\log_{10}(1 + x^2)\right]. \end{aligned} \tag{10}$$

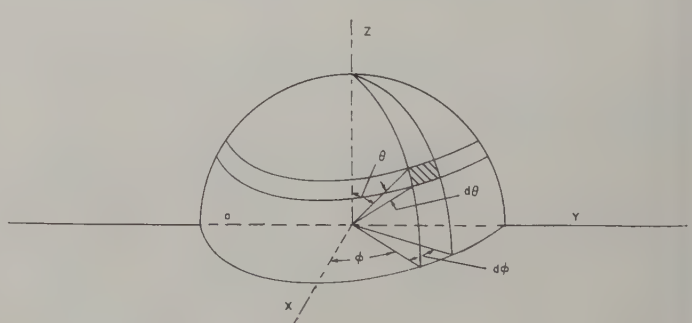

Fig. 2—Geometrical co-ordinates for the hemispherical dome.

The Hemispherical Dome

When the cockpit dome is not long compared with its diameter it is idealized as a hemisphere of diameter $d = 2a$ resting on a circular hole in the conducting plane, as is shown in Fig. 2. The same general approximations will be used for the fields as in the last section, and we give only the changes which are required by the altered geometrical conditions. The relationships between the

surface charge and current densities and the fields are

$$\sigma = 3\epsilon_v E_s \cos\theta, \tag{11}$$

$$k = \frac{E_0 + E_s}{R} \sin\theta. \tag{12}$$

The equation of charge conservation becomes

$$a \sin\theta \frac{\partial\sigma}{\partial t} + \frac{\partial}{\partial\theta}(k \sin\theta) = 0. \tag{13}$$

The calculational procedure used in the last section yields the following expression for the attenuation of the field inside the dome

$$A = -20\left[\log_{10} y - \frac{1}{2}\log_{10}(1 + y^2)\right], \tag{14}$$

with

$$y = (3/4)2\pi\epsilon_v fRd. \tag{15}$$

The Flat Circular Window

Our last example is that of a flat circular window of diameter $d = 2a$. Owing to the fact that the conducting surface on the window is in the plane of the aircraft skin the evaluation of the field which causes the flow over the window is more difficult than in the preceding cases. The electrostatic problem of a circular hole in an infinite conducting plane which forms one boundary of a uniform electric field directed towards the plane can be solved exactly.[4] If $\boldsymbol{E}_0$ is the electrical field at a great distance from the opening then the component of the field parallel to the plane, in the opening, is found to be

$$E_p = \frac{E_0}{\pi} \cdot \frac{\rho/a}{[1 - (\rho/a)^2]}, \tag{16}$$

at a distance ρ from the center of the window. When the external field is directed towards the plane the tangential field in the hole, which is given by (16), will be directed from the center of the hole towards its circumference. This formula shows the expected result that the field strength is unbounded at the edge of the hole, but with a window material of reasonable dielectric constant this strong local field will be smoothed out. We take it as a sufficiently accurate approximation to replace (16) by the relation

$$E_p = E_0\rho/\pi a. \tag{17}$$

When the window surface is made slightly conducting this tangential component of the incident field will lead to a flow of charge over the window, and this in turn gives rise to a secondary field $\boldsymbol{E}_s$. The resultant current flow over the window is determined by the tangential component of the resultant field on the window. It will be assumed that the tangential component of the secondary field on the window surface is determined by a relation of the form (17), just as for the incident field. While this cannot be proved in detail to be the case in the absence of a complete theory of the solution of the field equations, it will be seen below to be compatible with the equation of charge conservation and Ohm's law.

The formulas connecting surface charge and current densities on the window with fields take the form

$$\sigma = \epsilon_v E_s,$$
$$k = (E_0 + E_s)_p/R, \tag{18}$$

while the equation of charge conservation becomes

$$\frac{\partial\sigma}{\partial t} + \frac{1}{\rho}\frac{\partial(\rho k)}{\partial\rho} = 0. \tag{19}$$

Use is now made of (17) to write

$$(E_0 + E_s)_p = (E_0 + E_s)\rho/\pi a. \tag{20}$$

On elimination between (18) and (20), we find, that from (19),

$$\frac{dE_s}{dt} + \frac{4(E_0 + E_s)}{\pi\epsilon_v Rd} = 0. \tag{21}$$

The reduction procedure used in the previous cases leads to the attenuation formula

$$A = -20\left[\log_{10} w - \frac{1}{2}\log_{10}(1 + w^2)\right], \tag{22}$$

with

$$w = (\pi/4)2\pi\epsilon_v fRd. \tag{23}$$

Discussion

Comparison of formulas (10), (14), and (22) for the attenuation shows that they can be reduced to a standard form. If d is a mean linear dimension of the opening and $x = 2\pi\epsilon_v fRd$, then

$$A = -20\left[\log_{10}(\alpha x) - \frac{1}{2}\log_{10}(1 + (\alpha x)^2)\right], \tag{24}$$

with α as a scaling factor which is of the order of unity. It is not concluded that this form has any fundamental theoretical foundation, but in the absence of a more complete theory it might be expected to apply with reasonable accuracy to more irregularly shaped domes and windows than those of our special cases.

The curve of (24) is shown in Fig. 3 (next page), graphs for three cases ($\alpha = 1, \frac{3}{4}, \frac{1}{2}$) being drawn separately. Experimental points (X) are given for the case of a cockpit dome of diameter $d = 0.5$ meter, which was sufficiently long to be treated as a semicylinder ($\alpha = 1$). Surface resistivities of 5,000 and 50,000 ohms per square were used, with broadcast signals ranging from about 0.3 to 1.5 mc. The agreement with the theory is quite satisfactory.

There is also a phase shift between the incident and resultant fields. The complete expression connecting the

[4] Smythe, *op. cit.*, sec. 5.272.

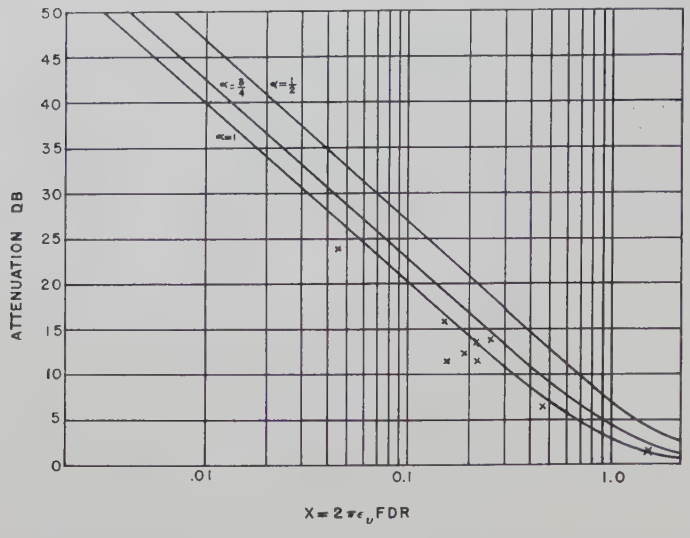

Fig. 3—Attenuation curves from (24) with experimental data (X).

fields is

$$E(t) = E_0(t) \cdot \frac{\alpha x e^{j\beta}}{[1 + (\alpha x)^2]^{1/2}}, \tag{25}$$

with

$$e^{j\beta} = (\alpha x + j)/[1 + (\alpha x)^2]^{1/2}. \tag{26}$$

This formula predicts that the resultant field leads the incident field in phase by an angle which equals 90 degrees at very low frequencies and diminishes to zero with increasing frequency with tan $\beta = 1/\alpha x$.

Acknowledgments

Acknowledgment is made of research support under a joint USAF, Wright Air Development Center (Air Research and Development Command), and Navy Department, Bureau of Aeronautics, sponsored program at the Lightning and Transients Research Laboratory.

VHF Auroral and Sporadic-*E* Propagation from Cedar Rapids, Iowa, to Ithaca, New York*

ROLF DYCE†

Summary—**A 50-mc transmitter operating continuously at Cedar Rapids, to the west of Ithaca, has been monitored for more than two years, using a northward-pointing antenna intended to reduce signals from the west due to *E*-scatter and bursts due to meteors. Associated with visible auroral activity, enhanced signals are heard, having a very rapid fading rate, characteristic of auroral propagation previously described. Continuous recordings are made on an Esterline-Angus chart moving 6 inches per hour. Much stronger sporadic-*E* signals are observed occasionally entering the sidelobes of the receiving antenna, but can usually be distinguished from auroral propagation by the appearance of the trace or clarity of the beat frequency. This method of identification and separation is thought to be effective because each mode of propagation has its own diurnal and seasonal variations agreeing with characteristics found previously by others.**

Introduction

FOR MANY YEARS, amateurs have been aware that, coincident with visual auroral displays, unusual radio propagation is possible on the vhf bands of 28, 50, 144,[1] and, most recently, 220 mc.[2] These contacts have been made using continuous waves, the fading being so rapid that a growling or hissing modulation is heard on the received signals which often makes telephony emission unusable.[3] During recent years, radar equipments operating at vhf frequencies have obtained echoes from ionization associated with the aurora.[4–7] Considerable emphasis at Cornell University has been placed on *cw* techniques for studying auroral propagation, using amateur emissions as well as remotely-located beacon transmitters. The continuous monitoring of a transmitter in Iowa, operating 24 hours per day, is described and some of the results obtained are presented.

Transmitting Equipment

Use has been made of unmodulated transmissions on 49.6 and 49.8 mc originating from Cedar Rapids, Iowa, intended for other propagation research purposes.[8] Each transmitter is equipped with a horizontally-polarized, extremely directive antenna, one aimed at Round Hill, Massachusetts, and the other at Sterling, Virginia.

* Original manuscript received by the PGAP, August 12, 1954; revised manuscript received, January 5, 1955.

† Geophysical Inst., College, Alaska.

[1] R. K. Moore, "A vhf propagation phenomenon associated with aurora," *Jour. Geophys. Res.*, vol. 56, pp. 97–106; March, 1951.

[2] E. P. Tilton, "The world above 50 mc," *QST*, vol. 38, pp. 61–62; June, 1954.

[3] K. L. Bowles, "The fading rate of ionospheric reflections from the aurora borealis at 50 mc," *Jour. Geophys. Res.*, vol. 57, pp. 191–196; June, 1952.

[4] A. Aspinall and G. S. Hawkins, "Radio echo reflections from the aurora borealis," *Jour. Brit. Astron. Assn.*, vol. 60, p. 130; April, 1950.

[5] B. W. Currie, P. A. Forsyth, and F. E. Vawter, "Radio reflections from aurora," *Jour. Geophys. Res.*, vol. 58, pp. 179–200; June, 1953.

[6] L. Harang and B. Landmark, "Radio echoes observed during aurorae and geomagnetic storms using 35 and 74 mc waves simultaneously," *Jour. Atmos. Terr. Phys.*, vol. 4, pp. 322–338; January, 1954.

[7] R. E. Thayer, Master's Thesis, Cornell University, Ithaca, N. Y.; 1952.

[8] D. K. Bailey, R. Bateman, L. V. Berkner, H. G. Booker, G. F. Montgomery, E. M. Purcell, W. W. Salisbury, and J. B. Wiesner, "A new kind of radio propagation at very high frequencies observable over long distances," *Phys. Rev.*, vol. 86, pp. 141–145; April, 1952.

There is probably considerable energy in the antenna sidelobes due to the high-transmitter power in use (approximately 30 kw). Suitably located auroral ionization is therefore believed to be capable of scattering signal to Ithaca, New York (see Fig. 1). In fact, although the Round Hill beam passes nearly overhead at Ithaca, the observed signal strength is not radically different from that due to the Sterling beam passing to the south. This supports the view that these auroral signals arise by scattering of radiation outside the main lobe of the transmitting antenna. These transmissions are useful for recording the incidence of auroral propagation because the radiation is already maintained by other parties on a continuous schedule, day and night.

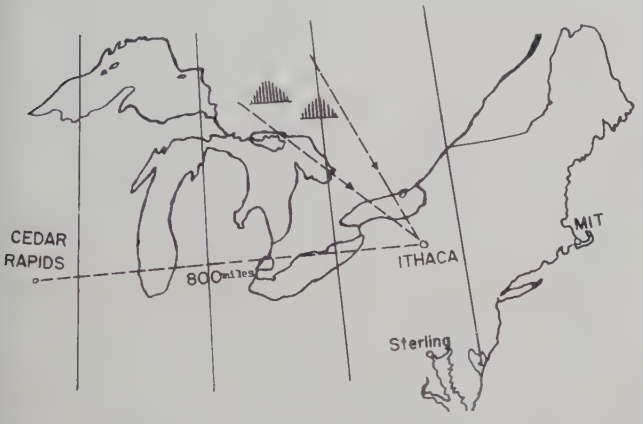

Fig. 1—Map showing approximate location of auroral scatterers.

Receiving Equipment

An 8-element Yagi antenna one wavelength above the ground is used for receiving at Ithaca. The antenna is fixed true north to enhance the auroral signal, when present, and to reduce unwanted signal from the west due to *E*-scatter or meteors. A low-noise cascode rf amplifier with a noise figure of about 3.5 db feeds a crystal-controlled converter with output at 15 mc. An HRO50T-1 communications receiver is used for detection with approximately 4 kc bandwidth. The signal can be aurally monitored and the dc output of the detector simultaneously used to actuate an Esterline-Angus recording milliameter. The beat-frequency oscillator in the communications receiver can be used to detect weak signals in the noise, or to judge the fading characteristics of the received signal. The recorder, running at 6 inches per hour chart speed, provides a permanent, 24-hour per day indication of auroral (and meteoric) propagation at this frequency. Some sporadic-*E* signals are of sufficient strength to leak into the sidelobes of the receiving antenna and are also recorded, as will be later described.

E-Scatter Propagation

If the receiving antenna is pointed west, toward Cedar Rapids, a weak, persistent signal can usually be heard, although the frequency of 49.8 mc is many times the MUF. This has been explained in the literature[8] as being due to ionospheric turbulent *E*-region scattering. With the equipment used at Ithaca, however, this signal is not sufficiently reliable for communication purposes and its rapid fluctuations suggest simply a summation of frequent, weak-meteor echoes.[9,10] Normally, while seeking auroral signals, the receiving antenna is pointed northward, further reducing this unwanted persistent mode of propagation.

Meteoric Propagation

Bursts of signal due to sporadic meteoric ionization are normally recorded many times per minute. The signal usually rises quickly to a large value, then decreases in a few seconds accompanied by deep fading. An amplifier has been used which limits at the top of its range, thus avoiding damage to the recording pen, but allowing most of the recording range to be linear. Typical meteor activity is shown during the first half-hour of the recording shown in Fig. 2, each meteor appearing as a single line due to the slow chart motion. Notice that, in the absence of auroral or sporadic-*E* signal, there is usually sufficient time between meteors for the pen to settle back to the no-signal noise level.

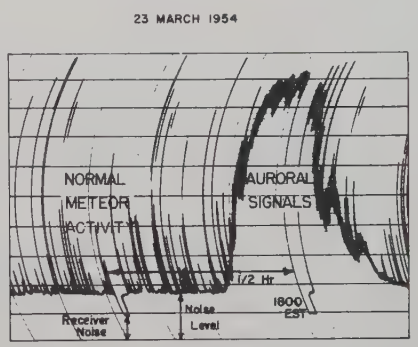

Fig. 2—Typical trace showing a short period of auroral propagation, March 23, 1954. The maximum signal level reached represents approximately 1 microvolt across the 50-ohm antenna input.

The occurrence of meteor bursts provides a permanent record of the fact that the transmitter and receiving equipment were both operating. Conversely, when meteor bursts on the record are missing, the recording is considered not valid. Meteor showers are also recorded but have not been studied with this equipment.

Auroral Propagation

During times of visible aurora, a signal can generally be heard which is believed to be propagated by auroral ionization. A typical record left by such a signal is

[9] O. G. Villard, Jr., A. M. Peterson, L. A. Manning, and V. R. Eshleman, "Extended-range radio transmission by oblique reflection from meteoric ionization," *Jour. Geophys. Res.*, vol. 58, pp. 83–93; 1953.

[10] D. W. R. McKinley, "Dependence of integrated duration of meteor echoes on wavelength and sensitivity," *Can. Jour. Phys.*, vol. 32, pp. 450–467; July, 1954.

shown in Fig. 2. The auroral type of signal has an unusually rapid fading rate, containing frequencies up to several hundred cycles per second.[3] However, the response of the recording pen falls off rapidly with frequency as shown in Fig. 3. The pen is therefore not able to follow all fluctuations in the auroral signal but deviates rapidly about a mean indication, producing a distinctive trace. Almost without exception, such recorded traces are accompanied by a characteristic auroral hissing or growling sound in the loudspeaker, due to the rapid fading rate at audio frequencies. With the beat frequency oscillator turned on during such conditions, a "fuzzy" note will be heard, rather than the clear single tone obtained, for instance, at the time of a long-enduring meteor. Thus, when an observer is present, the beat-frequency oscillator provides a sensitive test for the auroral type of signal.

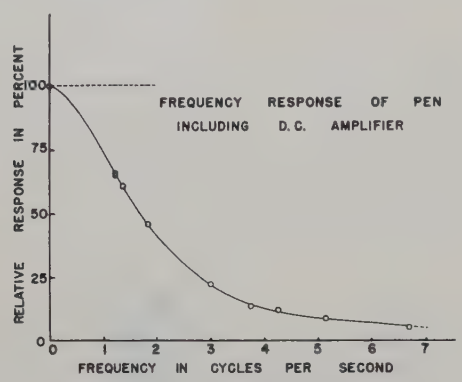

Fig. 3—The Esterline-Angus recorder frequency response.

The occurrence of the auroral type of signal observed with this equipment during a given hour is usually verified by similar reports from amateurs in the northeastern United States. Disturbances from the Agincourt magnetic station also correspond to indications of auroral propagation on the recorder, although minute-to-minute changes correlate only to a limited extent. On many clear nights, attempts were made to correlate the 49.8 mc record, minute-by-minute, with auroral forms seen visually. In general, a quiet arc will correspond with a weak radio signal or no signal at all. If, however, the arc breaks into rays, a sudden increase in signal is noted. There are occasions, however, when signals are heard without visible aurora and vice versa, as if auroral activity not visible were also contributing to the recorded signal. Visual data collected by C. W. Gartlein, and the 49.8-mc radio recordings from March 26 to April 20, 952, were broken into one-hour intervals and rated strong, weak, or nonauroral. These data showed a correlation of 61 per cent. For these and other reasons to follow, the auroral propagation indications obtained with this equipment are believed to be related to the visual auroral phenomena.

The average diurnal variation of auroral signals appears in Fig. 4, based on the percentage of time that signal occurred above the threshold of detectability, irrespective of intensity. The phenomenon is chiefly a night-time one although there are rare cases of auroral signals obtained near mid-day. There is a subsidiary dip near midnight which is believed to be statistically authentic. Also, if the data are broken into three-month periods, individual diurnal variation curves show the same shape. This curve does not conform with most diurnal variation curves based on visual observations, which tend to have a single maxima.[11] However, this is not surprising since there is even poor agreement between visually-obtained diurnal variation curves from one location to another.[12]

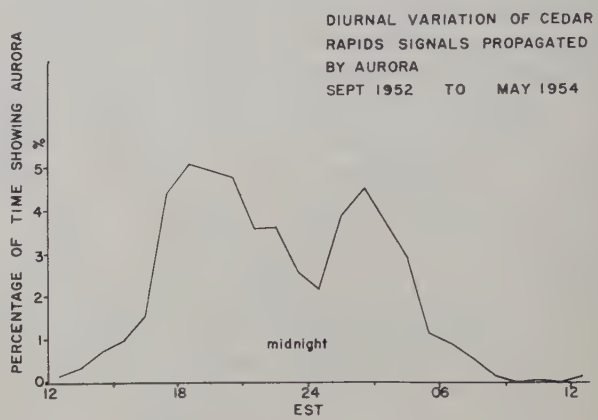

Fig. 4—The percentage of time that auroral propagation was recorded for each hourly segment of the day.

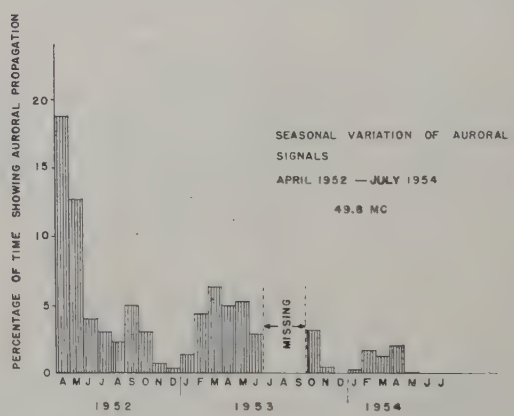

Fig. 5—The percentage of time that auroral propagation was recorded for each month.

Visual auroral observers have long known that maximum auroral activity occurs near the equinoxes.[13] The records showing auroral propagation occurrence have therefore been examined for this seasonal variation. For each month, the percentage of time that auroral propagation occurred was determined, the resultant seasonal variation appearing in Fig. 5. Maxima appear near the

[11] V. R. Fuller, "A report of work on the aurora borealis for the years 1932–1934," *Terr. Mag.*, vol. 40, pp. 269–275; September, 1935.
[12] E. O. Hulbert, "On the diurnal variation of aurora polaris," *Terr. Mag.*, vol. 36, pp. 23–28; 1931.
[13] Curves from several authors may be found in L. Harang, "The aurorae," John Wiley and Sons, Inc., New York, N. Y., pp. 9–10; 1951.

equinoxes and minima near the solstices. Also the plot shows a decrease in auroral propagation activity from 1952 to 1954. Since the equipment gain was maintained approximately constant, the decrease appears to be genuine. It is attributed to the decrease in the sunspot activity, expected to reach a minimum in 1954.

Measurements of the azimuth angle of arrival of the auroral signals were made at a separate location using a highly-directive antenna. Four Yagi antennas were mounted side-by-side, spaced so that the centers of the outside antennas were separated by two wavelengths. The array was motor-driven with provision for recording signal strength and position marks on fast recording chart. The great-circle route from Ithaca to Cedar Rapids lies due west. Maximum meteor rate and signal strength occur in that direction. The bearing of maximum auroral signal varied from sweep-to-sweep but averaged about northwest, within plus or minus 30 degrees. The signal was not expected to arrive from the north or the northeast because the transmitter is unable to illuminate the *E*-region at those geographic locations.

The receiving-antenna polarization was changed many times when auroral signals were present. Although the transmitter emits horizontally-polarized waves, an increase of 3 db in received power can be achieved by using vertical polarization. Since most of the received signal is probably arriving below the Brewster angle of vertical waves, the two polarizations should have little effect on the vertical polar diagram. Signals arriving from northwest are off the main beam of the receiving antenna so that possible differences in the patterns in the two planes would make a difference in the received signal. The explanation is felt to lie, however, in the fact that, over the Cedar Rapids-to-Ithaca path, the auroral ionization must scatter through a right angle for typical orientations. A horizontally-polarized wave sent from the transmitter and re-radiated by "scattering dipoles" composing the auroral ionization will have no component that can be detected at the receiver. But, because the sidelobe radiation of the transmitting antenna probably contains some vertical polarization, vertical waves should be detected at the receiver, so the receiving antenna has been vertically polarized since September, 1952.

Sporadic-*E* Propagation

Occasionally a different type of trace appears on the record as shown in Fig. 6. It is distinguished by frequent saturation of the recording system due to large signal strength and, more important, by the ability of the recording pen to register the slow fading. Except in rare cases, the beat frequency oscillator test gives a clear tone, unlike auroral signals. The ionosphere recorder at Cornell has detected appreciable sporadic-*E* when this kind of trace is present. Also amateur signals can be heard on 28 mc and sometimes 50 mc, arriving at Ithaca from directions not necessarily west. Traces such as in Fig. 6 have, for these reasons, been credited to sporadic-*E* propagation.

A few measurements were made of the azimuth direction of arrival of sporadic-*E* signals. The signals do not necessarily come from the north, where the receiving antenna points, or from the *E*-region midpoint to the west of Ithaca. For instance, one measurement showed signal from the southeast, first alone and then accompanied by a signal coming also from the west. The sidelobes of the northward-pointing receiving antenna are therefore involved in the reception of these signals.

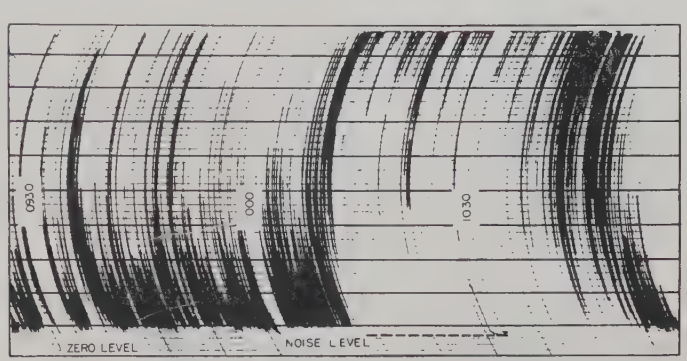

TYPICAL RESPONSE OF ESTERLINE—ANGUS RECORDER TO SPORADIC-E SIGNAL ON 49.6 MC, JUNE 21, 1952

Fig. 6—Sporadic-*E* propagation is indicated from approximately 1010 to 1050 EST

Sporadic-*E* indications on the Cedar Rapids-to-Ithaca path are less frequent and occupy less total time than either ionosphere recorder indications or amateur reception. Special orientation of sporadic-*E* clouds or unusually strong ionization are apparently necessary for an indication on this equipment. Thus traces indicating sporadic-*E* are only useful as a measure of relative sporadic-*E* activity. With this limitation in mind, the following studies have been attempted.

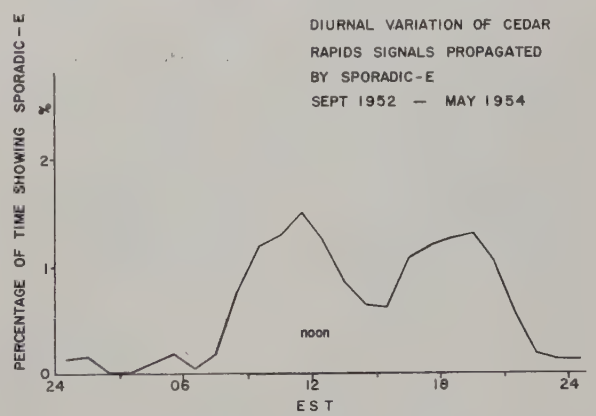

Fig. 7—The percentage of time that sporadic-*E* propagation was recorded for each hourly segment of the day.

First the diurnal variation curve was determined for the sporadic-*E* signals (see Fig. 7). The phenomenon occurs chiefly in the daytime, although there are many instances of nighttime activity having the same characteristics. (In comparing this figure with Fig. 4, note that the diurnal curve for auroral signals is centered on

midnight.) The peak value represents 8 hours of sporadic-E occurrence which is believed to be a sufficient quantity to authenticate the subsidiary minimum appearing at 1500 EST. Similar curves have been obtained from hf ionosphere recorder data.[14]

The seasonal variation was determined and the results are presented in Fig. 8. Inspection shows, contrary to auroral signals, sporadic-E maxima at the solstices with minima at the equinoxes. Prior to May 1954, the occurrence of sporadic-E appeared to decrease in conformity with decreasing sunspot number. However, the months of May, June, and July, 1954, have shown unusually high sporadic-E activity despite very low solar and magnetic activity. Thus, there is a lack of well-defined correspondence with sunspot cycle.

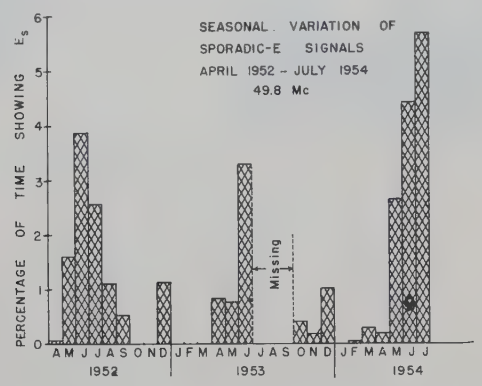

Fig. 8—The percentage of time that sporadic-E propagation was recorded for each month.

Conclusion

The recordings from April 1952 to May 1954 inclusive totaled 13,595 hours of valid observation. If the presence of sporadic-E is assumed to make that time "non-observable" for auroral propagation and vice versa, then auroral propagation was present 4.77 per cent of the time and sporadic-E 0.82 per cent. If July, August, and September of 1953 (for which all observations have been condemned due to low gain) are excluded, the valid observation time is 81 per cent of the total available 700 days (from April 1952 to May 1954). Most of the lost time was due to transmitter shutdown with receiver tuning drift of secondary importance. The occurrence of auroral propagation and, on this equipment, sporadic-E propagation, can thus be considered non-normal, each occurring less than 5 per cent of the time.

The simple techniques used on this vhf circuit for the separation of sporadic-E and auroral ionization appear to be effective. First, the diurnal variation has been determined for each type of trace. The results are opposite; one being a nighttime phenomenon and the other a daytime one. Second, the seasonal variation has been determined for each mode of propagation and again the results are different; sporadic-E signals having maxima at the solstices and auroral signals having minima at that time. Third, successful correlations have been made with visible aurora occurrence, in the one case, and ionospheric sounder data in the other case. The results, illustrated here, indicate that success has been largely achieved (1) in the determination of quantities proportional to auroral and sporadic-E propagation occurrence, and (2) in the separation of these two quantities.

Acknowledgment

The author wishes to express his appreciation to those parties responsible for the operation of the Cedar Rapids transmitters. The Cornell Radio Astronomy Laboratory staff has been most helpful in furnishing assistance as well as an electrically quiet location. Financial aid was supplied by the U. S. Signal Corps through the School of Electrical Engineering at Cornell University. The author gratefully acknowledges a Republic Aviation Corporation fellowship for the academic year 1953–54.

[14] E. K. Smith, "The Sporadic-E region of the ionosphere and its effect upon television," Tech. Rep. No. 7, School of Elec. Engng., Cornell Univ., Ithaca, N. Y.; October, 1951.

Endfire Slot Antennas*

B. T. STEPHENSON† AND C. H. WALTER†

Summary—The conditions for endfire radiation from a traveling-wave slot are discussed. These are that the phase velocity of the traveling wave be equal to or less than the velocity of light in free space and that the aperture be excited with a strong longitudinal component of electric field. Practical ways of achieving these conditions are mentioned and an approximate analysis based on partially dielectric-filled waveguide theory is used to determine the aperture fields as a function of the antenna geometry.

Far-field pattern characteristics are discussed. It is found that the actual pattern may differ considerably from that predicted by simple theory. This is attributed primarily to two things, a finite ground plane and the discontinuity produced by the abrupt aperture opening. Two practical discontinuity minimizers are described. The ground plane effect is analyzed by applying Huygens Principle, and a simple procedure is described for determining the first-order effect.

The problem of obtaining pencil-beam radiation in the horizontal (plane of the ground plane) pattern is solved quite simply by using wide-aperture antennas which can be made to operate satisfactorily over better than a 2:1 band. The efficiency and vswr of a practical antenna, with sidelobes in the horizontal pattern at least 20 db down, have been measured over a 2:1 band. The efficiency varied from 65 per cent at the high-frequency end of the band to 55 per cent at the low end. The vswr was less than 1.4 over the band.

Introduction

THE ENDFIRE slot antenna is a traveling-wave antenna[1] characterized by a phase velocity equal to or less than the velocity of light in free space. This paper deals with the type of aperture excitation required to produce endfire radiation, the spurious radiation produced by the discontinuity at the end of the slot, and the effect of the finite ground plane in which the slot is cut. Practical, broadband, endfire antennas are described whose apertures may be made wide enough to obtain pencil-beam radiation without the need for an array of slots.

Aperture Excitation for Endfire Radiation

In determining the aperture excitation necessary for a particular farfield polarization, it is convenient to think in terms of the equivalent current distribution in the aperture. Thus, to obtain a horizontally-polarized endfire beam, we need a distribution of horizontal electric current elements oriented at right angles to the endfire direction, or a distribution of vertical magnetic-current elements. To obtain a vertically-polarized endfire beam we need a distribution of horizontal magnetic-current elements oriented at right angles to the endfire direction, or a distribution of vertical electric-current elements. Since, for horizontally-polarized radiation, the signal in the plane of a horizontal ground plane is greatly reduced by the shorting-action of the ground plane, only vertically-polarized endfire antennas will be considered.

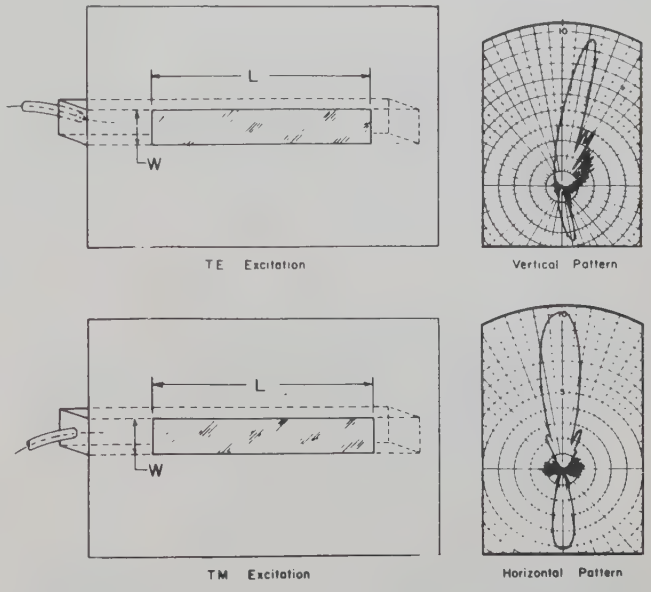

Fig. 1—Endfire antennas and typical radiation patterns for $L \geqq 10$ wavelengths.

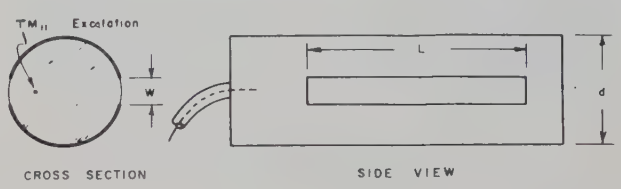

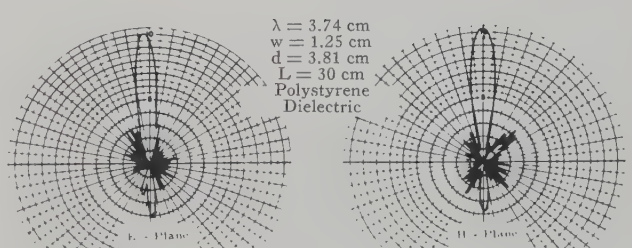

Fig. 2—Endfire pencil beam from diametrically opposed slots.

In practice vertically-polarized endfire radiation can be obtained by either TE or TM excitation of slotted, dielectric-filled waveguides. This is a type of hybrid mode operation[1] that produces a strong longitudinal component of electric field in the aperture. Practical endfire slot antennas and typical radiation patterns are shown in Fig. 1. Fig. 2 shows an endfire pencil beam obtained from diametrically opposed slots in a cylinder.

* Original manuscript received by the PGAP, June 9, 1954; revised manuscript received, December 15, 1954.

† Antenna Lab., The Ohio State Univ., Research Foundation, Columbus, Ohio.

[1] J. N. Hines, V. H. Rumsey, and C. H. Walter, "Traveling-wave slot antennas," PROC. I.R.E., vol. 41, pp. 1624–1631; November, 1953.

The back radiation caused by waves reflected from the far end of the slot can be eliminated by an absorbing load at the end of the aperture, or by tapering the depth of the guide to eliminate the abrupt termination. A TE-excited antenna with uniformly-tapered depth has been found to give very satisfactory endfire operation.[2] A sketch of a tapered-depth antenna and typical radiation patterns are shown in Fig. 3.

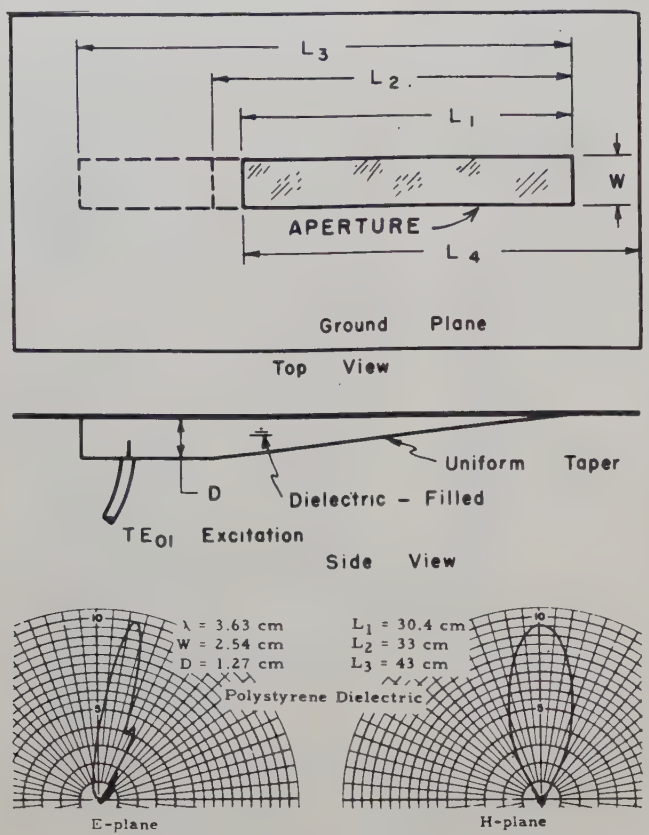

Fig. 3—A tapered-depth endfire antenna and typical radiation patterns.

In observing the radiation patterns of Figs. 1 and 3 it should be kept in mind that the vertical (E plane) pattern is not a good test of endfire operation because of the effect of a finite ground plane (which will be discussed later). The real test is the horizontal (H plane) pattern (i.e. the pattern in the plane of the ground plane). When the endfire conditions are met, this pattern has its maximum in the endfire direction, and is relatively independent of the size of the ground plane.

Analysis of the Aperture Field

A rigorous analysis of slotted dielectric-filled waveguide is extremely difficult and has been supplanted by approximate methods. Recently the problem has been treated by a variational method[3] which gives formulas for the propagation constant and ratio of longitudinal to transverse electric field. However, the formulas involve integrals that are rather difficult to evaluate and, if the phase velocity is of primary interest, there are several methods that are easier to apply.[4,5]

An analysis based on the partially-filled waveguide of Fig. 4 is quite useful and easy to apply. This method assumes that the phase velocity is not appreciably altered when the air-filled part of the guide is removed. From the partially-filled waveguide analysis two types of hybrid mode operation are possible. One type corresponds to $H_x=0$ and the other to $E_x=0$ (refer to Fig. 4 for co-ordinate system). In practice it is found that something close to the $H_x=0$ mode is produced by conventional TE excitation of a dielectric-filled guide with a side normal to the E field removed.

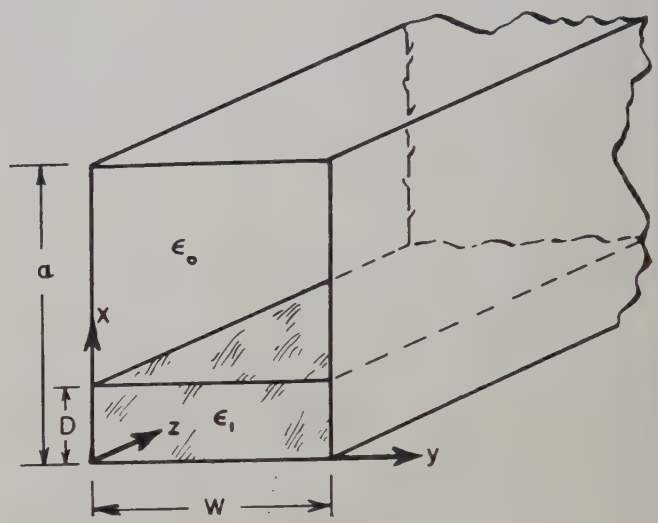

Fig. 4—Partially-filled waveguide used in endfire antenna analysis.

The phase velocity in the partially-filled waveguide is given by

$$c/v = \sqrt{1 - \left(\frac{k_0}{\beta}\right)^2 - \left(\frac{M}{2W/\lambda}\right)^2}, \qquad (1)$$

where

c = velocity in free space
v = phase velocity in the Z direction
$\beta = 2\pi/\lambda$
λ = free-space wavelength
M = mode number

and k_0 is the propagation constant in the x-direction in medium 0 (air). For the $H_x=0$ mode k_0 satisfies the

[2] P. W. Springer and E. L. Ellis, "An Experimental Study of Dielectric-Filled Traveling-Wave, Tapered-Guide Antennas," Tech. Rep. 52–173, Wright Air Dev. Center, Dayton, Ohio; January, 1952.
[3] V. H. Rumsey, "Traveling-wave slot antennas," *Jour. Appl. Phys.*, vol. 24, pp. 1358–1365; November, 1953.
[4] "Millimeter Wavelength Antenna Studies," 2nd Quart. Prog. Rep., Proj. 430, Stanford Res. Inst.; September, 1951.
[5] W. Rotman, "Metal-Clad Progressive Phase, Dielectric Antennas," AFCRC Report No. E5081, Air Force Cambridge Res. Labs., Cambridge, Mass.; January, 1951.

equation

$$k_1 \tan k_1 D = (\epsilon_1/\epsilon_0) k_0 \tan k_0(D - a), \qquad (2)$$

where k_1 is the propagation constant in the x-direction in medium 1. Curves of c/v for the $H_x = 0$ mode with $M = 1$ and $a = \infty$ are shown in Fig. 5 as a function of D/λ and W,λ for polystyrene dielectric. Fig. 6 shows a comparison of a measured and calculated velocity ratio c/v for a tapered-depth antenna.

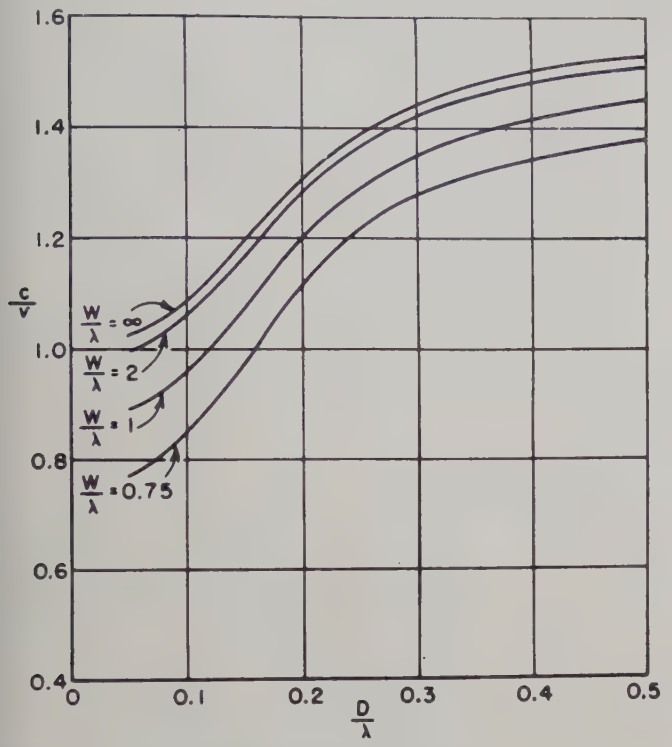

Fig. 5—Calculated c/v as a function of waveguide geometry for polystyrene dielectric.

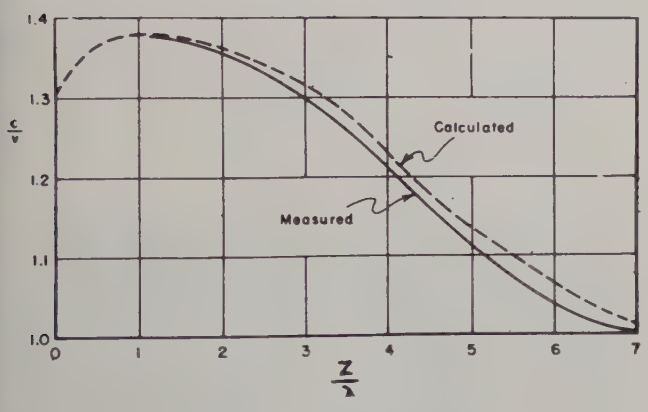

Fig. 6—Comparison of measured and calculated c/v for a flared slot antenna with $\psi = 30$ degrees (see Fig. 12).

It is interesting to note from Fig. 5 that c/v can be kept within the limits $\sqrt{\epsilon_1/\epsilon_0}$ and 1 over an extremely wide-frequency range. Hence the tapered-depth antenna results in an endfire antenna whose practical bandwidth is limited only by the feed and the discontinuity at the beginning of the aperture. These two problems will be discussed in some detail later.

The partially-filled waveguide analysis can also be used to calculate approximately the amplitude distribution in the aperture of the antenna. This is illustrated in Fig. 7, which shows a comparison of measured and calculated longitudinal field (E_z) along a tapered-depth antenna of uniform width. The magnitude of the longitudinal component of electric field is given by

$$|E_z| \sim k_1(c/v) \sin k_1 D. \qquad (3)$$

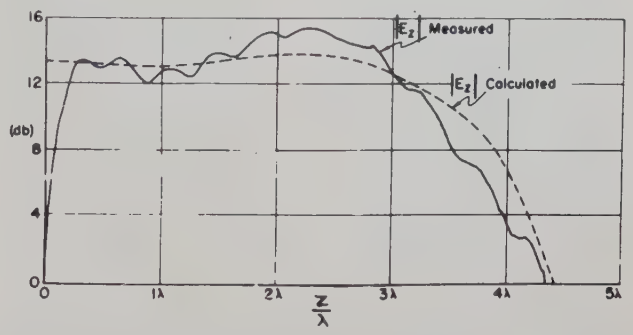

Fig. 7—Comparison of measured and calculated amplitude along a tapered-depth antenna of constant width.

Effect of Finite Ground Plane on Radiation Pattern

Because of ground plane currents, the size of the ground plane will have a serious effect on the radiation pattern of any antenna that has substantial radiation in the plane of the ground plane. From Huygens Principle, the radiation from the antenna is the same as the free-space radiation from the equivalent electric and magnetic currents on any surface enclosing the antenna. Provided the electric currents on the back of the ground plane can be ignored, the radiation is therefore the free-space radiation from the electric currents in the ground plane plus the equivalent electric and magnetic currents in the aperture. If the magnetic-current distribution (which exists in the aperture only) is given, the classical approach is to assume that the electric current distribution (of both actual and equivalent currents) is approximately the same as the current distribution which would exist on that portion of an infinite ground plane which corresponds to the finite ground plane.

A crude test has been made of this approach. A series of patterns was measured as the length of the ground plane of an endfire antenna was varied, and an attempt was made to calculate corresponding patterns from assumed electric and magnetic currents.

The calculated patterns were made by superimposing the radiation of a line source of transverse magnetic-current elements extending the length of the aperture and the radiation of a line source of longitudinal electric-current elements extending from the beginning of the aperture to the end of the ground plane. For simplicity the line sources were assumed to have uniform ampli-

tude distributions. The relative strengths of the sources were such that the maximum values of their patterns were equal in magnitude and phase. This is strictly true only for an aperture in an infinite ground plane; however, it is assumed to be true for large ground planes. The agreement between measured and calculated patterns is quite good as is shown in Fig. 8.

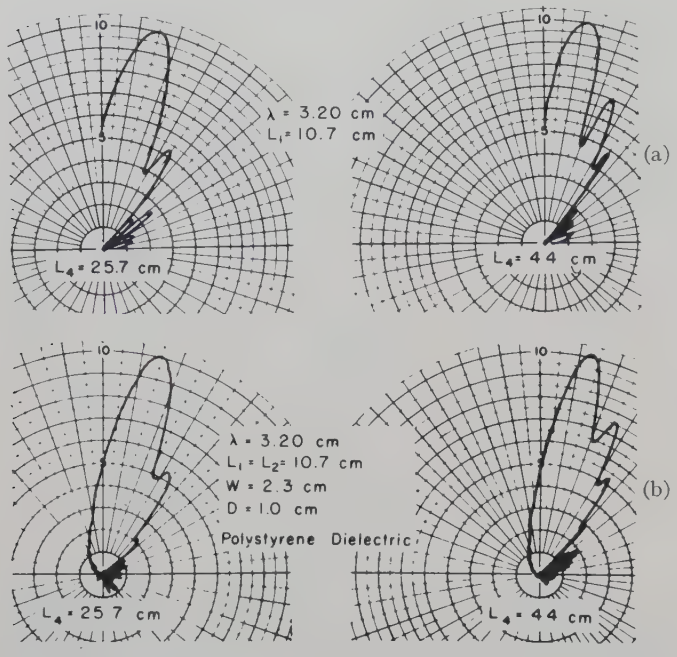

Fig. 8—(a) Calculated patterns showing the effect of ground plane length on the vertical pattern of an endfire antenna. (b) Measured patterns of the endfire tapered-depth antenna of Fig. 3 showing the effect of ground-plane length on the vertical pattern.

Because of the polarization of the assumed electric-current source, very little change would be expected in the horizontal pattern. This was verified by measurements. The horizontal pattern remained essentially the same over a wide range of ground plane lengths.

These calculations to determine the effect of the ground plane length are admittedly crude, but the remarkable agreement with measurements recommends this method as a simple way of determining the first-order effect of the ground plane size.

Discontinuity Minimizers

We have seen that the tapered-depth antenna is potentially capable of operating over an extremely wide bandwidth. In practice the primary factor restricting the bandwidth is the discontinuity effect created by the abrupt opening of the aperture. The spurious radiation caused by the discontinuity is superimposed on the traveling-wave pattern and sometimes results in serious degradation.

The ideal solution is to design the feed section so that it produces the same field configuration that exists in the aperture section. In practice it is desirable to feed the slotted waveguide section from conventional waveguide. This necessitates a transition section between the closed and slotted guide.

For air-filled slotted waveguides a V-taper replacing the abrupt opening of the slot has proven effective. However, the application of a V-taper to the endfire dielectric-filled antenna, while improving the vertical pattern, may seriously distort the pattern in the plane of the ground plane (horizontal pattern). The distortion in the horizontal pattern may be ascribed to a transverse electric field set up by the V-taper. This suggests that the transition should be designed to modify the longitudinal component of electric field without introducing a transverse component or if not possible to avoid the transverse component, then provide a means for restricting its radiation. Two discontinuity minimizers have resulted. These are called the "fingers" and the "tapered ladder."

The fingers are merely short stubs at the beginning of the aperture. Their purpose is to short-out the tangential fields of undesired modes present at the discontinuity. Fig. 9 shows the design used to obtain the results of Fig. 10.

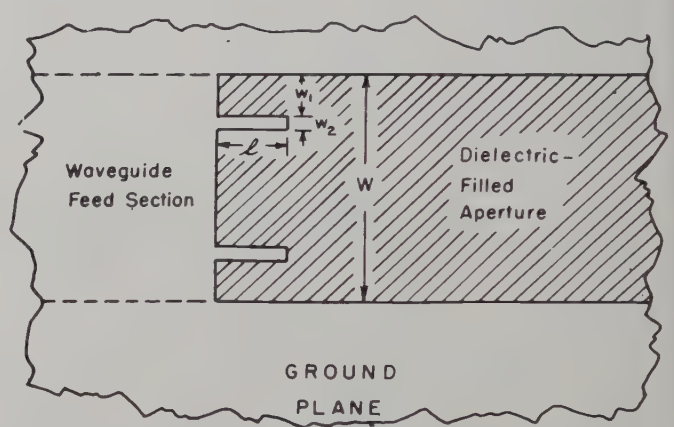

Fig. 9—Sketch of "fingers" discontinuity minimizer.

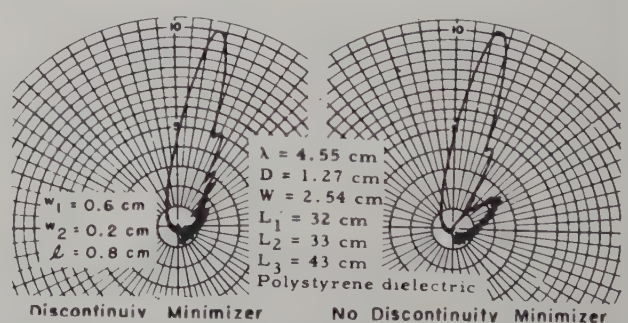

Fig. 10—Comparison of patterns with and without discontinuity minimizer for a tapered-depth antenna.

The tapered-ladder discontinuity minimizer appears to be more effective. It consists of a V-taper with transverse strips to restrict radiation from the transverse

lectric field. Fig. 11 shows a sketch of a tapered-ladder liscontinuity minimizer. Best results have been ob-ained with the transverse strips composed of lossy ma-erial. Perfectly conducting strips tend to scatter appre-iable radiation to the rear. A tapered-ladder discon-inuity minimizer approximately a wavelength long at nid-band has worked satisfactorily over a 3:1 band.

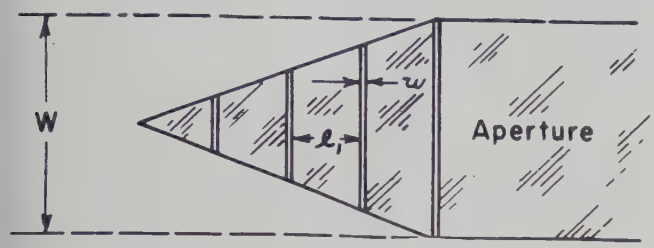

Fig. 11—Sketch of tapered-ladder discontinuity minimizer.

Large Aperture Endfire Antennas

We frequently encounter the problem of obtaining a narrow beam with low sidelobes. This can be accomplished by using a single large aperture instead of the conventional array of slots. Two large aperture endfire antennas are shown in Fig. 12. These antennas are simple to construct and they are inherently broadband.

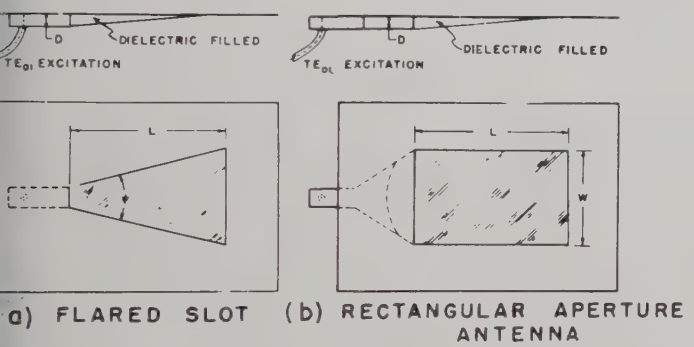

Fig. 12—Large aperture tapered-depth antennas.

The flared slot antenna which is shown in Fig. 12(a) is effectively a flush horn. With a tapered-ladder discontinuity minimizer this antenna operates over a 2:1 band with sidelobes in the horizontal pattern at least 20 db down. Fig. 13 shows a typical pattern.

If a rectangular aperture is desired the antenna of Fig. 12(b) can be used. The antenna illustrated utilizes a horn feed to excite the aperture although any suitable wide aperture feed can be used. For the horn feed it will generally be necessary to insert a lens to correct the phase distribution across the aperture. In practice it has been found convenient to combine the lens and the tapered transition from air to dielectric. An optical lens design procedure has been used with good results.

With ridged-waveguide feed and tapered-ladder discontinuity minimizer the antenna of Fig. 12(b) has operated from 3 to 9 cm with sidelobes in the horizontal

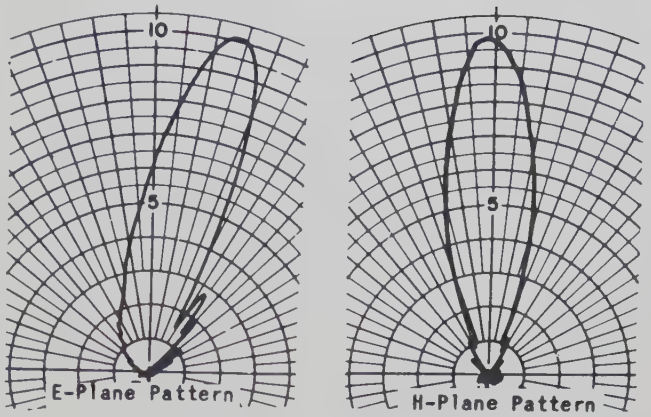

Fig. 13—Typical patterns of a flared slot antenna with $\psi = 30$ degrees and $L \geqq 10$ wavelengths.

pattern at least 18 db down. The antenna is shown in detail in Fig. 14.

Wide-band operation often entails some loss in efficiency. To ascertain the extent of the loss in a flush mounted endfire antenna, efficiency measurements were made on a flared slot antenna over a 2:1 band. The measurements were made by means of a 3-cm efficiency measuring equipment which measures the radiated power of an antenna.[6]

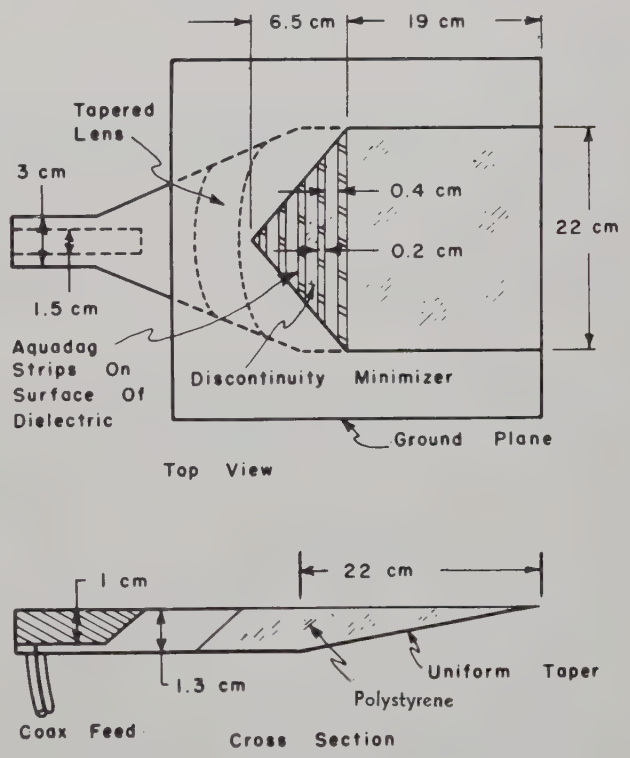

Fig. 14—A wide-aperture antenna with ridged-waveguide feed and discontinuity minimizer.

[6] J. Rowan, "A Direct Reading Efficiency Meter for *X*-Band Antennas," Interim Engrg. Rep. 301–26, Antenna Lab., The Ohio State Univ. Res. Found., prepared under Contract AF 33(038) ac 16520, with Air Materiel Command, Wright-Patterson AF Base, Dayton, Ohio; October, 1950.

With a silver-plated pyramidal horn as a standard, a flared slot antenna was tested from 3 to 6 cm with and without a tapered-ladder discontinuity minimizer. The antenna was made of brass and filled with polystyrene. It had a flare angle of 30 degrees and a length of 35 cm. The discontinuity minimizer had a 60 degree flare and 8 transverse strips of aquadag-coated paper 0.2 cm wide and 0.4 cm. apart. The efficiency ranged from 85 per cent at the shortest wavelength to 80 per cent at the longest wavelength of the 2:1 band for the flared slot antenna without discontinuity minimizer. Thus the dielectric itself accounts for an appreciable loss in efficiency. With the discontinuity minimizer in place, the efficiency ranged from 65 per cent at the shortest wavelength to 55 per cent at the longest wavelength of the band. The discontinuity minimizer introduces as much as 25 per cent loss in efficiency. However, it should be mentioned that the discontinuity minimizer used in this test resulted in sidelobes in the horizontal patterns at least 20 db down over the 2:1 band. If a less stringent sidelobe level or a narrower band is acceptable, fewer lossy strips are required and an increase in efficiency will result. In fact the flared slot has sidelobes 15 db down or better over a 50 per cent band with no discontinuity minimizer at all.

A vswr measurement was made also to see how well the flared slot matched the waveguide feed. With discontinuity minimizer the vswr was less than 1.4 over the 2:1 band. Without discontinuity minimizer the vswr was less than 2.2 over the 2:1 band.

Acknowledgment

This work was performed under Contract AF 18(600)-85 between Wright-Patterson Air Force Base and The Ohio State University Research Foundation. It is a pleasure to acknowledge the many suggestions of Prof. V. H. Rumsey, and the help given by W. E. Nexsen and other members of The Ohio State University Antenna Laboratory.

communications

The Various Theories on the Propagation of Ultra-Short Waves Beyond the Horizon*

JEAN ORTUSI†

Introduction

SINCE THE rapid development of television and radar, the use of ultra-short waves of length less than a few meters has considerably increased. The main characteristics of these waves is the almost complete absence of reflection from the ionospheric layers responsible for the long distance propagation of short waves. Thus the opinion is generally held that these waves are only propagated over optical paths, or more correctly, to take into account standard atmospheric refraction, in regions of radio visibility reckoned on the basis of an earth radius of 4/3 of the real radius. This opinion is strongly upheld by the diffraction calculations on the classical method known as the "phase integral" method. In this method, the field beyond the horizon consists of evanescent propagation modes and decreases very rapidly (exponentially) with distance.

Experimental Determination of the Received Field

However, numerous propagation experiments beyond direct visibility have been undertaken during the last few years. Their object was, on the one hand, to determine the ultimate possibilities of television transmitters, and, on the other, to make use of the inherent

* Original manuscript received by the PGAP, December 20, 1954.
† Compagnie Générale De Télégraphie Sans Fil, Paris, France.

advantages of these waves for long distance connections (absence of interference and wide band). These experiments have turned out to be in violent opposition with the prevailing opinion. They show the presence of relatively large fields beyond the horizon as well as behind local natural obstacles, such as mountains.

Two types of tests were undertaken:

1. In the VHF range, for frequencies between 40 and 200 mc, a series of propagation curves proposed by the "rapporteurs" of the United Kingdom were accepted by the CCIR at the Stockholm Conference in May, 1952.

2. In the SHF (or centimetric) band, numerous measurements of field strength were made in the United States up to distances beyond 1,000 km.

The results of these experimental data show that the main characteristics of this type of propagation appear to be as follows:[1]

(a) The received field varies approximately inversely as the *fourth* power of the distance but relatively little in terms of wavelength.

(b) The field depends very little on the height of the aerials or on the meteorological conditions along the path.

(c) The aerial gain appears to be maintained for all distances.

(d) The attenuation factor F (ratio of actual field to the field received at the same distance in free space) decreases rapidly close to the horizon. It then varies relatively slowly and takes up a value between -40 and -120 decibels when the distance increases from 100 to 1,000 km.

Thus, it is sometimes greater by several hundreds of decibels than the attenuation factor calculated according to the classical method.

General Principle Common to the Various Theories

To account for these experimentally established facts, various theories have been put forward in an attempt to explain this type of propagation and to examine the reasons why the measured field, even in the absence of abnormal propagation (ducts), has values so different from those obtained according to the classical theory.

All these theories are derived from the criticisms which can be levelled at the physical hypotheses of the classical theory.

It is well known that the latter rests on the calculation of the Sommerfeld integral representing the solution of the equation for propagation above the surface of the earth. This integral is calculated in the form of a series of real or of evanescent modes, according to the curve of the index profile.

In the case of normal refraction conditions, it can be shown, by the phase integral method, that the real modes are zero; therefore, at a sufficient distance, the first evanescent mode leading to an attenuation factor proportional to distance is considered.

However, although the general problem of the stability of the propagated wave is difficult to solve, it can be shown that, when the wavelength is small, the solution obtained remains stable so long as the distance is less than the distance corresponding to the conditions of optical path, but that it becomes *unstable* in the contrary case.[2] Hence, as a result, small variations in the boundary conditions or in the curve of the index profile (curve giving the index n or the modulus of refraction $M=(n-1)\ 10^6$ as a function of the altitude h), must effect important modifications of the first solution and, therefore, to the value of the calculated fields.

For example, when the field is calculated on the basis of a bilinear index, it is observed that the proper values obtained do not tend towards the values of a linear profile when the height of the discontinuity increases indefinitely.[3]

A consequence of the instability of the solution is that it is useless to attempt to obtain this rigorously for a given value of the parameters, but that it appears preferable to examine the physical phenomenon which, by introducing a small modification to the given data, profoundly transforms the solution and thus makes propagation possible.

The various theories differ according to the nature of this physical phenomenon.

1. *Effect of Wind:* The hypothesis of the homogeneity of the atmosphere has been challenged and it has been admitted that there exist, around the classical mean value of the index in standard atmosphere, small erratic variations of the latter in all directions. This is the *turbulence theory*, where the mean field at a distance is calculated on the basis of the diffusion caused by these variations.

2. *Effect of Gravity:* The hypothesis of a constant index gradient has been challenged and it has been admitted that the exponential variation of the modulus of refraction with altitude caused by gravity suffices to explain, as was shown above, the variations between the proper values which determine the attenuation factor.

This is the *theory of partial reflections*, so called because the variations between the proper values are attributed to the reflections caused by the discontinuities in the curve of the index profile.

3. *Effect of Terrain Irregularities:* The hypothesis of perfect sphericity of the earth has been challenged and it has been admitted that terrain irregularities the average dimensions of which are greater than the wavelength suffice, by the resulting modification of the boundary conditions, for obtaining a solution of the propagation equation differing greatly from the classical solution.

[1] K. Bullington, "Radio transmission beyond the horizon in the 40- to 4,000-mc band," Proc. IRE., vol. 41, pp. 132–135; January, 1953.

[2] J. Ortusi, *Annales de Radioélectricité*, p. 88; January, 1953.

[3] "Propagation of short waves," M.I.T. Collection, vol. 13, sec. 2–20, pp. 168–174.

This is the *theory of pure diffraction*, so called because the calculation of the field is no longer so closely tied to a particular hypothesis regarding the nature of the atmosphere.

The advantages and disadvantages of the various theories will now be examined one by one.

Turbulence Theory

According to this theory, the field is calculated by the usual method of diffusion calculations. First, the zone of the troposphere situated inside the beams of the transmitter and receiver is determined (Fig. 1). In this zone, each elementary volume of the dimension of the scale of turbulence is considered as an elementary dipole excited by a source uncorrelated to its neighbor.

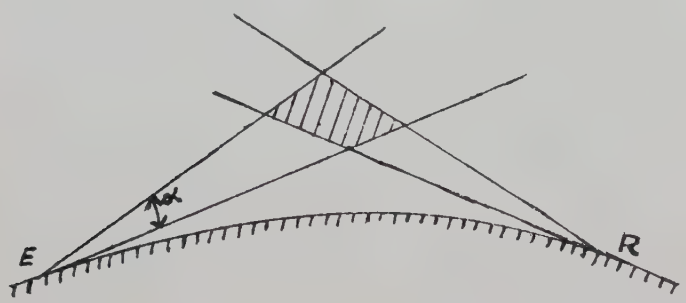

Fig. 1

Advantages of the Theory: The main advantage of the theory is that it stresses the importance of the erratic variations of the refraction index confirmed experimentally.

These experiments, carried out on aircraft with the aid of refractometers, furnish data corresponding approximately, for distances of the order of 300 km, with those needed in order to obtain fields in agreement with those measured.

It cannot seriously be denied that, even if the turbulence method does not give the value of the median field, it should enable the mean value of propagation laws to be determined as well as the loss of aerial gain sometimes observed at long distances.

Disadvantages of the Theory: Two objections can be raised regarding the application of this theory.

(a) It is often difficult to define the volume of diffusion. At first, Booker and Gordon assumed that the volume of diffusion was strictly limited by the locus of the points common to the two beams. The attenuation factor is then given by the formula (in decibels)

$$F = 20 \log_{10} \frac{2R^5\alpha^3}{d^4} S_p,$$

where R is the fictitious earth radius,
d, the distance between the transmitter and the receiver,
α, the angle of the two beams, assumed to be identical,

and S_p is called the mean "*diffusion parameter.*" It is equal to

$$S_p = \frac{2\bar{\Delta}_n^2}{\pi l},$$

where $\bar{\Delta}_n$ is the mean square value of the index variations and l the scale of turbulence.

This formula gives fields that are much too large when the aerials are of low gain. The diffusion volume then increases considerably, since the angle α of each beam is inversely proportional to the aerial gains.

More recently, in order to take into account the polar diffusion diagram of the atmosphere, Gordon assumed that the useful angle in each beam is limited to a critical value given by the relation $\alpha_c = 2/3 \cdot d/R$.[4] From this new hypothesis, the aerial gains can only decrease, at long distances, when the absolute value is such that the angle α of the beams is less than α_c. In the contrary case, the gain is maintained.

Finally, it is clear that this hypothesis considerably reduces the volume of diffusion when the distance is small and the aerial gain low.

(b) The "diffusion parameter S" depends on the altitude of each point in the volume of diffusion. It can be taken as roughly proportional to the square of the number of air molecules per cm^3; it then varies according to the function

$$f(z) = e^{-z/z_0},$$

where z is the altitude and z_0 a constant equal to 4 km for a temperature of 0 degrees C. The maximum mean diffusion parameter, obtained when the beam is very narrow, is thus proportional to the function

$$g(d) = e^{-d^2/8Rz_0} = e^{-(d/500\ \mathrm{km})^2}.$$

The field of turbulence should then begin to decrease exponentially from a distance of 500 km, at most.

The experiments, though difficult of interpretation, clearly show the rapid decrease of the diffusion parameter at high altitudes. However, in the curves of the field received the function of distance, no marked discontinuity appears at distances greater than 500 km. This seems to show that, at least at great distances, the turbulence field does not constitute the median field.

Theory of Multiple Reflections

In this theory, as in the case of the classical theory, the field is calculated by the phase integral method. But the atmosphere is taken as real standard, for which the index does not always vary linearly with altitude—a physical phenomenon which was shown above to be due to the action of gravity. The gradient of the profile index curve is then no longer constant and it can be taken as a series of straight elements of varying slope. It is then necessary to apply new boundary conditions at all

[4] W. E. Gordon, URSI Meeting, Washington; April, 1953.

points of the profile curve where the slope changes (see Fig. 2).

These new boundary conditions imply the presence of spatial charges equivalent to a polarization of the atmosphere in about the same manner as in the turbulence theory and so enable relatively strong fields at great distances to be obtained.

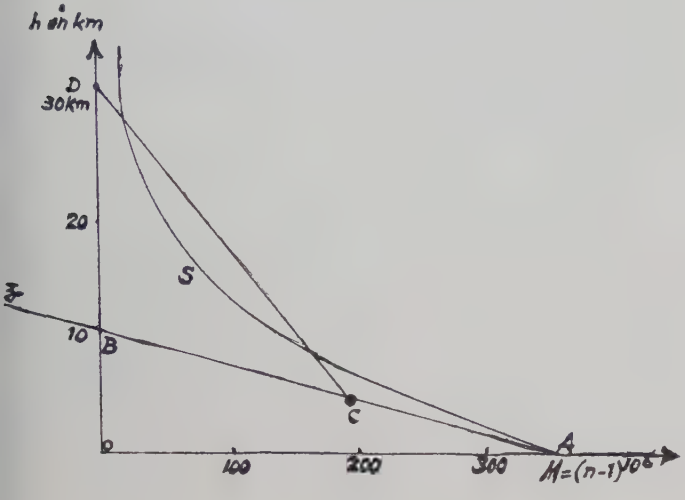

Fig. 2

However, to make calculations possible, certain hypothesis have to be made regarding the index profile curve. Fig. 2 shows the approximations made on this curve. Curve S is the curve for the real standard atmosphere. The straight line Az is the straight line corresponding to the radio standard atmosphere.[5] It will be noted that negative refraction moduli are assumed for $h>10$ km. The two straight segments AB and Bh constitute the bilinear model. It was seen earlier that this model introduces propagation modes whose proper values differ from those of the standard atmosphere. However, at great distances, point B is again located beyond the horizon and the field produced by the equivalent source at B becomes very weak.

To overcome this difficulty use is made of the trilinear model consisting of the three straight segments AC, CD, and Dh. In this case, one of the fictitious sources at D always remains above the horizon. To investigate the effect of the fictitious sources at B or D, an examination is made of the effect of the boundary conditions applied at these points on the different modes of propagation.

It is found that *modes of maximum contribution* exist, the order number of which (always high) depends on the height of the aerials and on the wavelength.[6]

Advantages of the Theory: There are three important advantages.

(a) It is based, as in the case of the classical method, on the solution of the propagation equation. It is therefore rigorous, in principle.

(b) It supplies field values which agree very well with the values of the fields in the neighborhood of the horizon. In this case, the influence of multiple reflections is slight, and the calculation is therefore that which applies in the classical method which, as is well known, then gives fields agreeing with experiment.

(c) It takes into account, as far as possible, the actual nature of the index profile.

Disadvantages of the Theory: The main disadvantage of the theory is the uncertainty regarding the real choice of the boundary conditions which have considerable effect on the form of the solution. The choice of points B, C, or D in Fig. 2 is independent of distance.

Fig. 3 shows the intersection of the transmitter and receiver beams with the layer of height OC, OB, or OD. These layers cut at rather arbitrary points the vertical of the point of intersection M of the beams assumed indefinitely narrow.

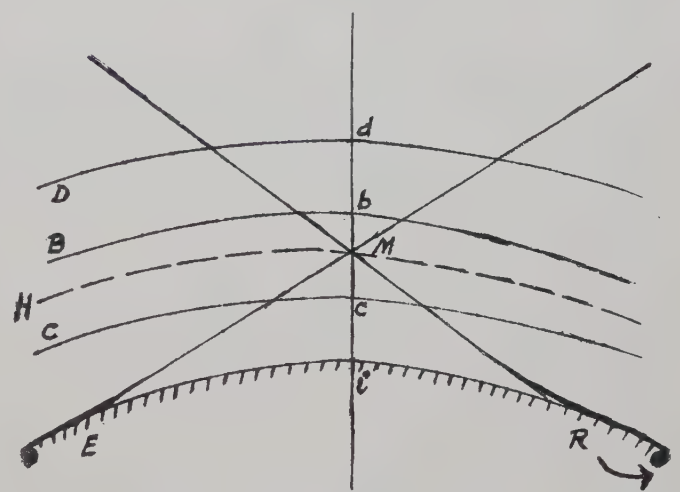

Fig. 3

When the field along this vertical is considered, the limiting conditions have to be applied at the point i of intersection with the ground and at one of the points b, c, or d. Two difficulties then arise.

(a) Points b, c or d being different from point M, the limited development of the field at b, c, or d must be taken to quite an advanced stage, since the chief discontinuity occurs near M.

(b) The influence of the field value at i is of major importance in calculating the maximum modes of excitation. And this field is highly dependent on terrain irregularities.

Modification to the Multiple Reflection Theory: To overcome these two disadvantages, it appears possible to choose an index profile curve so determined that the limiting conditions are exactly applied at point M.

Fig. 4, on the following page, shows the bilinear model of the corresponding index profile curve. The at-

[5] Radio standard atmosphere is sometimes so-called to indicate a fictitious state of the atmosphere where the index varies as the tangent Az to the curve S of the real standard atmosphere.

[6] Thomas J. Caroll, Document presented by the delegation of the U.S.A. at the URSI Meeting; August, 1954.

mosphere is assumed to be radio standard up to the value of layer H corresponding to point M, and the index is taken as constant above point M (elements AH, Hy layer H shown dotted in Fig. 3).

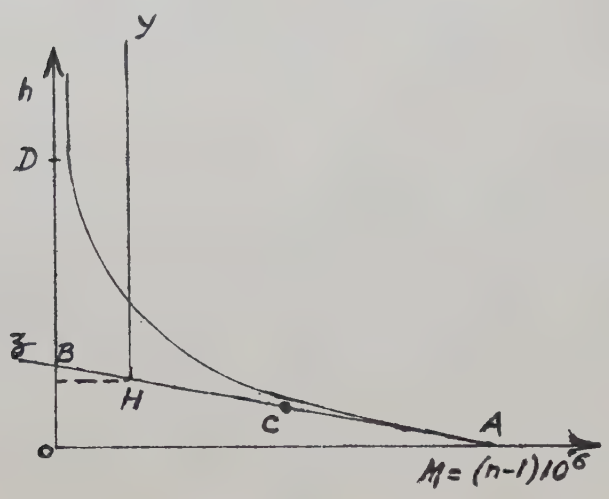

Fig. 4

This method allows the limiting conditions to be applied at point M, that is to say for a value of altitude where the field has a marked discontinuity and where it may consequently be assumed that the modification introduced by the boundary conditions can be of major importance for the form of the solution.

Pure Diffraction Theory

This theory was developed by the author.[7] In it the index profile curve shown in Fig. 4 is assumed so as to apply the limiting conditions at the point M as was shown above. Further, in view of the presence of terrain irregularities the average dimension of which is large compared to the wavelength, it is assumed that the boundary conditions applied at the earth's surface introduce only a slight disturbance when determining the field along the vertical on point M. The diagram of the equivalent earth is thus shown in Fig. 5.

The earth is assumed to be conducting up to points Eh and Rh corresponding to the transmitter and receiver radio horizon. It is then assumed that *no terrain exists* between Eh and Rh. Also, the atmosphere is taken as radio standard up to point M and with a constant index above point M.

It was shown that these simplifying physical hypotheses correspond to the choice of a bilinear index curve allowing, by neglecting also the influence of field discontinuity at point i, a solution to be obtained in the form of a rapidly convergent series. To this end, the propagation equation is replaced by the equivalent integral equation giving the field data along the vertical on point M. The real part of the proper values of the propagation modes then corresponds to the Huyghens sources set out along $y\,y'$ (or, more exactly, along the vertical plane through $y\,y'$ and perpendicular to ER). In this latter plane, the integrals of the sources in surfaces S_1 and S_2 above and below point M are replaced by a contour integral along the perpendicular at M to the plane of Fig. 5.[8] The integrals in surfaces S_1 and S_2 appear, as in the case of the calculation of propagation modes by the phase integral method, in the form of two series the main parts of which are equal and opposite, and the second order terms of which supply, by neglecting the discontinuity at point i, the values of the diffracted field at R.

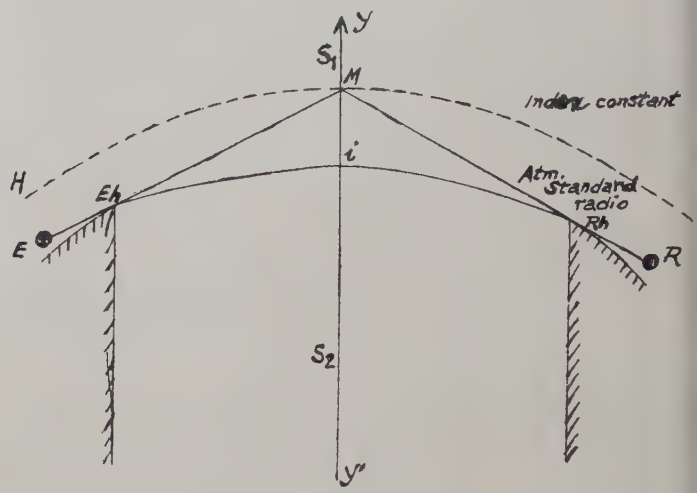

Fig. 5

This procedure provides median field values given by the following formulae, when the distance is sufficiently great.

1. When the height of one of the aerials is less than a limiting value

$$h_m = \frac{R\lambda}{2d},$$

there is a negative gain of height, depending on the terrain conditions in the neighborhood of this aerial.

2. When the sum of the heights of the aerials h_1+h_2 is greater than a limiting value

$$h_L = \frac{d^2}{4\pi R},$$

there is a positive gain of height, independent of the terrain conditions and given by the formula

$$G_A = \left(\frac{h_1 + h_2}{h_L}\right)^3.$$

3. When the aerial heights are between the preceding limits, the median field received is independent both of the aerial heights and of the terrain conditions. It is given by the formula

[7] J. Ortusi, *Annales de Radioélectricité*, p. 227; July, 1954.

[8] According to the classical method of the Kottler formulae See L. de Broglie, "Problems of Guided Propagation," p. 102.

$$F = \frac{E}{E^0} = \frac{R^2\lambda}{\pi^2 d^3},$$

where F, R and, d have the significations given previously.

Advantages of the Theory: This theory has two advantages.

(a) From the physical point of view, as in the case of the bilinear model in the multiple reflection theory, the field beyond the horizon is attributed in part to the discontinuity of the index profile curve. It is also due, however, to the presence of terrain irregularities. From the mathematical point of view, the method allows the important difference between the solution obtained and the unstable solution of the classical method, to be attributed to a modification of the boundary conditions occurring in fact near the zone of heights where the field varies considerably.

(b) The formulae obtained *agree to within a few decibels* with the median field as well as the height gains of the experimental data supplied by the Stockholm curves and by the U.S.A. delegation at the CCIR (Document 201 London 1953).

Disadvantages of the Theory: The main disadvantage of the method is the impossibility of bringing the solution into agreement with that given by the classical method in the neighborhood of the horizon. In this case, point M is low and the index profile curve of Fig. 4, AH, Hy departs considerably from the real curve. Similarly, the limited development over short distances is obtained with excessive values of the variable.

It must be admitted that the theory can be rigorously applied only for distances in excess of 300 km, corresponding to points H in Fig. 4 higher than the fixed point C. On the other hand, because of the suppression of the influence of ground discontinuity, the absolute value of the index at point M is of far less importance than in the two previous theories and the formulae obtained, as confirmed by experiment, show no marked discontinuity at distances greater than 500 km.

Conclusion

The three theories for the calculation of fields beyond the horizon have been reviewed. It has been seen that these theories rest on the instability of the propagated wave in respect various physical factors (meteorological or due to terrain conditions). It appears that the three methods, each having its own advantages, can be used jointly by engineers concerned with long-range communication.

1. Near the horizon, the multiple reflection theory, in good agreement with the classical method, is preferable.

2. For distances greater than 200 kmn, the pure diffraction theory, providing a simplified form of calculation of the preceding theory, is preferable, especially when using simplified formulae for the calculation of the median field and height gains.

3. Neither of these two methods supplies the law around the median value. The calculation of the turbulence field must then be made in order to obtain that law. The same applies in the case of the highly directional aerials calculation of the loss of gain obtained from the polar diagram of the turbulence sources.

Office of Naval Research—Naval Electronics Laboratory Symposium

A Symposium on "Normal Mode Theory" will be held at the Navy Electronics Laboratory, San Diego, California, on July 5–7, 1955, under the chairmanship of Dr. S. A. Schelkunoff of Bell Telephone Laboratories. This Symposium will consist of a roundtable discussion. The major objective is to offer an opportunity for interchange of ideas, stimulating discussion, and elucidation of controversial or seemingly controversial questions and conclusions.

International Council of Scientific Unions: Mixed Commission of the Ionosphere

A Symposium under the general title "Solar Eclipses and the Ionosphere" will be held in the rooms of the Royal Society, Burlington House, London, on August 22–24, 1955. Topics to be discussed include: (1) Ionospheric and Other Geophysical Eclipse Phenomena; (2) Recent Ionospheric Eclipse Results; (3) Ionospheric Processes—Ion Production and Recombination; (4) Sources of Ionizing Radiation; and (5) Radio Astronomical Eclipse Observations.

Contributors include Professor S. Chapman, Professor H. S. W. Massey, Mr. J. A. Ratcliffe, Dr. M. Nicolet, Dr. J. Bartels, Mr. L. V. Berkner, Professor D. R. Bates, Professor J. Sayers, R. P. Lejay, Dr. K. Weekes, Professor C. W. Allen, Mr. W. R. Piggott, Mr. C. M. Minnis.

The Proceedings of the Symposium will be published as a special report by the International Union of Scientific Radio (URSI). Those wishing to attend the Symposium or to submit written contributions are invited to communicate with Dr. W. J. G. Beynon, Secretary, Mixed Commission on the Ionosphere, Department of Physics, University College, Swansea, U. K.

URSI-University of Michigan Symposium

An International Symposium on Electromagnetic Wave Theory sponsored by Commission VI of URSI (The International Scientific Radio Union) and the University of Michigan will be held on June 20–25, 1955, at the University of Michigan.

The Symposium will be devoted to these major topics: (1) Propagation in Doubly Refracting Media in Wave Guides (e.g., Ferrites); (2) Boundary Value Problems of Diffraction and Scattering Theory; (3) Contributions in Antenna Theory of Fundamental Importance; (4) Forward Scattering; (5) Multiple Scattering (i.e., of Light by Colloidal Particles). Of particular interest are millimeter developments in the above topics.

The program will consist of invited and contributed papers in any of the above or related topics. Those who wish to present papers at the meeting should submit abstracts (not more than 200 words) to K. M. Siegel, Symposium Chairman, Willow Run Research Center of the Engineering Research Institute, University of Michigan, Ypsilanti, Michigan, by March 31, 1955.

INSTITUTIONAL LISTINGS

The IRE Professional Group on Antennas and Propagation is grateful for the assistance given by the firms listed below, and invites application for Institutional Listing from other firms interested in the field of Antennas and Propagation.

ANDREW CORPORATION, 363 E. 75th Street, Chicago 19, Ill.
Development and Production of Antenna and Transmission Line Systems.

DORNE AND MARGOLIN, INC., 30 Sylvester Street, Westbury, L. I., New York
Antenna Research and Development—Radiation Pattern Measuring Services.

THE GABRIEL LABORATORIES, Div. of the Gabriel Co., 135 Crescent Road, Needham Heights 94, Mass
Research and Development of Antenna Equipment for Government and Industry.

I-T-E CIRCUIT BREAKER CO., Special Products Div., 601 E. Erie Ave., Philadelphia 34, Pa.
Design, Development and Manufacture of Antennas and Related Equipment.

JANSKY & BAILEY, INC., 1339 Wisconsin Ave. N.W., Washington 7, D.C.
Radio & Electronic Engineering; Antenna Research & Propagation Measurements; Systems Design & Evaluation

WHEELER LABORATORIES, INC., 122 Cutter Mill Road, Great Neck, New York
Consulting Services, Research and Development, Microwave Antennas and Waveguide Components.

The charge for an Institutional Listing is $25.00 per issue or $75.00 for four consecutive issues. Application for listing may be made to the Technical Secretary, The Institute of Radio Engineers, 1 East 79th Street, New York 21, New York